Winter 12-4-2015

Reactive Oxygen Species Homeostasis and Proline Catabolism

Lu Zhang
University of Nebraska-Lincoln, juliazhang87@gmail.com

Reactive Oxygen Species Homeostasis and Proline Catabolism

by

Lu Zhang

A DISSERTATION

Presented to the Faculty of

The Graduate College at the University of Nebraska

In Partial Fulfillment of Requirements

For the Degree of Doctor of Philosophy

Major: Biochemistry

Under the Supervision of Professor Donald Becker

Lincoln, Nebraska

December, 2015

Reactive Oxygen Species Homeostasis and Proline Catabolism

Lu Zhang, Ph.D.

University of Nebraska, 2015

Advisor: Donald Becker

The role of proline metabolism in regulating cellular redox status was first proposed three decades ago. Proline catabolism was then later found to induce programed cell death and cell apoptosis by regulating ROS signaling. Proline oxidation was also found to promote cell survival under oxidative stress. Proline catabolism-mediated reactive oxygen species (ROS) were suggested to be involved in both cases by serving as a regulatory signal. In this work, the sources of proline oxidation-induced ROS production were explored in both bacteria and animal cells. Proline oxidation-induced ROS was found to be shared by bacteria (*Escherichia coli*) and animals (human and pig), suggesting it is a common occurance for many if not all organisms. The source of proline oxidation–mediated ROS was found to be the respiratory chain, where reducing equivalents generated during proline catabolism transfer electrons to molecular oxygen. Proline dehydrogenase (PRODH), the enzyme that catalyzes the first and rate limiting step of proline oxidation, does not directly contribute to proline oxidation-induced ROS formation. For instance, we found recombinant human PRODH1 has low reactivity with molecular oxygen (*kcat* = 0.06 min^{-1}), which is

300-700 times slower than with an artificial electron acceptor (*kcat* =0.75 s^{-1}) or the physiological electron acceptor ubiquinone-1 (*kcat* =0.35 s^{-1}). We also studied the mechanism of proline treatment in regulating oxidative stress resistance, since proline supplementation was able to promote the survival of wild-type *E. coli* under oxidative stress. Depletion of PutA in *E. coli* resulted in increased sensitivity to oxidative stress, suggesting the role of proline oxidation in regulating oxidative stress resistivity. We found that ROS generated during proline oxidation activates the OxyR regulon leading to increased *katG* expression and oxidative stress tolerance. In addition, the level of proline oxidation induced ROS in *E. coli* are sufficient to serve as an adaptive signal to oxidative stress. In mitochondria, proline oxidation also led to ROS generation suggesting that a conserved feature of proline catabolism in different organisms in the formation of ROS as a by product.

ACKNOWLEDGEMENTS

I would never have been able to finish my Ph.D. study without the guidance of my committee members, help from my co-workers and support from friends and my family.

Foremost I would like to gratefully and sincerely thank my advisor, Dr. Donald F. Becker, for taking me originally as a master student of “3+1” program and a Ph.D. student afterwards. Without him, I would not be standing in the place where I am. I am grateful for all of the mentorship, guidance, understanding and patience that he has given me. I also highly appreciate his support and encouragement for my internships at both NUtech Ventures and Dow AgroSciences. I know that not many graduate students are given the opportunity to participate in multiple internship during their Ph.D. program. I felt I owned a debt of gratitude to Dr. Becker and I will forever remember his kindness, support and great work ethics.

I would also like to express my gratitude to members of my advisory committee, Dr. Mark Wilson, Dr. Melanie Simpson, Dr. Nicole Buan and Dr. James Alfano, for their input, valuable discussion and accessibility.

I am thankful to my former and present co-workers in Dr. Becker’s lab for their helpful discussion and assistance. I would like to express my appreciation to all office personal and colleagues at the Beadle Center for their help and suggestion. They make the Beadle Center a friendly and enjoyable place to learn and work.

I would like to thank all my friends for their friendship, help and support. They make Lincoln, Nebraska as my second home. They also help me to stay strong and calm during the tough period of graduate school.

Finally, I thank my parents for their faith in me, and my dog Tiantian for his silent love and patience.

TABLE OF CONTENTS

ABBREVISTIONS

AKT	Protein Kinase B
AMPK	AMP-activated protein kinase
ATP	Adenosine- 5'-riphosphate
Bcl-2	B-cell lymphoma 2
CoQ1	Ubiquinone -1
EDTA	Ethylenediaminetetraacetic acid
ETC	Electron transport chain
FAD	Flavin adenine dinucleotide
GK	γ-Glutamyl kinase
GPR	γ-Glutamyl phosphate reductase
GSA	Glutamate-γ-semialdehyde
GSH	Reduced glutathione
H_2O_2	Hydrogen peroxide
HR	Hypersensitive Response
IPTG	Isopropyl β-D-thiogalatopyranoside
JA	Jasmonic acid
JNK	c-Jun N-terminal protein kinases
KEAP1	Kelch-Like ECH-Associated Protein 1
[Fe-S]	Iron–sulphur cluster
mTOR	mechanistic target of rapamycin
MAPK	Mitogen-activated protein kinases

MEK	Mitogen-activated protein kinase kinase
ERK	Extracellular signal-regulated kinases
MKK	Mitogen-activated protein kinase kinase
MPK	Mitogen Activated Protein Kinase
NAD^+	Nicotinamide adenine dinucleotide
NADH	Reduced nicotinamide ademine dinucleotide
NADPH	Nicotinamide adenine dinucleotide phosphate
Nrf	Nuclear respiratory factor
o-AB	*o*-aminobenzaldehyde
$^{\bullet}OH$	Hydroxyl radical
$^1O_2$	Singlet oxygen
$O_2^{\bullet-}$	Superoxide anion
OAT	Ornithine-δ-aminotransferase
OGDH	α-ketoglutarate dehydrogenase
PCD	Programmed cell death
PI3K	Phosphatidylinositol-3,4,5-triphosphate dependent kinase
PPAR	Peroxisome proliferator-activated receptor
PRODH	Proline dehydrogenase
PutA	Proline utilization A
P5C	Δ^1-Pyrroline-5-carboxylate dehydrogenase
P5CR	Δ^1-Pyrroline-5-carboxylate reductase
P5CS	Δ^1-Pyrroline-5-carboxylate synthase

RHH	Ribbon-helix-helix
ROS	Reactive oxygen spices
SDS-PAGE	Sodium dodecyl sulfate polyacrylamide gel electrophoresis
SDH	Succinate Dehydrogenase
SOD	Superoxide dismutase
TCA	Tricarboxylic acid cycle
TGF	Transforming growth factor
THFA	Tetrahydro-2-furoic acid
TTC	Triphenyltetrazolium chloride

CHAPTER 1

Reactive Oxygen Species, Oxidative Stress and Redox Signaling

1.1 REACTIVE OXYGEN SPECIES

Aerobic organisms inevitably encounter reactive oxygen species (ROS), which are generated as by-products from molecular oxygen (O_2) during respiration (1). ROS such as superoxide anion ($O_2^{\bullet -}$), hydroxyl radical (•OH), hydrogen peroxide (H_2O_2) and singlet oxygen ($^1O_2$) are the chemical species that are formed when molecular oxygen accepts electrons from cellular redox components (2). $O_2^{\bullet -}$ is produced by the one-electron reduction of O_2 and is the most abundant ROS (3). As a charged molecule, $O_2^{\bullet -}$ is not capable of crossing membranes passively, therefore its deleterious effect is limited to its site of generation (1). With its high electrostatic attraction, $O_2^{\bullet -}$ reacts readily with iron–sulfur clusters (4) disrupting the function of several iron-sulfur proteins which have vital physiological roles, such as in the electron transport chain (NADH dehydrogenase, Coenzyme Q-cytochrome C reductase) and the tricarboxylic acid cycle (TCA) (aconitase) (5). Another consequence of iron-sulfur destruction, however, is the release of iron that can lead to the production of highly reactive •OH. Superoxide dismutase (SOD) is responsible for scavenging $O_2^{\bullet -}$ (2), a process that results in the formation of H_2O_2 ($2O_2^{\bullet -} + 2H^+ \rightarrow H_2O_2 + O_2$). H_2O_2 is more stable than $O_2^{\bullet -}$. It is capable of passing through membranes and, can also be transported via aquaporins into different cellular compartments (1). Main sources of H_2O_2 include flavin enzymes, respiratory electron transport chain, and NAPDH oxidase (7). H_2O_2 itself is not generally reactive, however, H_2O_2 reacts quickly with transition metals to generate •OH, a process known as the Fenton reaction ($Cu^+/ Fe^{2+} + H_2O_2 \rightarrow Cu^{2+}/ Fe^{3+} + \bullet OH + OH^-$) (1). H2O2 can also down

regulate the catalytic activity of many enzymes, including protein tyrosine phosphatases, cysteine proteases, and metalloenzymes, by oxidization of irons-sulfur clusters and certain residues (tryptophan, methionine, histidine and cysteine) (8). In some cases, a reactive cysteine on the enzyme acts as a nucleophile by attacking H_2O_2, resulting in the formation of a cysteine sulfenic species (SOH) that can lead to glutathiolation or a disulfide bond (8). Because H_2O_2 has multiple effects on cellular processes by either causing oxidative damage or regulating various cell signaling pathways (6), numerous enzymes are dedicated to regulating H_2O_2 levels. These include catalase and alkyl hydroperoxidase in gram-negative bacteria such as *Escherichia coli* (2), and in eukaryotes, additional glutathione peroxidase and peroxiredoxin (1). With a half-life of only 2-4 ms, $^{\bullet}OH$ is the most potent oxidant causing damage to cellular macromolecules, including DNA, lipids and protein. The reaction between macromolecular and $^{\bullet}OH$ produces a variety of organic peroxides, such as malonaldehyde and 4-hydroxyalkenals, which can further propagate oxidative damage (9). Unlike H_2O_2 and $O_2^{\bullet -}$, $^{\bullet}OH$ cannot be eliminated by an enzymatic reaction (10). Instead, antioxidants, such as melatonin, glutathione and vitamin E, are responsible for $^{\bullet}OH$ scavenging (10). Considering the difference of efficiency between enzyme-mediated and antioxidants-mediated scavenge of $^{\bullet}OH$, it is important to tightly regulate the level of H_2O_2 and $O_2^{\bullet -}$. Therefore, this thesis will be mainly focusing on the biological response and endogenous production of H_2O_2 and $O_2^{\bullet -}$.

1.2 OXIDATIVE STRESS AND ROS SENSORS IN *ESCHERICHIA COLI*

Oxidative stress arises when the concentration of ROS exceeds the cell's defense capacity (6). Oxidative stress is inevitably encountered by aerobic organisms. *E. coli*, the model organism of Gram-negative bacteria, generate up to 10 μM of H_2O_2 and 5 μM of $O_2^{\bullet -}$ during respiration at exponential phase of aerobic growth (11). Irradiation, heavy metals, and certain antibiotics and redox cycling compounds will also boost the endogenous production of ROS (2). Besides these sources, bacteria also face ROS derived from exogenous sources, such as a host phagocyte and other competing microorganisms (2). To regulate the oxidative stress defense system, *E. coli* utilizes two ROS sensors, namely, the SoxRS system and the OxyR regulon.

OxyR is a H_2O_2-sensing transcriptional activator belonging to the LysR family of transcriptional regulators (12). OxyR contains a N-terminal helix-turn-helix DNA binding domain, a central recognition and response domain that senses the regulatory signal, and a C-terminal domain that is responsible for multimerization and activation (4). In its inactive non-DNA binding form, two cysteine thiols of OxyR are reduced. Upon exposure to as low as 20 nM H_2O_2, a concentration that is well below the toxic threshold (1 mM) (13), the cysteine thiols become oxidized thereby leading to activation of OxyR DNA-binding. Based on structural information, the Cys199 residue of OxyR attacks H_2O_2 to generate a sulfenic acid, which then condenses with nearby Cys208 to form an intramolecular disulfide bond (14). The formation of the disulfide bond changes the conformation of OxyR and triggers the activation of OxyR allowing it to bind

site-specifically to DNA promoters of the OxyR regulon (14). The OxyR regulon of *E. coli* is comprised of over 20 genes, including genes involved in H_2O_2 detoxification, heme biosynthesis, reducing equivalents supply, thiol-disulfide isomerization, [Fe-S] repair, iron binding, and the transport of iron and manganese (2). When H_2O_2 stress abates, OxyR is reduced and de-activated by glutaredoxin 1, which contributes to OxyR auto-regulation together with alkyl hydroperoxidase and catalase (4).

The SoxRS system contains two proteins SoxR and SoxS, whose encoding genes are adjacent to each other (15). SoxR, an iron-sulfur transcription factor, is activated when its $[2Fe\text{-}2S]^{1+}$ cluster is oxidized by $O2^{\bullet -}$ to a $[2Fe\text{-}2S]^{2+}$ state (2). Oxidized SoxR then induces the transcription of SoxS, which subsequently activates the expression of more than 100 genes of the SoxRS regulon, including manganese-containing SOD (SodA) and the ferric uptake regulation protein (Fur) (16). With activated SodA, the level of $O_2^{\bullet -}$ is kept around 0.1 nM (17). When $O2^{\bullet -}$ stress subsides, SoxR is reduced and SoxS is degraded via proteolysis using the Clp protease system (15).

1.3 ROS ACTIVATED INTRINSIC AND EXTINSIC APOPTOSIS SIGNALING PATHWAY

ROS induced cell apoptosis is mediated by either intrinsic or extrinsic pathways in animals (18). In either case, apoptosis is associated with the activation of caspases, belonging to cysteine protease family (19). Activated caspases cleave a number of proteins, such as inhibitor of caspase-activated

DNase and cytoskeletal protein, leading to DNA fragmentation, nuclear shrinking and loss of cell shape (19).

1.3.1 ROS induced extrinsic apoptosis pathway

In the extrinsic pathway, caspase is activated at the plasma membrane by activation of the death receptor (DR) (18). Factors that activate DR are members of the tumor necrosis factor (TNF) receptor superfamily, such as TNF-related apoptosis-inducing ligand (TRAIL) receptor. Activation of the DR leads to recruitment of the Fas-associated death domain (FADD) protein and caspase-8, which eventually activates downstream effector caspases such as caspase-3 to induce apoptosis (20). A link between oxidative stress and the extrinsic cell death pathway was discovered to involve nuclear factor of activated T cells (NFAT), which activates TRAIL promoter activity and increases the expression of TRAIL (21). H_2O_2 has been shown to activate the Ca^{2+}-calcineurin-NFAT pathway (22). In the Ca^{2+}-calcineurin-NFAT pathway, Ca^{2+} binds to the regulatory subunit of calcineurin as well as to calmodulin, therefore leading to the activation of calcineurin phosphatase (23). Dephosphorylation of several phosphorylated residues in the N-terminus of NFAT by calcineurin phosphatase results in increased transportation of NFAT into nucleus. Nuclear localized NFAT binds to the promoter region of target genes such as TRAIL, and regulate their expression (23). Therefore, ROS potentially induces or can at least amplify the extrinsic apoptosis pathway through Ca^{2+}-calcineurin- NFAT pathway (24) (Figure 1.1).

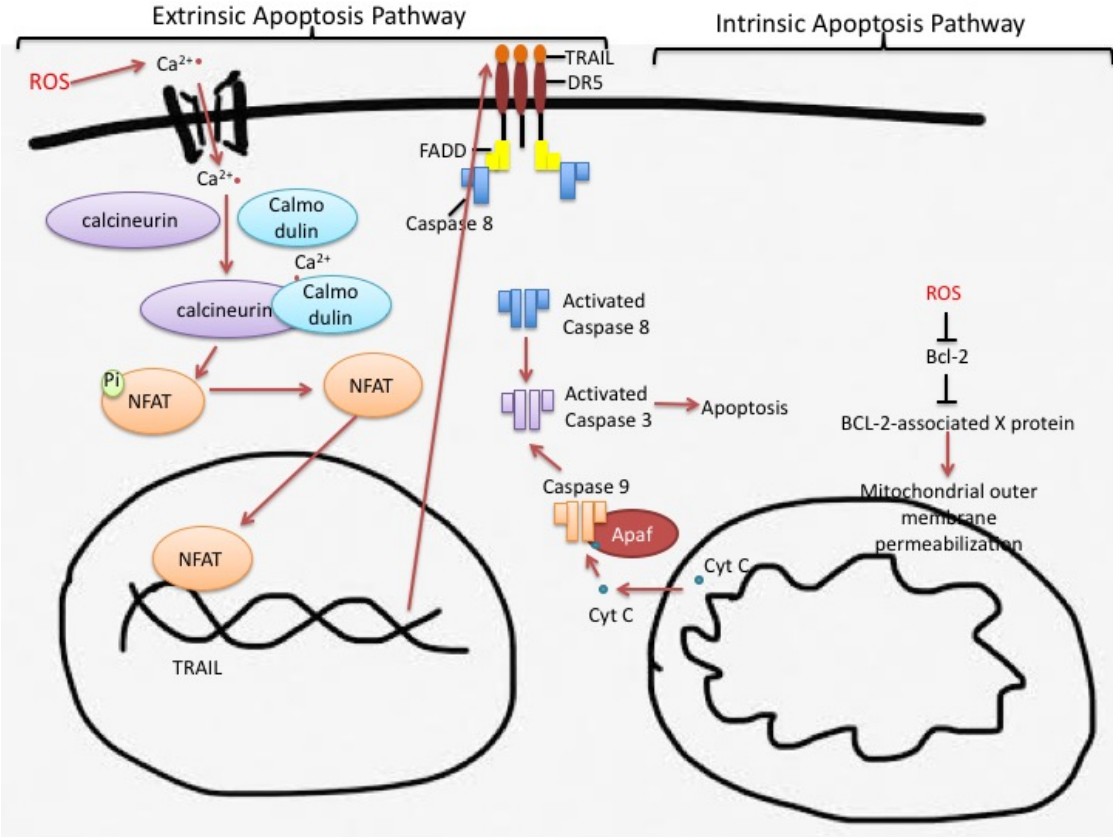

Figure 1.1 ROS induction of extrinsic and intrinsic apoptosis pathways. In the extrinsic pathway, ROS induces Ca^{2+}-calcineurin-NFAT pathway and TRAIL expression, which activates caspases 8 and 3. In the intrinsic pathway, ROS inhibits the expression of Bcl-2, resulting in increased mitochondrial membrane permeabilization and release of cytochrome C (Cyt C) and activation of caspases 9 and 3.

1.3.2 ROS induced intrinsic apoptosis pathway

In the intrinsic pathway, caspase in the mitochondria is activated independent of a receptor (18). B-cell lymphoma 2 (Bcl-2) family proteins, localized on the outer mitochondrial membrane, play a vital role in regulating permeability of outer and inner mitochondria membrane and apoptosis cascades (25). ROS oxidizes Bcl-2 and decreases the expression of Bcl-2, thereby increases the permeability of the mitochondria membrane (26) (Figure 1.1). Upon disruption of the outer mitochondria membrane, cytochrome C localized at the intermembrane space is released into the cytosol (26), thereby triggers apoptosis by either activating caspases or acting as caspase-independent death effectors (18). Cytochrome c binds to the C-terminal of the apoptotic protease activating factor 1 (Apaf-1), a cytosolic protein with an N-terminal recruitment domain (20). The interaction between Apaf-1 and cytochrome c results in the oligomerization of Apaf-1 and the recruitment of caspase-9 (20). The formation of the cytochrome c/Apaf-1/caspase-9-containing apoptosome complex leads to the recruitment and activation of caspase 3, a protease that cleaves key substrates for initiation of apoptosis (18).

1.4 ROS REGULATED MITOGEN-ACTIVATED PROTEIN KINASE CASCADE

Mitogen-activated protein kinase (MAPK) cascades consist of three kinases: MAPK kinase kinases (MEKKs), MAPK kinases (MKKs) and MAPKs (MPKs), each of which phosphorylates its target and acts sequentially (27). Elevated ROS production leads to the activation of members of MPK family,

including extracellular-signal-regulated kinases (ERKs), c-Jun N-terminal Kinases (JNKs) and p38 MAPKs (28) (Figure 1.2). In the ERK pathway, Ras-GTPase in response to growth hormone, activates RAF proto-oncogene serine/threonine-protein kinase (Raf), an MEKK, followed by phosphorylation and activation of MKK and ERK (29). MKK4 and MKK7 in the JNK pathway phosphorylates threonine (Thr) and tyrosine (Tyr) residues within a Thr-Pro-Tyr motif located in JNK subdomain VIII, which activates JNK (30). The p38 MAPKs are usually activated in response to inflammatory cytokines, by MKK3 and MKK6 (27). Upon activation by growth factors, the ERK pathway is involved in cell growth, differentiation and development, while JNK and p38 MAPK pathway are associated with inflammation, apoptosis, cell growth and differentiation when activated by stress stimulation (27).

ROS has been shown to induce the activation of Ras-GTPase through cAMP and protein kinase A, followed by the activation of Raf and ERKs (31). In both p38 MAPK and JNK pathways, apoptosis signal-regulating kinase 1 (ASK-1) is one of the MEKKs in the pathway. In the absence of oxidative stress, ASK-1 binds to reduced thioredoxin, which promotes ASK-1 ubiquitination and degradation to inhibit ASK-1-mediated tumor growth factor (TGF)-α-induced apoptosis (32). Upon oxidative stress, oxidized thioredoxin disassociates from ASK-1, leading to the oligomerization of ASK-1 and activation of the JNK and p38- MAPK pathways (33). MAPK phosphatases (MPKs), which dephosphorylate and deactivate MAPKs, are regulated by ROS (7). In murine embryo fibroblasts, ROS generated by TGF-β1 stimulates NADPH oxidase 4

(Nox4) expression resulting in the modification of a catalytic cysteine residue in MKP-1, leading to activation of the JNK and p38 MAPK pathways (7). Besides thiol modification, ROS can also affect the expression level of MKP-1, thereby regulating the activation of MAPK cascades (34). In addition, ROS also impacts multiple MEKs. In plant, ROS activation of MAPK cascades through MEKs regulate the expression of antioxidant enzymes (27,35). H_2O_2 activates *Arabidopsis* MEKK ANP1, which initiates a phosphorylation cascade involving MKK4/5 and MPK3/6 (36). In the process of pathogen defenses, H_2O_2 activates the MEKK1-MPK4 pathway in Arabidopsis (35). H_2O_2 also induces nucleoside-diphosphate kinases 2, which activates ROS scavenging enzymes by phosphorylation of MPK3/6 (37).

1.5 THE EFFECT OF ROS ON PI3K/AKT/mTOR PATHWAY

The phosphoinositide 3-kinase (PI3K)/protein kinase B (Akt)/ mechanistic target of rapamycin (mTOR) pathway is a signaling pathway regulating cell proliferation while inhibting cell apoptosis (38). PI3K activation phosphorylates and activates Akt, which can regulate a series of down-stream targets, including mTOR and Forkhead box O (FOXO) (38). Akt inhibits FOXO through direct phosphorylation, and indirectly activates mTORC1, which is associated with protein synthesis and cell growth (39). FOXO is involved in the regulation of cell metabolism, proliferation, and stress response (38). PI3K is negatively regulated by phosphatase and tumor suppressor (PTEN) (40). In *vitro*, H_2O_2 oxdizes

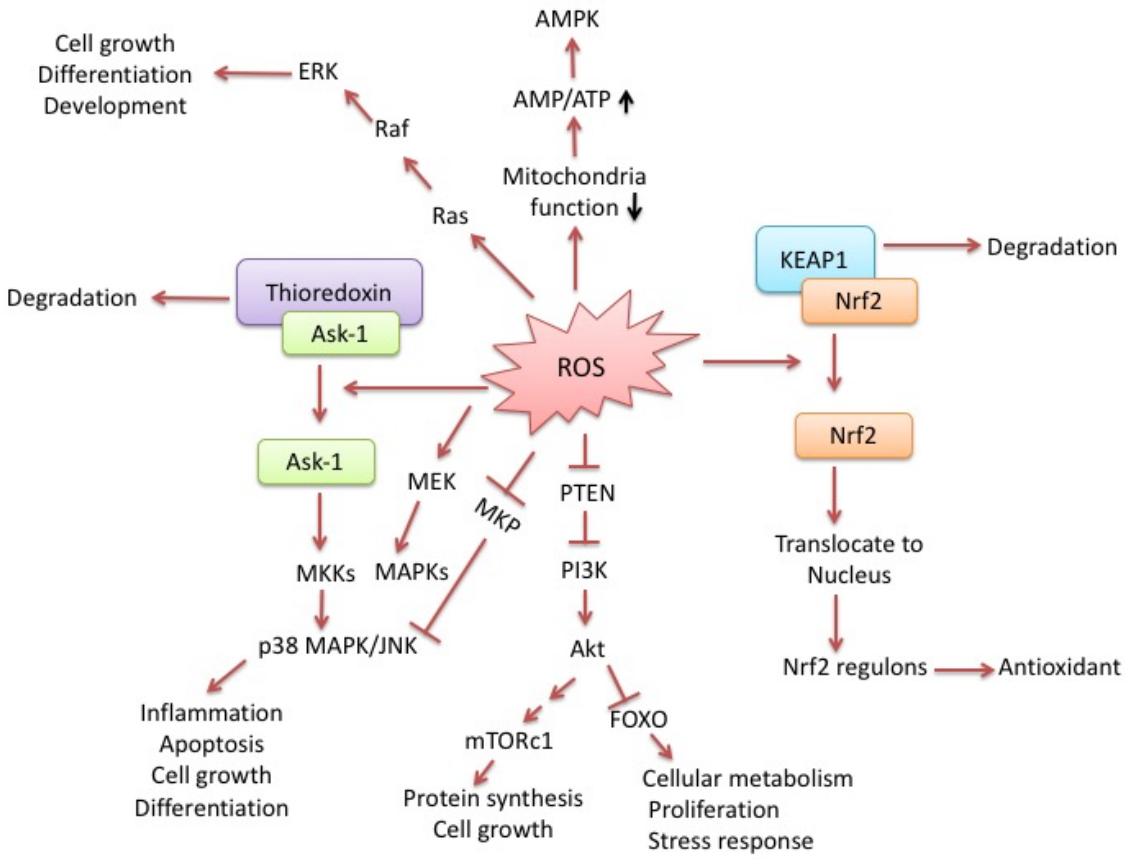

Figure 1.2 Scheme for how ROS can regulate various signaling pathways such as MAPKs, PI3K/AKT/mTOR, Nrf2 and AMPK pathways. In the presence of oxidative stress, MAPKs cascades are activated by inhibition of MKP, and activated Ras, Ask-1 and MEK. By oxidizing PTEN, PI3K/Akt pathway is induced by ROS, leading to activation of mTORC1 and inhibition of FOXO. ROS induces dysfunction of mitochondria ATP production resulting in activation of the AMPK pathway. ROS can also promote the dissociation of Nrf2 from KEAP1 leading to the expression of several antioxidant defense genes.

Cys121 and Cys71 of PTEN, generating a disulfide bond and inactivating PTEN, thus relieving inhibition of PI3K. In *vivo*, increased amounts of oxidized PTEN and activated PI3K due to growth factor induced ROS were observed (42). Therefore, upon oxidiative stress, PTEN inhibition of PI3K is disrupted, leading to activation of Akt/mTORC and inhibition of the FOXO pathway (Figure 1.2).

1.6 ROS ACTIVATED KEAP1/NRF2 PATHWAY

A cysteine–zinc complex constitutes the redox sensor of the Kelch-like ECH associated protein-1 (KEAP1) in mammals. Residues Cys273 and Cys288 of KEAP1 are crucial to zinc coordination and the degradation of the nuclear factor erythroid 2-related factor 2 (Nrf2) (43). Nrf2 is a transcription factor responsible for the regulation of antioxidant proteins (40). In the absence of oxidative stress, Nrf2 forms a complex with KEAP1, leading to proteasome degradation of Nrf2 (44). Upon oxidative stress, Cys273 and Cys288 become oxidized, leading to the release of Nrf2 from KEAP1. Subsequently, Nrf2 is translocated into the nucleus and binds to antioxidant-response elements of antioxidant genes, which are associated with regulating glutathione homeostasis, stress response, calcium homeostasis, and iron metabolism (44) (Figure 1.2). Besides KEAP1, MAPKs and PI3K are also responsible for the activation of Nrf2 under oxidative stress, although the mechanism is still under investigation (45). In the MAPKs, ERK and JNK appear to positively regulate Nrf2, whereas p38 MAPK was reported to regulate Nrf2 both positively and negatively (45).

1.7 SUMMARY

Although oxidative stress is toxic and may initiate cell apoptosis, ROS is required for cellular regulation and is integrated with several different signaling pathways, including MAPKs cascades, and the PI3K/Akt/mTOR and Nrf2 pathways (6). In addition, impaired mitochondrial function due to ROS leads to intracellular increases in AMP, which can activate the AMP-dependent protein kinase (AMPK) pathway (31) (Figure 1.2). The mechanisms by which organisms respond to ROS as an adaptive signal for protection and cell survival during oxidative stress will be explored in Chapters 3 and 4.

REFRENCES:

1. Mittler, R., Vanderauwera, S., Suzuki, N., Miller, G., Tognetti, V. B., Vandepoele, K., Gollery, M., Shulaev, V., and Van Breusegem, F. (2011) ROS signaling: the new wave? *Trends Plant Sci* **16**, 300-309
2. Imlay, J. A. (2008) Cellular defenses against superoxide and hydrogen peroxide. *Annu Rev Biochem* **77**, 755-776
3. Cabiscol, E., Tamarit, J., and Ros, J. (2000) Oxidative stress in bacteria and protein damage by reactive oxygen species. *International microbiology : the official journal of the Spanish Society for Microbiology* **3**, 3-8
4. Dubbs, J. M., and Mongkolsuk, S. (2012) Peroxide-sensing transcriptional regulators in bacteria. *J Bacteriol* **194**, 5495-5503
5. Lill, R. (2009) Function and biogenesis of iron-sulphur proteins. *Nature* **460**, 831-838
6. Apel, K., and Hirt, H. (2004) Reactive oxygen species: metabolism, oxidative stress, and signal transduction. *Annual review of plant biology* **55**, 373-399
7. Liu, R. M., Choi, J., Wu, J. H., Gaston Pravia, K. A., Lewis, K. M., Brand, J. D., Mochel, N. S., Krzywanski, D. M., Lambeth, J. D., Hagood, J. S., Forman, H. J., Thannickal, V. J., and Postlethwait, E. M. (2010) Oxidative modification of nuclear mitogen-activated protein kinase phosphatase 1 is involved in transforming growth factor beta1-induced expression of plasminogen activator inhibitor 1 in fibroblasts. *The Journal of biological chemistry* **285**, 16239-16247
8. Johnston, P. A. (2011) Redox cycling compounds generate H2O2 in HTS buffers containing strong reducing reagents--real hits or promiscuous artifacts? *Current opinion in chemical biology* **15**, 174-182
9. Tejero, I., Gonzalez-Lafont, A., Lluch, J. M., and Eriksson, L. A. (2007) Theoretical modeling of hydroxyl-radical-induced lipid peroxidation reactions. *The journal of physical chemistry. B* **111**, 5684-5693
10. Reiter, R. J., Melchiorri, D., Sewerynek, E., Poeggeler, B., Barlow-Walden, L., Chuang, J., Ortiz, G. G., and Acuna-Castroviejo, D. (1995) A review of the evidence supporting melatonin's role as an antioxidant. *Journal of pineal research* **18**, 1-11
11. Seaver, L. C., and Imlay, J. A. (2004) Are respiratory enzymes the primary sources of intracellular hydrogen peroxide? *Journal of Biological Chemistry* **279**, 48742-48750
12. Zheng, M., Wang, X., Templeton, L. J., Smulski, D. R., LaRossa, R. A., and Storz, G. (2001) DNA microarray-mediated transcriptional profiling of the Escherichia coli response to hydrogen peroxide. *J Bacteriol* **183**, 4562-4570
13. Seaver, L. C., and Imlay, J. A. (2001) Hydrogen peroxide fluxes and compartmentalization inside growing Escherichia coli. *Journal of bacteriology* **183**, 7182-7189

14. Choi, H., Kim, S., Mukhopadhyay, P., Cho, S., Woo, J., Storz, G., and Ryu, S. E. (2001) Structural basis of the redox switch in the OxyR transcription factor. *Cell* **105**, 103-113
15. Pomposiello, P. J., and Demple, B. (2001) Redox-operated genetic switches: the SoxR and OxyR transcription factors. *Trends in biotechnology* **19**, 109-114
16. Wu, J., and Weiss, B. (1992) Two-stage induction of the soxRS (superoxide response) regulon of Escherichia coli. *J Bacteriol* **174**, 3915-3920
17. Baez, A., and Shiloach, J. (2013) Escherichia coli avoids high dissolved oxygen stress by activation of SoxRS and manganese-superoxide dismutase. *Microbial cell factories* **12**, 23
18. Fulda, S., and Debatin, K. M. (2006) Extrinsic versus intrinsic apoptosis pathways in anticancer chemotherapy. *Oncogene* **25**, 4798-4811
19. Degterev, A., Boyce, M., and Yuan, J. (2003) A decade of caspases. *Oncogene* **22**, 8543-8567
20. Jiang, X., and Wang, X. (2000) Cytochrome c promotes caspase-9 activation by inducing nucleotide binding to Apaf-1. *The Journal of biological chemistry* **275**, 31199-31203
21. Wang, Q., Zhou, Y., Weiss, H. L., Chow, C. W., and Evers, B. M. (2011) NFATc1 regulation of TRAIL expression in human intestinal cells. *PloS one* **6**, e19882
22. Huang, C., Li, J., Costa, M., Zhang, Z., Leonard, S. S., Castranova, V., Vallyathan, V., Ju, G., and Shi, X. (2001) Hydrogen peroxide mediates activation of nuclear factor of activated T cells (NFAT) by nickel subsulfide. *Cancer Res* **61**, 8051-8057
23. Crabtree, G. R., and Schreiber, S. L. (2009) SnapShot: Ca2+-calcineurin-NFAT signaling. *Cell* **138**, 210, 210 e211
24. Zou, W., Liu, X., Yue, P., Khuri, F. R., and Sun, S. Y. (2007) PPARgamma ligands enhance TRAIL-induced apoptosis through DR5 upregulation and c-FLIP downregulation in human lung cancer cells. *Cancer Biol Ther* **6**, 99-106
25. Harris, M. H., and Thompson, C. B. (2000) The role of the Bcl-2 family in the regulation of outer mitochondrial membrane permeability. *Cell death and differentiation* **7**, 1182-1191
26. Hildeman, D. A., Mitchell, T., Aronow, B., Wojciechowski, S., Kappler, J., and Marrack, P. (2003) Control of Bcl-2 expression by reactive oxygen species. *Proceedings of the National Academy of Sciences of the United States of America* **100**, 15035-15040
27. Sinha, A. K., Jaggi, M., Raghuram, B., and Tuteja, N. (2011) Mitogen-activated protein kinase signaling in plants under abiotic stress. *Plant signaling & behavior* **6**, 196-203
28. Matsuzawa, A., and Ichijo, H. (2008) Redox control of cell fate by MAP kinase: physiological roles of ASK1-MAP kinase pathway in stress signaling. *Biochim Biophys Acta* **1780**, 1325-1336

29. Rao, V. N., and Reddy, E. S. (1994) elk-1 proteins interact with MAP kinases. *Oncogene* **9**, 1855-1860
30. Ip, Y. T., and Davis, R. J. (1998) Signal transduction by the c-Jun N-terminal kinase (JNK)--from inflammation to development. *Current opinion in cell biology* **10**, 205-219
31. Cardaci, S., Filomeni, G., and Ciriolo, M. R. (2012) Redox implications of AMPK-mediated signal transduction beyond energetic clues. *Journal of cell science* **125**, 2115-2125
32. Liu, Y., and Min, W. (2002) Thioredoxin promotes ASK1 ubiquitination and degradation to inhibit ASK1-mediated apoptosis in a redox activity-independent manner. *Circulation research* **90**, 1259-1266
33. Song, J., Park, K. A., Lee, W. T., and Lee, J. E. (2014) Apoptosis signal regulating kinase 1 (ASK1): potential as a therapeutic target for Alzheimer's disease. *International journal of molecular sciences* **15**, 2119-2129
34. Hou, N., Torii, S., Saito, N., Hosaka, M., and Takeuchi, T. (2008) Reactive oxygen species-mediated pancreatic beta-cell death is regulated by interactions between stress-activated protein kinases, p38 and c-Jun N-terminal kinase, and mitogen-activated protein kinase phosphatases. *Endocrinology* **149**, 1654-1665
35. Pitzschke, A., Djamei, A., Bitton, F., and Hirt, H. (2009) A major role of the MEKK1-MKK1/2-MPK4 pathway in ROS signalling. *Molecular plant* **2**, 120-137
36. Kovtun, Y., Chiu, W. L., Tena, G., and Sheen, J. (2000) Functional analysis of oxidative stress-activated mitogen-activated protein kinase cascade in plants. *Proc. Natl. Acad. Sci. U.S.A* **97**, 2940-2945
37. Moon, H., Lee, B., Choi, G., Shin, D., Prasad, D. T., Lee, O., Kwak, S. S., Kim, D. H., Nam, J., Bahk, J., Hong, J. C., Lee, S. Y., Cho, M. J., Lim, C. O., and Yun, D. J. (2003) NDP kinase 2 interacts with two oxidative stress-activated MAPKs to regulate cellular redox state and enhances multiple stress tolerance in transgenic plants. *Proc. Natl. Acad. Sci. U.S.A* **100**, 358-363
38. Liou, G. Y., and Storz, P. (2010) Reactive oxygen species in cancer. *Free radical research* **44**, 479-496
39. Chen, C. C., Jeon, S. M., Bhaskar, P. T., Nogueira, V., Sundararajan, D., Tonic, I., Park, Y., and Hay, N. (2010) FoxOs inhibit mTORC1 and activate Akt by inducing the expression of Sestrin3 and Rictor. *Developmental cell* **18**, 592-604
40. Schieber, M., and Chandel, N. S. (2014) ROS function in redox signaling and oxidative stress. *Current biology : CB* **24**, R453-462
41. Lee, S. R., Yang, K. S., Kwon, J., Lee, C., Jeong, W., and Rhee, S. G. (2002) Reversible inactivation of the tumor suppressor PTEN by H2O2. *The Journal of biological chemistry* **277**, 20336-20342
42. Leslie, N. R., Bennett, D., Lindsay, Y. E., Stewart, H., Gray, A., and Downes, C. P. (2003) Redox regulation of PI 3-kinase signalling via inactivation of PTEN. *The EMBO journal* **22**, 5501-5510

43. Vriend, J., and Reiter, R. J. (2015) The Keap1-Nrf2-antioxidant response element pathway: a review of its regulation by melatonin and the proteasome. *Molecular and cellular endocrinology* **401**, 213-220
44. Ma, Q. (2013) Role of nrf2 in oxidative stress and toxicity. *Annual review of pharmacology and toxicology* **53**, 401-426
45. Tufekci, K. U., Civi Bayin, E., Genc, S., and Genc, K. (2011) The Nrf2/ARE Pathway: A Promising Target to Counteract Mitochondrial Dysfunction in Parkinson's Disease. *Parkinson's disease* **2011**, 314082

CHAPTER 2

Reactive Oxygen Species and Signaling Pathways Associated with Proline Oxidation

Note: Part of this chapter has been published as the review articles: “Connecting proline metabolism and signaling pathways in plant senescence.” Zhang L and Becker DF. *Front. Plant Sci*. (2015) 6:552. “Proline Mechanisms of Stress Survival.” Xinwen Liang, Lu Zhang, Sathish Kumar Natarajan, and Donald F. Becker. *Antioxidants & Redox Signaling*. September 20, 2013, 19(9): 998-1011. Frontiers in Plant Science and Antioxidants & Redox Signaling granted permission for use in dissertation.

2.1 THE EFFECT OF PROLINE ON ROS HOMEOSTASIS

Besides its proteogenic function, the imino acid proline plays numerous roles in cellular processes, including bioenergetics, cell differentiation, tumor growth, lifespan, and cell apoptosis (1-9). The function of free proline is normally connected to the regulation of ROS homeostasis. Generally, proline may directly scavenge certain types of ROS (e.g. $^{\bullet}OH$) or protect antioxidant enzymes from metal, osmotic and oxidative stress. Free and polypeptide-bound proline can react with $O_2^{\bullet-}$ and $^{\bullet}OH$ to form a variety of hydroxyproline derivatives (e.g., 4-hydroxyproline and 3-hydroxyproline) (10,11). The reaction rate of proline with H_2O_2 is too slow to effectively diminish cellular ROS by a direct chemical mechanism (10,11). However, the pyrrolidine ring of proline has a low ionization potential and effectively quenches $^1O_2$ most likely through a charge transfer mechanism in which molecular oxygen returns to the ground triplet state ($^3O_2$) (12-14). Alia and coworkers used irradiation of various photosensitizers to produce $^1O_2$ and showed that 20 mM proline completely inhibits $^1O_2$ formation (15). However, recent evidence suggests that proline cannot quench $^1O_2$ in aqueous buffer causing the potential scavenging role of proline against $^1O_2$ to be reconsidered (16). As an osmolyte, proline acts as a chaperone and stabilizes proteins, including antioxidant enzymes. Proline (1 molar concentration) *in vitro* protected nitrate reductase under osmotic, metal, and H_2O_2 stress (17). However, relative to other osmolytes, proline is categorized as a weak stabilizer of protein folding and ranks lower in its ability to induce protein folding (18,19). In addition, the concentration of proline used for osmoprotectant experiments *in*

vitro is > 1 M which is significantly higher than intracellular proline concentrations found under stress conditions (100-400 mM). Therefore, the role of proline as a chaperone in protecting antioxidant enzymes at physiological condition remains to be determined.

2.2 PROLINE METABOLIC PATHWAYS

Proline metabolism involves the interconversion of proline and glutamate. The oxidation of proline is coordinated by the flavin-adenine dinucleotide (FAD) dependent proline dehydrogenase (PRODH; EC 1.5.99.8) and nicotinamide adenine dinucleotide (NAD^+) dependent Δ^1-pyrroline-5-carboxylate dehydrogenase (P5CDH; EC 1.5.1.2) (20) (Figure 2.1). In Gram-negative bacteria, these two enzymes are fused into a single protein known as proline utilization A (PutA) (21). PRODH catalyzes the first and the rate-determining step by coupling the two-electron oxidation of proline to the reduction of membrane-associated ubiquinone (22). Δ^1-pyrroline-5-carboxylate (P5C), the product of PRODH, spontaneously converts into glutamate-γ-semialdehyde
(GSA), which is oxidized to glutamate by P5CDH using NAD^+ as an electron acceptor (23). In eukaryotes, PRODH and P5CDH localize in the mitochondrial matrix with PRODH associating with the inner mitochondrial membrane. In prokaryotes, P5CDH is in the cytosol while PRODH binds peripherally to the cytoplasmic membrane (24).

The biosynthesis of proline from glutamate requires the bifunctional

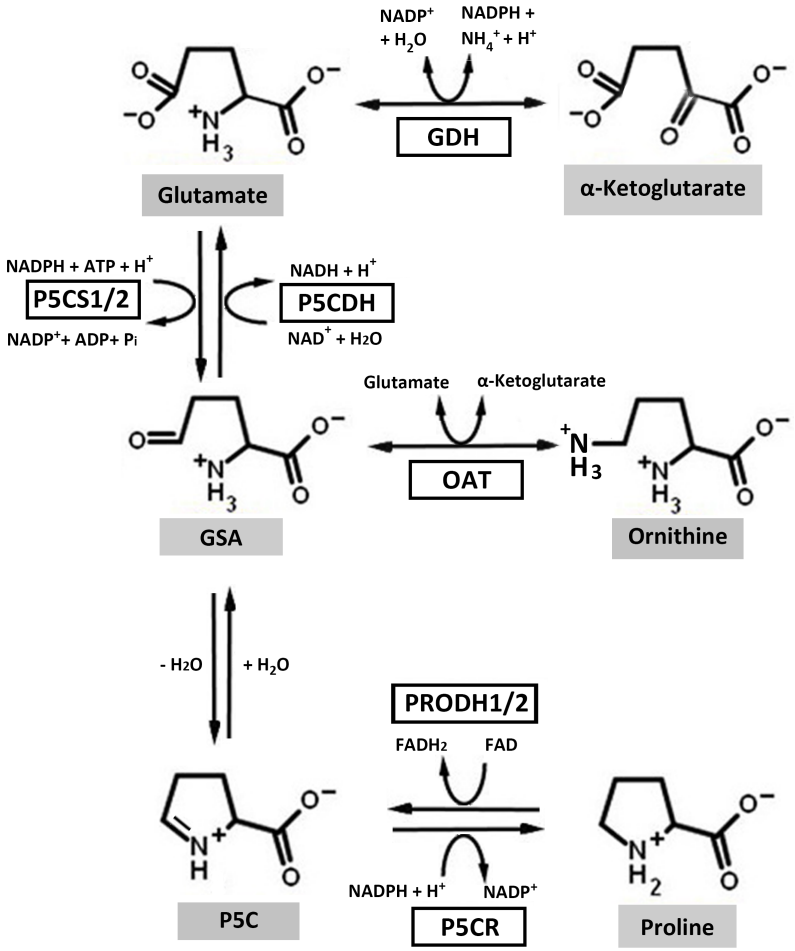

Figure 2.1 Proline metabolic pathways. In the biosynthesis pathway, ornithine and glutamate can be converted to glutamate-γ-semialdehyde (GSA) by ornithine-δ-aminotransferase (OAT) and $^{1}\Delta$-pyrroline-5-carboxylate (P5C) synthetase (P5CS), respectively. GSA then spontaneously cyclizes to P5C, which is the substrate for P5C reductase (P5CR). P5CR catalyzes the last step in proline synthesis. In the catabolic pathway, proline dehydrogenase (PRODH) and P5C dehydrogenase (P5CDH) catalyze the oxidation of proline to glutamate. Electrons from reduced flavin ($FADH_2$) are transferred to the respiratory electron transport chain to regenerated oxidized flavin (FAD). Glutamate dehydrogenase (GDH) interconverts glutamate and α-ketoglutarate.

enzyme P5C synthetase (P5CS), which contains both activities of γ-glutamyl kinase (GK, EC 2.7.2.11) and γ-glutamyl phosphate reductase (GPR, EC 1.2.1.41) (Figure 2.1). In bacteria and yeast, GK and GPR are monofunctional enzymes (23). P5CS, the rate-limiting enzyme of proline biosynthesis, requires ATP and NAD(P)H for the reduction of glutamate to GSA, which then spontaneously cyclizes to P5C (25). P5C is then reduced to proline by P5C reductase (P5CR, EC 1.5.1.2) using NAD(P)H as an electron donor (26). Proline derived from ornithine requires ornithine-δ-aminotransferase (OAT, EC 2.6.1.13), which converts ornithine into GSA (27). In yeast, OAT is cytosolic (28), whereas in plants and humans, OAT is localized in the mitochondria (29-31).

2.3 MECHANISMS OF ROS FORMATION FROM PROLINE CATABOLISM

PRODH dependent ROS signaling has been implicated in cell proliferation, cell survival, apoptosis and autophagy (1,32-34). The amount of ROS generated depends on the availability of proline and the level of PRODH activity in the mitochondrion. Low ROS generation (i.e., constitutive PRODH expression) was predicted to stimulate protective effects such as activation of Nrf2 and life span extension as found in *C. elegans* (34). High ROS generation due to elevated PRODH expression would lead to apoptosis and cell death, contributing to physiological processes such as the hypersensitive response (HR) in plants. Several ROS sources have been linked to proline catabolism-mediated ROS formation, including PRODH itself, electron transport chain

(ETC), proline-P5C cycle, accumulated P5C and ROS-generating pathways regulated by proline catabolism.

PRODH is also known as proline oxidase, indicating its potential ability to use molecular oxygen as an electron acceptor, a common property of many flavoenzymes. This implies that PRODH itself may serve as a source of proline oxidation-dependent ROS formation. The reactivity of PRODH with molecular oxygen during catalytic turnover of proline leads to the formation of $O_2^{\bullet -}$, which is converted into H_2O_2 by SOD (Figure 2.2). Oxygen reactivity and H_2O_2 formation were reported in several purified PRODH enzymes. By measuring the rate of H_2O_2 formation in air-saturated buffer, PutA from *Escherichia coli* was shown to have only minimal turnover with proline and molecular oxygen (< 0.3 min^{-1}) whereas PutAs from *Helicobacter pylori* and *H. hepaticus* exhibited > 200-fold higher activity with oxygen (35). PRODH from *Thermus thermophilus* also exhibited higher proline:O_2 reactivity than *E. coli* PutA with a k_{cat} of 12.7 min^{-1} (36). Crystallographic studies of various PRODH enzymes have identified an α-helix near the FAD that appears to shield the cofactor from solvent oxygen. The α-helix may help direct electrons from the reduced flavin to ubiquinone or allow exposure of the reduced FAD to solvent oxygen thereby allowing for the generation of superoxide anion. Whether mammalian and plant enzymes exhibit significant proline:O_2 reactivity is not yet clear, but if they behave similarly to the yeast PRODH enzyme (Put1p), then it is likely that the human and plant enzymes have only minimal reactivity with molecular oxygen as Put1p was shown to have a turnover number of only 0.54 min^{-1} with proline and molecular

oxygen (35-37).

Instead of being directly formed in the FAD active site, a second source of proline-mediated ROS is the downstream electron transfer events of proline oxidation in the ETC of prokaryotes or the mitochondrion of eukaryotes. Every catalytic turnover of PRODH and P5CDH generates $FADH_2$ and NADH, respectively, which provide electrons for the ETC, leading ultimately to reduction of oxygen into water by cytochrome C oxidase. The ETC chain, however, is not 100% efficient with estimates of 1-2% $O_2^{\bullet-}$ and H_2O_2 being generated per water molecule formed. The formation of ROS by proline via the ETC is supported by the fact that in isolated *Drosophila* mitochondria using proline as a substrate, ROS production can be inhibited by malate, an inhibitor of mitochondrial Complex II (succinate dehydrogenase) (38). Similarly, isolated mitochondria of a human breast cancer cell line (ZR75-30) was shown to generate H_2O_2 during incubation with proline (38).

Even though proline is likely to drive ROS formation by the ETC, little is known about which sites in the ETC actually generate ROS during proline oxidation. The logical sites of ROS formation are those to which proline oxidation directly feeds reducing equivalents. PRODH has been shown in bacteria and yeast to utilize Coenzyme Q as an electron acceptor, thus PRODH directly passes electrons into the ubiquinone pool. The NADH generated by the P5CDH reaction is a second source of electrons for the ubiquinone pool. In prokaryotes, such as *E. coli*, NADH is oxidized by NADH dehydrogenase and reduced ubiquinone is transferred to cytochrome bd (quinol:O_2 oxidoreductase) and

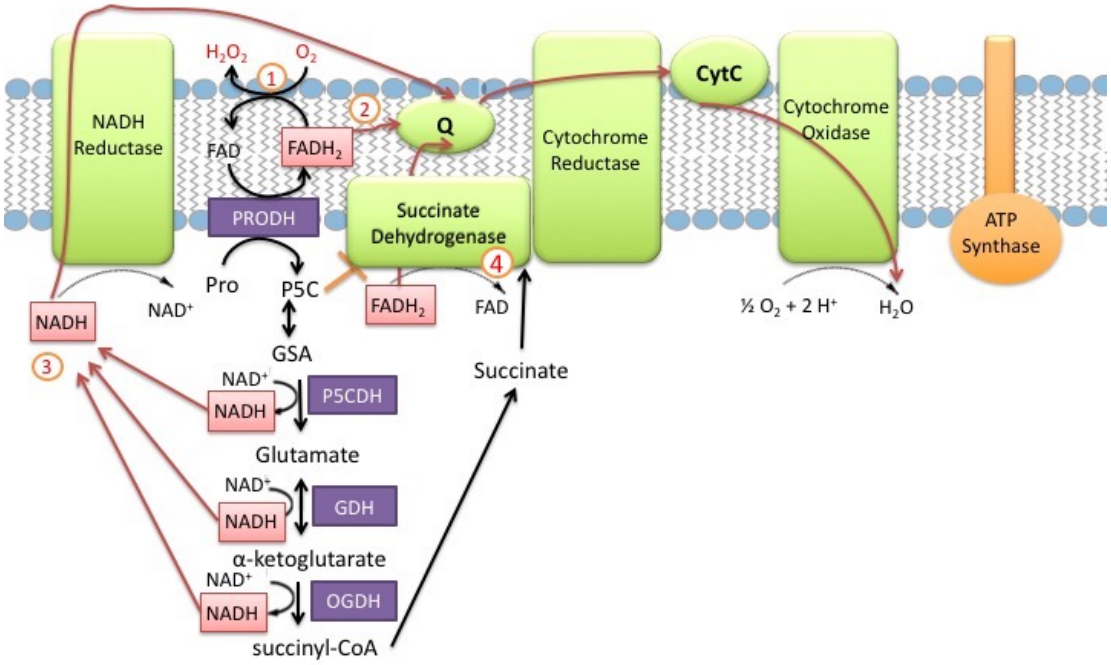

Figure 2.2 Potential sites for electron flow of proline oxidation into the ETC and ROS production. (1) PRODH may directly react with molecular oxygen to generate superoxide ($O_2^{\bullet-}$) and hydrogen peroxide (H_2O_2). **(2)** PRODH feeds electrons directly into the ubiquinone pool. **(3)** NADH generated by P5CDH is a substrate for complex I and another potential source of electrons for the ubiquinone pool. **(4)** Conversion of glutamate into α-ketoglutarate and eventually to succinate provides another route for electrons to enter the ubiquinone pool via succinate dehydrogenase.

cytochrome bo_3 (quinol oxidase) complexes (39). In eukaryotes, complex I (NADH dehydrogenase complex) transfers electrons from NADH to ubiquinone with reduced ubiquinone being oxidized by Complex III (ubiquinol-cytochrome c reductase complex) (39). A third possible route for reduction of ubiquinone during proline oxidation is succinate dehydrogenase. Glutamate produced by proline oxidation can be deaminated to α-ketoglutarate by glutamate dehydrogenase (GDH, EC 1.4.1.2). Subsequently, α-ketoglutarate dehydrogenase (OGDH, EC 1.2.4.2) and succinyl-CoA synthetase (EC 6.2.1.4) convert α-ketoglutarate into succinate which is oxidized to fumarate by succinate dehydrogenase (SDH, EC 1.3.5.1) or complex II. Therefore, proline oxidation can pass electrons into the ubiquinone pool of the ETC via PRODH, NADH dehydrogenase complex, and SDH (Figure 2.2). A few studies have been reported to explore the mitochondrial sites of proline induced ROS production. Isolated mouse liver mitochondria were shown to generate ROS using proline as substrate (9). The sites of proline-dependent ROS production in mouse mitochondria were suggested to be Complex III, because inhibition of complex III with myxothiazol or antimycin A resulted in a dramatic increase of ROS (9). On the other hand, with proline as substrate, isolated mitochondria from a human breast cancer cell line (ZR75-30) consumes O_2 and produces H_2O_2 presumably at complex I and α-ketoglutarate dehydrogenase (38). As mentioned above, isolated *Drosophila* mitochondria oxidize proline and generate ROS at complex I and complex II (38). Thus far, no information on ETC sites that contribute to proline-mediated ROS formation in prokaryotes has been reported. The

preliminary study of sites associated with proline oxidation-mediated ROS in *E.coli* will be discussed in Chapter 3. It is still unclear whether different organisms share the same sites of proline-dependent ROS formation or if each organism has unique sites of proline oxidation-induced ROS.

An important component of proline-induced ROS formation is the potential of a proline-P5C cycle that further feeds reducing equivalents into the ETC (Figure 2.3). The proline-P5C cycle has been mostly studied in mammalian cells and plants with NADPH as the fuel source for the cycle. When plants are exposed to certain biotic or abiotic stress, such as pathogen infection or exogenous high proline application, PRODH activity significantly increases (20). When PRODH activity exceeds the capacity of P5CDH, P5C accumulates and is reduced back to proline by P5CR and NAPDH (31). This is so called proline-P5C cycle. Significant cycling of proline-P5C is thought to enhance ROS production by increased electron flow to the ubiquinone pool of the ETC (6). Indeed, down-regulation of P5CDH in Arabidopsis by 24-nt SRO5-P5CDH natural silencing RNAs during salt treatment led to an increase in ROS production, consistent with the proline-P5C cycle enhancing ROS formation (40,41). In flax (*Linum usitatissimum*) it was also found that reduced expression of the flax homologue of *Arabidopsis* P5CDH, FIS1, resulted in increased sensitivity to exogenous proline and higher levels of H_2O_2 (42,43). Besides plant, evidence for the proline-P5C cycle has also been found in mammals (44). The proline-P5C cycle in mammalian cell lines is closely linked to maintenance of proper $NADP^+$/NADPH levels in the cytosol, enhancing the oxidative pentose phosphate pathway in

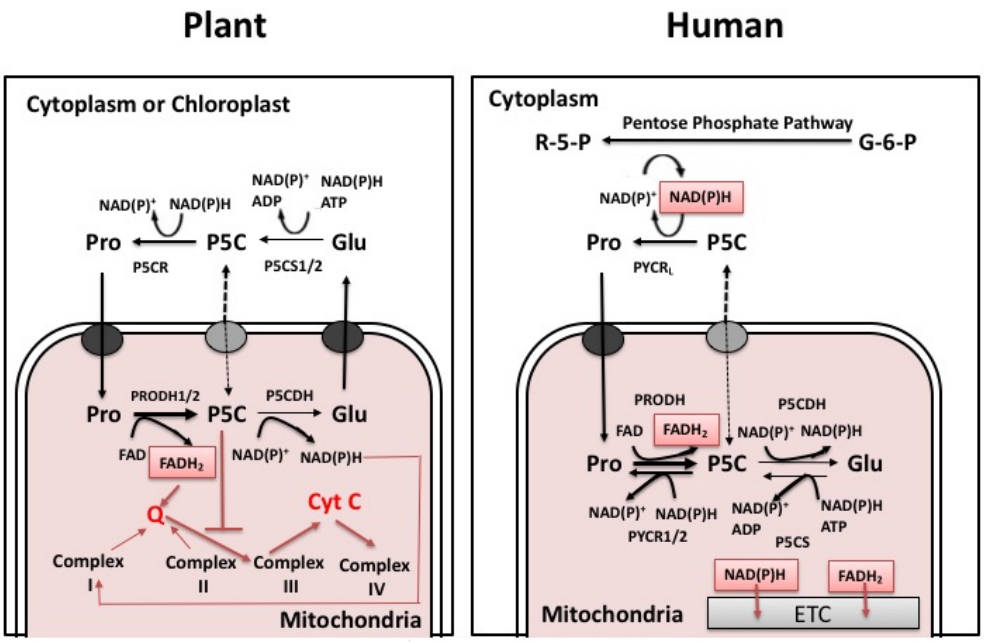

Figure 2.3 Proline-P5C cycle in plant and human. Left Panel: In plant, proline oxidation enzymes localize in mitochondria while proline biosynthesis enzymes localize in cytoplasm and chloroplast. When PRODH activity exceeds the capacity of P5CDH, accumulated P5C in the mitochondria is transported to the cytoplasm by unknown transporter and reduced back to proline by P5CR. Accelerated proline-P5C cycle increases the electron flow from PRODH to the ubiquinone pool of ETC, thereby inducing the production of ROS. Accumulated P5C in the mitochondria also inhibits the activity of Complex II, potentially resulting in increased ROS production. **Right Panel:** There are 3 isoforms of human PYCR (P5CR): $PYCR_L$ localizes in cytoplasm and PYCR1/2 localize in mitochondria. Human P5CS is also found in mitochondria. With excessive activity of PRODH, accumulated P5C can be converted back to proline by PYCR1/2 or $PYCR_L$. In cytoplasm, $NAD(P)^+$ generated by $PYCR_L$ induces the pentose phosphate pathway, where NAD(P)H is produced. NAD(P) H is then transported into mitochondria and enters ETC, where ROS is produced. (G-6-P: glucose-6-phosphate; R-5-P: ribose-5-phosphate)

cytoplasm (7). The production $NAPD^+$ by the proline-P5C cycle has been shown to up-regulate the oxidative pentose phosphate pathway, which produces NADPH. Because NADPH is vital for maintenance of key redox molecules such as thioredoxin and glutathione via thioredoxin reductase and glutathione reductase, respectively, NADPH has a critical supportive role in many cellular processes including cell survival and proliferation. The direct link of the proline-P5C cycle to NADPH balance can therefore potentially have a profound impact on redox balance and cellular processes.

Another mechanism by which proline metabolism has been proposed to affect ROS production is the accumulation of P5C/GSA (46). In *Saccharomyces cerevisiae* knocking out the *PUT2* gene encoding P5CDH (Put2p) resulted in higher levels of P5C, enhanced ROS production and inhibition of growth. In a *put2* mutant of *Cryptococcus neoformans,* proline supplementation led to increased mitochondrial $O_2^{\bullet-}$ and cell death (48). In a human bladder tumor cell line (ECV-304), application of P5C initiated an oxidative burst followed by cell apoptosis (47). The mechanism by which P5C induces ROS formation is not clear and remains to be studied. In *S. cerevisiae*, however, evidence was reported for P5C inhibiting mitochondrial respiration in a dose-dependent manner, presumably at complex II (49) (Figure 2.3 left panel). Although it is unknown whether P5C-induced inhibition of complex II will generate ROS, loss of function of complex II will lead to increased ROS formation in mammalian cells (50).

In summary, although PRODH as a flavoenzyme may react with

molecular oxygen during turnover to generate H_2O_2, the most likely mechanism by which PRODH induces ROS production is by transferring electrons to the ubiquinone pool of the ETC. Additionally, PRODH expression that is disproportionate to P5CDH levels may propel a proline-P5C cycle or result in accumulation of P5C, both of which will lead to increased ROS formation. Proline catabolism may also induce ROS-generating signaling pathway, such as NADPH oxidases through Ca^{2+} as secondary signaling molecule. Further investigations into these aforementioned mechanisms are needed to better understand the linkages between proline catabolism and the associated increases in ROS.

2.4 SIGNALING PATHWAYS LINKED TO PROLINE CATABOLISM IN PLANTS

Proline catabolism has been shown to be down-regulated in response to exogenous ROS treatment presumably as a mechanism to accumulate proline. For instance, deleterious concentration of exogenous H_2O_2 treatment of maize seedlings and *Nitraria tangutorum* callus significantly decreased PRODH activity, which would be expected to facilitate proline accumulation and resistance to further oxidative stress (53).

In contrast to the response found with exogenous ROS, proline catabolism is manipulated under other stress conditions to generate endogenous ROS via mechanisms described in the previous section, can have an important signaling role in pathogen defense and stress resistance in plants. It was established that proline oxidation mediated ROS production is vital for the

Pseudomonas syringae pathogen induced HR in plants (55). HR is a localized reaction stimulated by ROS against pathogens to induce programed cell death of infected tissue (55). Upon infection by *P. syringae*, both expression and activity of PRODH1 in *Arabidopsis* are up-regulated through a salicylic acid-sensitive pathway at the initial stage of HR, prior to the oxidative burst (56). Between the two isoforms of PRODH found in plants, PRODH1 is considered to be the main isoform responsible for proline oxidative flux (57). Plants with silenced PRODH1 expression had significantly lower ROS levels and exhibited increased susceptibility to infection relative to wild-type plants (56). Therefore, PRODH1 is required for ROS production and promotes HR during infection. In addition, at the oxidative stage of HR when oxidative stress occurs, the expression of PRODH and P5CDH was uncoupled with reciprocal upregulation of PRODH and downregulation of P5CDH. In HR, P5C levels remained constant thereby enabling the futile proline-P5C cycle and promoting ROS generation (31).

Proline oxidation induced ROS has been linked to programed cell death in plant (52). In cells with excessive PRODH activity, or limited P5CDH activity, the hyperactivity of the proline-P5C cycle is anticipated to increase ROS generation. Accordingly, *Arabidopsis* wild-type and *p5cdh*-mutant plants treated with exogenous proline exhibited HR-like lesions, a marker of programed cell death (42,43). Besides, the proline-P5C cycle, NADPH oxidase was another source of ROS induced by exogenous proline treatment (58). Proline-treated plant cells undergo cell death with features consistent with the production of ROS and DNA fragmentation (51). As discussed above, in a model proposed by

Chen et al. (52), exogenous proline can induce calcium-dependent generation of ROS through NADPH oxidase. It subsequently induces the production of salicylic acid probably via NDR1-mediated signaling resulting in a HR-like lesion (52).

Another cellular process linked to proline catabolism is senescence which is an age-dependent, development regulated programed cell death phenomenon (59). *PRODH2* was shown to have stronger expression in leaf vascular tissues at senescence in *Arabidopsis thaliana* and *Brassica napus* (rapeseed) (60,61). *P5CDH* expression was also found to increase in older leaves of *Arabidopsis* as observed using a *AtP5CDH* promoter-β-glucuronidase fusion construct (62). One possibility of upregulated proline degradation during leaf senescence is to facilitate nitrogen recycling in the phloem from old leaves to sink organs which would be consistent with the stronger expression of *PRODH2* in vascular tissues (60,61) and induced cytosolic *GS1* and *GDH* during leaf senescence (63). On the other hand, PRODH1 may be involved in plant hormone induced senescence, although *PRODH1* expression in attached leaves did not change during senescence (61). The mechanism by which plant hormones such as methyl jasmonic-acid (JA) (64) and ABA (65) induced senescence, involves phosphatidylinositol-3,4,5-triphosphate dependent kinase (PI3K) signaling and H_2O_2 generation. Inhibiting PI3K activity by wortmannin or LY294002 aborts H_2O_2 production and delays JA induced-senescence in rice leaves (66). Phosphatidylinositol-3-phophate (PI3P), the product of PI3K, has also been shown to be necessary for ABA-induced H_2O_2 production and senescence (64). Thus, PI3K and PI3P promote plant hormone (ABA and methyl

JA)-induced senescence by facilitating H_2O_2 production. Inhibition of PI3K by LY294002 under salt stress resulted in lower *P5CS1* transcripts, higher *PRODH1* expression and decreased endogenous proline content in *Arabidopsis* (64). Consistent with these results, *PRODH1* expression was higher in a *pi3k*-hemizygous *Arabidopsis* mutant, although there was no change in *P5CS1* transcription level (66). Thus, PI3K appears to negatively regulate proline catabolism by repressing PRODH1 expression. Whether proline metabolism has an important role in PI3K signaling and plant hormone induced-senescence in leaves remains to be explored. Repression of *PRODH1* by PI3K could potentially decrease oxidative stress resistance as discussed above due to loss of proline-mediated ROS signaling and a lower ability to adapt to oxidative stress.

2.5 SIGNALING PATHWAYS LINKED TO PROLINE OXIDATION IN ANIMALS

2.5.1 Proline oxidation mediated ROS and cell apoptosis

The function of PRODH as a tumor suppressor has been established by different studies using cancer cell lines (67) and xenograft tumor models in immunodeficient mice (68) and, by analysis of tissue samples from cancer patients (69). As a tumor suppressor, PRODH induces cell apoptosis when its expression is upregulated (68).

The tumor suppressor protein p53 and the peroxisome proliferator-activated receptor γ (PPARγ) are involved in up-regulating *PRODH1* gene expression (Figure 2.4). *Homo sapiens PRODH1*, encoding human proline dehydrogenase, was first identified as a p53 target gene in 1997 and the role of

p53 in activating *PRODH1* expression in cancer cells is well documented (67). Recent analysis of the *PRODH1* promoter identified p53 responsive binding elements further establishing *PRODH1* as a p53 regulated gene. PPARγ, a ligand-dependent transcription factor that controls lipid metabolism and cell apoptosis, has also been shown to induce *PRODH1* expression (70). PPARγ ligand troglitazone was found to activate the *PRODH1* promoter in colon cancer HCT116 cells, by enhancing the binding of PPARγ to PPAR-responsive element in the *PRODH1* promoter (70). However, blocking PPARγ activation with an antagonist only partially decreased *PRODH1* expression, indicating the existence of both PPARγ dependent and independent mechanisms of PRODH1 induction (70). Because troglitazone also induces p53 protein expression in HCT116 cells, p53 may be responsible for the PPARγ-independent PRODH activation (70). PRODH1 was also found to be regulated by microRNA. Ectopic expression of miR-23b* in normal renal endothelial cells decreased PRODH1 protein expression, PRODH-induced ROS generation and cell apoptosis (71). miR-23b* was shown to post-transcriptionally downregulate PRODH1 by binding to the 3'-UTR of the *PRODH1* gene (71). The level of miR-23b* is negatively controlled by the transcription factor c-MYC (MYC). Thus, loss of c-MYC results in higher levels of miR-23b* thereby lower PRODH1 expression, a mechanism that could potentially decrease PRODH1-dependent apoptosis and promote cancer progression (69).

The mechanism by which upregulation of PRODH1 induces apoptosis is thought to rely on increased mitochondrial ROS production. Upregulation of

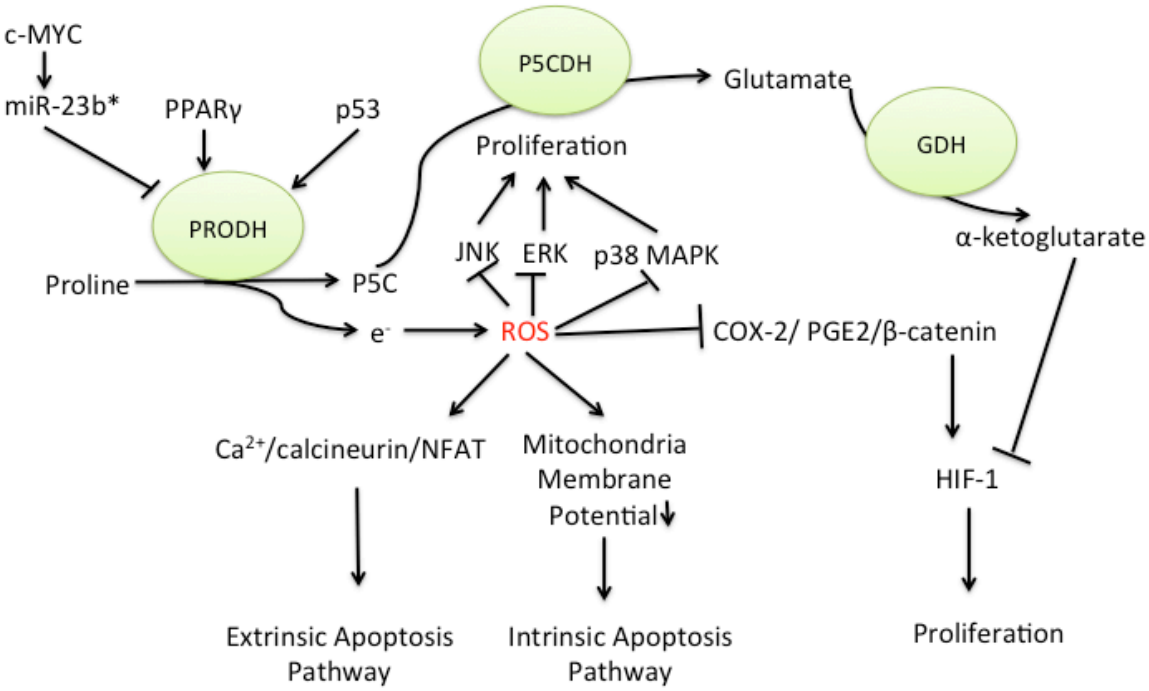

Figure 2.4 Proline oxidation mediated ROS and cell apoptosis. The expression of PRODH1 is negatively regulated by c-MYC via miR-23b* and positively regulated by PPARγ and p53. During proline oxidation, ROS is generated as a byproduct. ROS can induce apoptosis by intrinsic and extrinsic apoptosis pathway and down-regulate proliferation by inhibiting MAPKs and Cox-2/PGE2/β-catenin pathway. α-ketoglutarate derived from proline oxidation can also inhibit HIF-1 pathway by promoting degradation of hydroxylated HIF-1.

PRODH by p53 or PPARγ leads to increased mitochondrial $O_2^{\bullet-}$ production, which can be inhibited by antioxidant NAC or co-expression of mitochondrial SOD (MnSOD) (67). Proline catabolism induces cell apoptosis by intrinsic (mitochondrial) and extrinsic (death receptor) pathways (72) (Figure 2.4). In the intrinsic pathway which involves non-receptor mediated intracellular signaling, proline oxidation-induced $O_2^{\bullet-}$ alters mitochondrial membrane potential allowing for the release of cytochrome c into the cytosol, followed by the activation of caspase 9 and the caspase cascade (72). In the extrinsic (death receptor) pathway, proline-derived ROS activates apoptotic pathways through the calcineurin-dependent expression of nuclear factor of activated T cells (NFAT) (73). NFAT is a potent activator of the tumor necrosis factor-related apoptosis inducing ligand (TRAIL) promoter (73). Overexpression of PRODH induces the expression of TRAIL and death receptor 5 through NFAT, resulting in the cleavage of caspase-8 and thus death by extrinsic apoptosis (74).

ROS produced during proline oxidation has also been shown to affect MAPK signaling by decreasing the phosphorylation of all three subtypes of MAPK, namely, ERK, JNK and p38 (74) (Figure 2.4). Constitutive expression of MEK markedly reduced PRODH-mediated cell apoptosis (74). Therefore, proline-dependent ROS down-regulates MPAK pathway, which promotes cell apoptosis.

PRODH1 also inhibits signaling pathways associated with tumor cell proliferation (16). PRODH inhibits cyclooxygenase-2 (COX-2)/prostaglandin E2 (PGE2) signaling by down-regulating the expression of COX-2 and suppresses the production of PGE2. It was found that PRODH also reduces the

phosphorylation of GSK-3β and increases the phosphorylation of β-catenin (16) (Figure 2.4). Expression of MnSOD reversed the effect of PRODH on the aforementioned phenomenon and abolished cell apoptosis (16), indicating a role for proline oxidation induced ROS in driving the COX2-PGE2-β-catenin pathway. PGE2, produced by COX2, stimulates the direct association of the G-protein α subunit ($G_{\alpha s}$) with Axin through the EP2 receptor (75). In concert with the coupling of APC (adenomatous polyposis coli protein) to the EP2-associated $G_{\alpha s}$ subunit and Axin, was the release of unphosphorylated β-catenin from the axin-glycogen synthase kinase 3β (GSK3β) complex (75). Phosphorylated β-catenin by GSK3β results in its subsequent degradation via the 26S proteasome (75). Unphosphorylated β-catenin accumulated in the cytoplasm will enter into the nucleus and activate genes that stimulate cell survival, proliferation, and angiogenesis, including hypoxia-inducible factor-1 (HIF-1) (75). Thus, PRODH inhibits COX2-PGE2- β-catenin pathway and negatively impacts cancer cell survival. Interestingly, PRODH also down regulates HIF-1 independent of COX2-PGE2- β-catenin pathway (9). By using glutamate, the final product of proline oxidation, α-ketoglutarate can be generated by GDH. α-ketoglutarate is a substrate of prolyl hydroxylase (PHD), which catalyzes posttranslational hydroxylation of specific proline and asparagine residues in the α-subunit of HIF-1 (76). Hydroxylated HIF-1 is then degraded by ubiquitin and proteasomal degradation systems (76). Dimethyloxalylglycine, a α-ketoglutarate analogue and inhibitor of PHD, blocked PRODH dependent degradation of HIF-1 (9). Interestingly, the effects of PRODH on HIF-1 signaling could not be reversed by

MnSOD (9), suggesting ROS is not the mediator of HIF inhibition by PRODH.

2.5.2 Proline oxidation mediated ROS and cell survival under starvation and hypoxia

In environments with limited nutrients or oxygen supply, proline oxidation can provide benefits to the cell by promoting autophagy, ATP production, or mitochondrial oxidative metabolism of available substrates.

The AMP-activated protein kinase (AMPK) is the energy sensor in eukaryotes, activated by rising cellular AMP level (82). Under nutrient energy stress, AMPK is activated and mTOR is downregulated. In RKO colon cancer cells, inhibition of mTOR activity by rapamycin stimulated degradation of proline and increased PRODH catalytic activity (16) (Figure 2.4). On the other hand, activation of AMPK, by 5-aminoimidazole-4-carboxamide ribonucleoside (AICAR), also markedly upregulated PRODH and increased ATP levels. Under these conditions, PRODH was responsible, at least in part, for the maintenance of ATP levels (16). Thus, AMPK and mTOR pathways coordinately up-regulate PRODH under nutrient starvation to enable cells to use proline as an alternative energy source. Increases in PRODH are also associated with upregulation of the pentose phosphate pathway in colorectal cancer cells grown with low glucose, consistent with the proline-P5C cycle helping support thepentose phosphate pathway flux (83).

Autophagy, literally "self-eating", is a mechanism for survival and is mainly regulated through the mTOR pathway under nutrient depletion or metabolic stress (84). The link between autophagy and hypoxia is connected by proline oxidation in cancer cells. Under hypoxic conditions, proline metabolism was induced, leading to mitochondria ROS production and autophagic signaling, which could be abolished by inhibiting PRODH or treating cells with the antioxidant N-acetyl cysteine (NAC)(84). The mechanism by which PRODH contributes to the survival of cancer cells under hypoxia appears to involve ROS as *prodh* knockdown under hypoxia diminished ROS production but had no effect on ATP levels (84). Because AMPK both positively regulated mRNA and protein expression of PRODH, it was considered to be responsible for the hypoxia induced PRODH expression. Accordingly, compound C ((6-[4-(2-piperidin-1-yl-ethoxy)- phenyl)]3-pyridin-4-yl-pyrazolo[1,5-a] pyrimidine), a specific inhibitor of AMPK activation, completely blocked hypoxia-induced increase of PRODH expression (85). Also, hypoxia inducible factor-1 (HIF-1) which mediates the transcriptional response to hypoxia, was determined not to be responsible for hypoxia induced PRODH (9). Therefore, AMPK induces the expression of PRODH under hypoxia, leading to increased mitochondria ROS and pro-survival autophagy.

The adipose tissues in aged animals are poorly vascularized, therefore adipocytes suffer from nutrient starvation, which results in increased activity of PRODH and mitochondrial ROS production (9). The ROS produced by proline oxidation promotes the upregulation and the nuclear translocation of fork head

transcription factor class O1 (FoxO1), a transcriptional factor with the capacity to sense nutrient availability and tune several adaptive responses (9). Nuclear localized FoxO1 binds to the promoter of adipose triglyceride lipase (ATGL), which promotes mitochondrial oxidative metabolism and triglyceride utilization that supplies energy to starved adipocytes and prevents cell death, as well as adipose tissue inflammation (9).

2.5.3 PRODH protects cells from oxidative stress

Exogenous addition of proline has been shown to protect mammalian cells against oxidative stress (8,77) (Figure 2.5). Treatment with 5 mM proline decreased the H_2O_2 induced cell apoptosis in HEK293 cells by more than 2-fold (77). The activity of PRODH is required for proline-dependent oxidative stress protection, as either knockdown of *prodh* expression or inhibition of PRODH activity by L-tetrahydro-2-furoic acid (L-THFA), a competitive inhibitor of L-proline, abolished the protective role of proline (8). PRODH mediated protection against oxidative stress may involve ATP production and the activation of the Akt survival pathway (8). For the former, treatment of WM35 cells with proline retained ATP and NADPH levels after exposure to H_2O_2. Inhibition of TCA cycle enzymes by H_2O_2 is well established (58). Therefore, proline oxidation may help maintain ATP levels when the TCA cycle is shutdown under H_2O_2 stress. Akt activation and its downstream phosphorylation of the fork head transcription

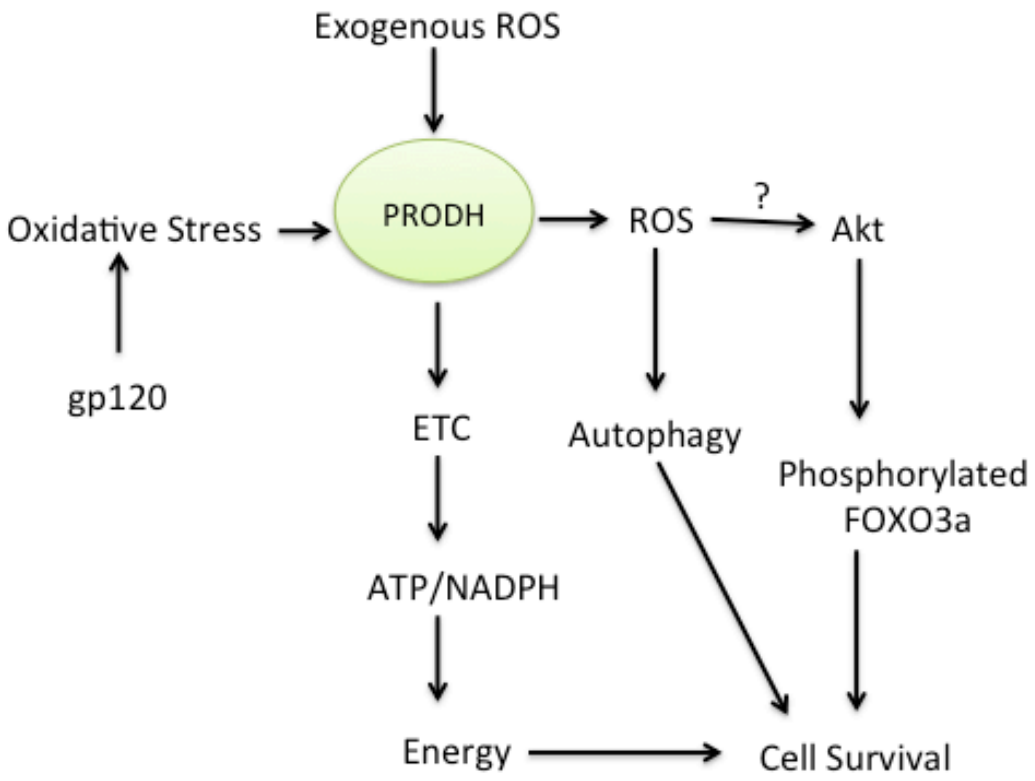

Figure 2.5 PRODH protects cell from oxidative stress. In response to exogenous ROS stress, PRODH can provide ATP/NADPH and activate Akt/FOXO3a pathway to protect cell survival. Under oxidative stress due to cytotoxic compound, such as gp120, ROS produced during proline oxidation induces pro-survival autophagy.

factor class O3a (FOXO3a), were significantly increased in proline treated cells under H_2O_2 stress, whereas knockdown of *prodh* in PC3 cells attenuated phosphorylated levels of Akt and FoxO3a (8). Therefore, PRODH can provide ATP to cells under oxidative stress and activate Akt resulting in increased phospho-FoxO3a which blocks FoxO3a from inducing cell death. The result is increased survival of proline treated cells during oxidative stress. The mechanism for how PRODH activates Akt is not yet known, however, ROS is well known to stimulate Akt signaling (8), suggesting ROS may be the link between PRODH and Akt activation.

In addition to protecting cells against exogenous oxidative stress , PRODH and proline oxidation were recently shown to protect cells from virulent agent or cytotoxic compound induced oxidative stress. HIV-1 glycoprotein 120 (gp120) is an envelope protein that mediates entry of the virus into host cells, including microglia, astrocytes and neurons (78). HIV-1 gp120 is a neurotoxic factor that is associated with HIV-1 associated neurological disorders (88). The neurotoxic effect of HIV-1 gp120 is partially due to its induction of oxidation stress (89). In astrocytes and microglia, HIV-1 gp120 has been shown to induce oxidative stress through the cytochrome P450 and NADPH oxidase, two major ROS production sites in mammalian cells (90). Recently, gp120 treatment has been shown to up-regulate transcription and activity of PRODH in SH-SY5Y (human neuroblastoma) cells (79). Concurrently, gp120 also increased intracellular ROS levels, which mostly depends on proline oxidation, since the inhibition of proline oxidation by dehydroproline attenuated ROS levels (79).

Although gp120 can induce both the apoptosis and autophagy of neurons (78), PRODH-dependent ROS was found to be only associated with autophagy (79). Parallel with increased ROS was the induction of autophagy markers, beclin 1 and LC3-II. The appearance of these autophagic markers was dependent on PRODH with inhibition of PRODH decreasing marker levels and over-expression of PRODH increasing the levels of the markers (79). The gp120 induced PRODH was suggested to be mediated by p53, since gp120 induces p53 via binding to CXCR4, the receptor of gp120 (79). Collectively, by binding to CXCR4, HIV-1 gp120 induces p53, which up-regulates PRODH expression and proline oxidation induced ROS, resulting in ROS-dependent autophagy. PRODH-mediated autophagy prevents HIV-1-induced neuron apoptosis, and may explain the resistance of neurons to HIV-1.

2.5.4 Proline oxidation and lifespan

Evidence for proline oxidative metabolism being linked to aging is mostly from studies of *Caenorhabditis elegans*. In *C. elegans* PRODH and proline catabolism was shown to significantly increase the lifespan of the worm. In a daf-2 mutant containing impaired insulin and IGF1 signaling, knockdown of *prodh* significantly decreased lifespan (34). Complementary to the effect of *prodh* knockdown on lifespan, proline treatment extended the lifespan of wild-type worms expressing PRODH (34). The mechanism of increased lifespan was shown to involve transient ROS signals generated by PRODH via the mitochondria ETC (34). Proline derived ROS is proposed to activate the worm

homologues of p38 MAP kinase (PMK-1) and Nrf2 (SKN-1), which defend against exogenous and endogenous cellular stress, leading to increased expression of antioxidant enzymes and extended lifespan (34). Although transient low levels of ROS benefit longevity, high ROS levels have also been shown to decrease lifespan. In *C. elegans*, knockdown of *alh-6* (*p5cdh*) by RNAi resulted in the activation of SKN-1, the worm ortholog of the mammalian Nrf2 (34). With an activated SKN-1, *alh-6* mutant had a 40% reduction in lifespan when fed on standard laboratory *E. coli* B strains OP50 and BL21, whereas, overexpression of *alh-6* extended life span, suggesting *alh-6* is a longevity gene (47). Interestingly, the effect of P5CDH on the life span of *C. elegans* is diet-dependent because the *alh-6* mutant and *alh-6* overexpressed worms had normal lifespans when fed on *E. coli* K-12 strains HT115 and HMS174 (47). Mechanistically, the expression of PRODH was induced by *E. coli* B strains but not *E. coli* K-12 strains (80). With impaired P5CDH and induced PRODH, the shorter lifespan may be due to accumulated P5C or an overactive proline-P5C cycle that results in toxic levels of ROS. In the *alh-6* mutant fed on *E. coli* OP50, ROS accumulation was confirmed and treatment of the worms with the antioxidant NAC reversed the shortened lifespan without affecting SKN-1 activation (80). Therefore, the continuous production of ROS due to dysregulated PRODH/P5CDH expression (i.e., high PRODH and low P5CDH) affects the longevity of *C. elegans* via a SKN-1 independent pathway. Instead, the neuromedin U receptor-1 (NMUR-1), which regulates food-associated activities in invertebrates, was responsible for the decreased lifespan found in *alh-6*

mutant as *nmur-1/alh-6* double mutants lived a normal lifespan (80). To summarize the experiments in C. elegans, low amounts of ROS produced during proline oxidation benefit longevity by activating PMK-1 and SKN-1 pathways whereas high levels of ROS generated by down-regulation of P5CDH and increased proline-P5C cycling or accumulated P5C, lead to shorten lifespan via NUMR-1.

2.6 SUMMARY

The function of the proline metabolic pathway in the regulation of redox homeostasis and cell survival has been known for 30 years (7). Consistent with this hypothesis, many studies have shown that proline oxidation induces ROS generation, which propels cellular signaling pathways that influence cell reprogramming, cell death and cell survival, and therefore facilitate proline-induced stress resistance, development and aging (8,34,81,84).

There are four major sources of ROS generated by proline oxidation: 1. PRODH with solvent exposed active site can directly reduce O_2 during turnover with proline and generate H_2O_2 (36); 2. The $FADH_2$ and NADH generated by proline oxidation ultimately feed electrons into the ETC where $O_2^{\bullet-}$ and H_2O_2 can form in reactions O_2 (38); 3. Enhanced proline-P5C cycling due to imbalanced activities of PRODH and P5CDH, can fuel additional reducing equivalents to the ETC where ROS is generated (31); 4. PRODH induces ROS-generating signaling pathways involving NADPH oxidases (52).

Although proline metabolism may regulate cellular signaling pathways in a ROS-independent manner, such as using α-ketoglutarate derived from proline oxidation to regulate the level of HIF-1 (9), in most cases, the effect of proline metabolism on signaling pathway depends on ROS generated from proline oxidation (12, 34, 29). Depending on the level of ROS ($O_2^{\bullet-}$ and H_2O_2) produced by proline oxidation, the effect of proline metabolism can be beneficial or detrimental. For instance, modest amounts of ROS produced during proline metabolism in mammalian cell lines are necessary to proline-mediated adaption to oxidative stress (12,29), cytotoxic compounds (79), nutrient starvation and hypoxia (84). Modest ROS levels are also beneficial for worm longevity (34). On the other hand, excess ROS produced because of imbalanced PRODH and P5CDH results in programed cell death (64), including hypersensitive response (55), cell apoptosis (47,72-74,85-88), senescence and shortened lifespan (80).

In summary, the role of proline metabolism as a source of ROS appears to be an important phenomenon in plants and animals. ROS generated by proline oxidation can have pro-death and pro-survival effects depending on the ROS production rate. Understanding the mechanisms by which proline-dependent ROS impacts cellular signaling and survival will improve human health by further defining the roles of proline metabolism in cancer, aging, and in plants, senescence and pathogen defense.

REFERENCES:

1. Phang, J. M., Liu, W., Hancock, C., and Christian, K. J. (2012) The proline regulatory axis and cancer. *Front Oncol* **2**, 60
2. Liu, W., Glunde, K., Bhujwalla, Z. M., Raman, V., Sharma, A., and Phang, J. M. (2012) Proline oxidase promotes tumor cell survival in hypoxic tumor microenvironments. *Cancer Res* **72**, 3677-3686
3. Donald, S. P., Sun, X. Y., Hu, C. A., Yu, J., Mei, J. M., Valle, D., and Phang, J. M. (2001) Proline oxidase, encoded by p53-induced gene-6, catalyzes the generation of proline-dependent reactive oxygen species. *Cancer Res* **61**, 1810-1815
4. Zarse, K., Schmeisser, S., Groth, M., Priebe, S., Beuster, G., Kuhlow, D., Guthke, R., Platzer, M., Kahn, C. R., and Ristow, M. (2012) Impaired insulin/IGF1 signaling extends life span by promoting mitochondrial L-proline catabolism to induce a transient ROS signal. *Cell Metab* **15**, 451-465
5. Pistollato, F., Persano, L., Rampazzo, E., and Basso, G. (2010) L-Proline as a modulator of ectodermal differentiation in ES cells. Focus on "L-Proline induces differentiation of ES cells: a novel role for an amino acid in the regulation of pluripotent cells in culture. *Am J Physiol Cell Physiol* **298**, C979-981
6. Miller, G., Honig, A., Stein, H., Suzuki, N., Mittler, R., and Zilberstein, A. (2009) Unraveling delta1-pyrroline-5-carboxylate-proline cycle in plants by uncoupled expression of proline oxidation enzymes. *The Journal of biological chemistry* **284**, 26482-26492
7. Phang, J. M. (1985) The regulatory functions of proline and pyrroline-5-carboxylic acid. *Curr Top Cell Regul* **25**, 91-132
8. Kumar Natarajan, S., Zhu, W., Liang, X., Zhang, L., Demers, A. J., Zimmerman, M. C., Simpson, M. A., and Becker, D. F. (2012) Proline dehydrogenase is essential for proline protection against hydrogen peroxide-induced cell death. *Free Radic Biol Med*
9. Liu, W., Le, A., Hancock, C., Lane, A. N., Dang, C. V., Fan, T. W., and Phang, J. M. (2012) Reprogramming of proline and glutamine metabolism contributes to the proliferative and metabolic responses regulated by oncogenic transcription factor c-MYC. *Proceedings of the National Academy of Sciences of the United States of America* **109**, 8983-8988
10. Buxton, G. V., Greenstock, C. L., Helman, W. P., and Ross, A. B. (1988) Critical-Review of Rate Constants for Reactions of Hydrated Electrons, Hydrogen-Atoms and Hydroxyl Radicals (.Oh/.O-) in Aqueous-Solution. *J Phys Chem Ref Data* **17**, 513-886
11. Smirnoff, N., and Cumbes, Q. J. (1989) Hydroxyl Radical Scavenging Activity of Compatible Solutes. *Phytochemistry* **28**, 1057-1060
12. Young, R. H., Martin, R. L., Feriozi, D., Brewer, D., and Kayser, R. (1973) On the mechanism of quenching of singlet oxygen by amines-III. Evidence for a charge-transfer-like complex. *Photochemistry and Photobiology* **17**, 233-244

13. Clennan, E. L., Noe, L. J., Wen, T., and Szneler, E. (1989) Solvent effects on the ability of amines to physically quench singlet oxygen as determined by time-resolved infrared emission studies. *J. Org. Chem.* **54**, 3581-3584
14. Matysik, J., Alia, Bhalu, B., and Mohanty, P. (2002) Molecular mechanisms of quenching of reactive oxygen species by proline under stress in plants. *Curr. Sci.* **82**, 525-532
15. Alia, Mohanty, P., and Matysik, J. (2001) Effect of proline on the production of singlet oxygen. *Amino Acids* **21**, 195-200
16. Signorelli, S., Arellano, J. B., Melo, T. B., Borsani, O., and Monza, J. (2013) Proline does not quench singlet oxygen: evidence to reconsider its protective role in plants. *Plant Physiol Biochem* **64**, 80-83
17. Sharma, P., and Dubey, R. S. (2005) Modulation of nitrate reductase activity in rice seedlings under aluminium toxicity and water stress: role of osmolytes as enzyme protectant. *Journal of Plant Physiology* **162**, 854-864
18. Bolen, D. W., and Baskakov, I. V. (2001) The osmophobic effect: natural selection of a thermodynamic force in protein folding. *J Mol Biol* **310**, 955-963
19. Auton, M., and Bolen, D. W. (2005) Predicting the energetics of osmolyte-induced protein folding/unfolding. *Proc Natl Acad Sci U S A* **102**, 15065-15068
20. Liang, X., Zhang, L., Natarajan, S. K., and Becker, D. F. (2013) Proline mechanisms of stress survival. *Antioxidants & redox signaling* **19**, 998-1011
21. Menzel, R., and Roth, J. (1981) Regulation of the genes for proline utilization in Salmonella typhimurium: autogenous repression by the putA gene product. *J Mol Biol* **148**, 21-44
22. Moxley, M. A., Tanner, J. J., and Becker, D. F. (2011) Steady-state kinetic mechanism of the proline:ubiquinone oxidoreductase activity of proline utilization A (PutA) from Escherichia coli. *Arch Biochem Biophys* **516**, 113-120
23. Arentson, B. W., Sanyal, N., and Becker, D. F. (2012) Substrate channeling in proline metabolism. *Front Biosci* **17**, 375-388
24. Tanner, J. J. (2008) Structural biology of proline catabolism. *Amino Acids* **35**, 719-730
25. Savoure, A., Jaoua, S., Hua, X. J., Ardiles, W., Van Montagu, M., and Verbruggen, N. (1995) Isolation, characterization, and chromosomal location of a gene encoding the delta 1-pyrroline-5-carboxylate synthetase in Arabidopsis thaliana. *FEBS Lett* **372**, 13-19
26. Adams, E. (1970) Metabolism of proline and of hydroxyproline. *Int Rev Connect Tissue Res* **5**, 1-91
27. Fichman, Y., Gerdes, S. Y., Kovacs, H., Szabados, L., Zilberstein, A., and Csonka, L. N. (2014) Evolution of proline biosynthesis: enzymology, bioinformatics, genetics, and transcriptional regulation. *Biological reviews of the Cambridge Philosophical Society*

28. Jauniaux, J. C., Urrestarazu, L. A., and Wiame, J. M. (1978) Arginine metabolism in Saccharomyces cerevisiae: subcellular localization of the enzymes. *J Bacteriol* **133**, 1096-1107
29. Szabados, L., and Savoure, A. (2010) Proline: a multifunctional amino acid. *Trends Plant Sci* **15**, 89-97
30. Simmaco, M., John, R. A., Barra, D., and Bossa, F. (1986) The primary structure of ornithine aminotransferase. Identification of active-site sequence and site of post-translational proteolysis. *FEBS Lett* **199**, 39-42
31. Kobayashi, T., Nishii, M., Takagi, Y., Titani, K., and Matsuzawa, T. (1989) Molecular cloning and nucleotide sequence analysis of mRNA for human kidney ornithine aminotransferase. An examination of ornithine aminotransferase isozymes between liver and kidney. *FEBS Lett* **255**, 300-304
32. Phang, J. M., Liu, W., and Zabirnyk, O. (2010) Proline metabolism and microenvironmental stress. *Annu Rev Nutr* **30**, 441-463
33. Phang, J. M., Donald, S. P., Pandhare, J., and Liu, Y. (2008) The metabolism of proline, a stress substrate, modulates carcinogenic pathways. *Amino Acids* **35**, 681-690
34. Zarse, K., Schmeisser, S., Groth, M., Priebe, S., Beuster, G., Kuhlow, D., Guthke, R., Platzer, M., Kahn, C. R., and Ristow, M. (2012) Impaired insulin/IGF1 signaling extends life span by promoting mitochondrial L-proline catabolism to induce a transient ROS signal. *Cell metabolism* **15**, 451-465
35. Krishnan, N., and Becker, D. F. (2006) Oxygen reactivity of PutA from Helicobacter species and proline-linked oxidative stress. *J Bacteriol* **188**, 1227-1235
36. White, T. A., Krishnan, N., Becker, D. F., and Tanner, J. J. (2007) Structure and kinetics of monofunctional proline dehydrogenase from Thermus thermophilus. *The Journal of biological chemistry* **282**, 14316-14327
37. Wanduragala, S., Sanyal, N., Liang, X., and Becker, D. F. (2010) Purification and characterization of Put1p from Saccharomyces cerevisiae. *Arch Biochem Biophys* **498**, 136-142
38. Goncalves, R. L., Rothschild, D. E., Quinlan, C. L., Scott, G. K., Benz, C. C., and Brand, M. D. (2014) Sources of superoxide/H2O2 during mitochondrial proline oxidation. *Redox biology* **2**, 901-909
39. Kracke, F., Vassilev, I., and Kromer, J. O. (2015) Microbial electron transport and energy conservation - the foundation for optimizing bioelectrochemical systems. *Frontiers in microbiology* **6**, 575
40. Borsani, O., Zhu, J., Verslues, P. E., Sunkar, R., and Zhu, J. K. (2005) Endogenous siRNAs derived from a pair of natural cis-antisense transcripts regulate salt tolerance in Arabidopsis. *Cell* **123**, 1279-1291
41. Verbruggen, N., and Hermans, C. (2008) Proline accumulation in plants: a review. *Amino Acids* **35**, 753-759

42. Ayliffe, M. A., Roberts, J. K., Mitchell, H. J., Zhang, R., Lawrence, G. J., Ellis, J. G., and Pryor, T. J. (2002) A plant gene up-regulated at rust infection sites. *Plant Physiology* **129**, 169-180
43. Roberts, J. K., and Pryor, A. (1995) Isolation of a flax (Linum usitatissimum) gene induced during susceptible infection by flax rust (Melampsora lini). *Plant Journal* **8**, 1-8
44. Liu, W., and Phang, J. M. (2012) Proline dehydrogenase (oxidase) in cancer. *BioFactors* **38**, 398-406
45. Cairns, R. A., Harris, I. S., and Mak, T. W. (2011) Regulation of cancer cell metabolism. *Nature reviews. Cancer* **11**, 85-95
46. Nomura, M., and Takagi, H. (2004) Role of the yeast acetyltransferase Mpr1 in oxidative stress: regulation of oxygen reactive species caused by a toxic proline catabolism intermediate. *Proceedings of the National Academy of Sciences of the United States of America* **101**, 12616-12621
47. Maxwell, S. A., and Davis, G. E. (2000) Differential gene expression in p53-mediated apoptosis-resistant vs. apoptosis-sensitive tumor cell lines. *Proceedings of the National Academy of Sciences of the United States of America* **97**, 13009-13014
48. Lee, I. R., Lui, E. Y., Chow, E. W., Arras, S. D., Morrow, C. A., and Fraser, J. A. (2013) Reactive oxygen species homeostasis and virulence of the fungal pathogen Cryptococcus neoformans requires an intact proline catabolism pathway. *Genetics* **194**, 421-433
49. Nishimura, A., Nasuno, R., and Takagi, H. (2012) The proline metabolism intermediate Delta1-pyrroline-5-carboxylate directly inhibits the mitochondrial respiration in budding yeast. *FEBS letters* **586**, 2411-2416
50. Drose, S. (2013) Differential effects of complex II on mitochondrial ROS production and their relation to cardioprotective pre- and postconditioning. *Biochim Biophys Acta* **1827**, 578-587
51. Deuschle, K., Funck, D., Forlani, G., Stransky, H., Biehl, A., Leister, D., van der Graaff, E., Kunze, R., and Frommer, W. B. (2004) The role of [Delta]1-pyrroline-5-carboxylate dehydrogenase in proline degradation. *Plant Cell* **16**, 3413-3425
52. Chen, J., Zhang, Y., Wang, C., Lu, W., Jin, J. B., and Hua, X. (2011) Proline induces calcium-mediated oxidative burst and salicylic acid signaling. *Amino Acids* **40**, 1473-1484
53. Yang, S. L., Lan, S. S., and Gong, M. (2009) Hydrogen peroxide-induced proline and metabolic pathway of its accumulation in maize seedlings. *J Plant Physiol* **166**, 1694-1699
54. Mittler, R., Vanderauwera, S., Suzuki, N., Miller, G., Tognetti, V. B., Vandepoele, K., Gollery, M., Shulaev, V., and Van Breusegem, F. (2011) ROS signaling: the new wave? *Trends Plant Sci* **16**, 300-309
55. Cecchini, N. M., Monteoliva, M. I., and Alvarez, M. E. (2011) Proline dehydrogenase is a positive regulator of cell death in different kingdoms. *Plant signaling & behavior* **6**, 1195-1197

56. Cecchini, N. M., Monteoliva, M. I., and Alvarez, M. E. (2011) Proline dehydrogenase contributes to pathogen defense in Arabidopsis. *Plant Physiol* **155**, 1947-1959
57. Funck, D., Eckard, S., and Muller, G. (2010) Non-redundant functions of two proline dehydrogenase isoforms in Arabidopsis. *Bmc Plant Biol* **10**, 70
58. Tretter, L., and Adam-Vizi, V. (2000) Inhibition of Krebs cycle enzymes by hydrogen peroxide: A key role of alpha-ketoglutarate dehydrogenase in limiting NADH production under oxidative stress. *J Neurosci* **20**, 8972-8979
59. Zhang, L., and Becker, D. F. (2015) Connecting proline metabolism and signaling pathways in plant senescence. *Front Plant Sci* **6**, 552
60. Faes, P., Deleu, C., Ainouche, A., Le Caherec, F., Montes, E., Clouet, V., Gouraud, A. M., Albert, B., Orsel, M., Lassalle, G., Leport, L., Bouchereau, A., and Niogret, M. F. (2015) Molecular evolution and transcriptional regulation of the oilseed rape proline dehydrogenase genes suggest distinct roles of proline catabolism during development. *Planta.* **241**, 403-419
61. Funck, D., Eckard, S., and Muller, G. (2010) Non-redundant functions of two proline dehydrogenase isoforms in *Arabidopsis*. *BMC Plant Biol.* **10**, 70
62. Deuschle, K., Funck, D., Forlani, G., Stransky, H., Biehl, A., Leister, D., van der Graaff, E., Kunze, R., and Frommer, W. B. (2004) The role of [Delta]1-pyrroline-5-carboxylate dehydrogenase in proline degradation. *The Plant cell* **16**, 3413-3425
63. Masclaux-Daubresse, C., Carrayol, E., and Valadier, M. H. (2005) The two nitrogen mobilisation- and senescence-associated GS1 and GDH genes are controlled by C and N metabolites. *Planta.* **221**, 580-588
64. Hung, K. T., Hsu, Y. T., and Kao, C. H. (2006) Hydrogen peroxide is involved in methyl jasmonate-induced senescence of rice leaves. *Physiol Plantarum* **127**, 293-303
65. Hung, K. T., and Kao, C. H. (2005) Phosphatidylinositol 3-phosphate is required for abscisic acid-induced hydrogen peroxide production in rice leaves. *Plant Growth Regul.* **45**, 95-101
66. Leprince, A. S., Magalhaes, N., De Vos, D., Bordenave, M., Crilat, E., Clement, G., Meyer, C., Munnik, T., and Savoure, A. (2015) Involvement of Phosphatidylinositol 3-kinase in the regulation of proline catabolism in *Arabidopsis thaliana*. *Front Plant Sci* **5**
67. Donald, S. P., Sun, X. Y., Hu, C. A., Yu, J., Mei, J. M., Valle, D., and Phang, J. M. (2001) Proline oxidase, encoded by p53-induced gene-6, catalyzes the generation of proline-dependent reactive oxygen species. *Cancer Res.* **61**, 1810-1815
68. Liu, Y. M., Borchert, G. L., Donald, S. P., Diwan, B. A., Anver, M., and Phang, J. M. (2009) Proline Oxidase Functions as a Mitochondrial Tumor Suppressor in Human Cancers. *Cancer Research* **69**, 6414-6422

69. Galoian, K., Scully, S., and Galoyan, A. (2009) Myc-oncogene inactivating effect by proline rich polypeptide (PRP-1) in chondrosarcoma JJ012 cells. *Neurochemical research* **34**, 379-385
70. Pandhare, J., Cooper, S. K., and Phang, J. M. (2006) Proline oxidase, a proapoptotic gene, is induced by troglitazone: evidence for both peroxisome proliferator-activated receptor gamma-dependent and -independent mechanisms. *The Journal of biological chemistry* **281**, 2044-2052
71. Liu, W., Zabirnyk, O., Wang, H., Shiao, Y. H., Nickerson, M. L., Khalil, S., Anderson, L. M., Perantoni, A. O., and Phang, J. M. (2010) miR-23b*targets proline oxidase, a novel tumor suppressor protein in renal cancer. *Oncogene* **29**, 4914-4924
72. Liu, Y., Borchert, G. L., Surazynski, A., and Phang, J. M. (2008) Proline oxidase, a p53-induced gene, targets COX-2/PGE2 signaling to induce apoptosis and inhibit tumor growth in colorectal cancers. *Oncogene* **27**, 6729-6737
73. Zou, W., Liu, X., Yue, P., Khuri, F. R., and Sun, S. Y. (2007) PPARgamma ligands enhance TRAIL-induced apoptosis through DR5 upregulation and c-FLIP downregulation in human lung cancer cells. *Cancer Biol Ther* **6**, 99-106
74. Liu, Y., Borchert, G. L., Surazynski, A., Hu, C. A., and Phang, J. M. (2006) Proline oxidase activates both intrinsic and extrinsic pathways for apoptosis: the role of ROS/superoxides, NFAT and MEK/ERK signaling. *Oncogene* **25**, 5640-5647
75. Dorsam, R. T., and Gutkind, J. S. (2007) G-protein-coupled receptors and cancer. *Nature reviews. Cancer* **7**, 79-94
76. Legendre, C., Mooij, M. J., Adams, C., and O'Gara, F. (2011) Impaired expression of hypoxia-inducible factor-1alpha in cystic fibrosis airway epithelial cells - a role for HIF-1 in the pathophysiology of CF? *Journal of cystic fibrosis : official journal of the European Cystic Fibrosis Society* **10**, 286-290
77. Krishnan, N., Dickman, M. B., and Becker, D. F. (2008) Proline modulates the intracellular redox environment and protects mammalian cells against oxidative stress. *Free Radic. Biol. Med.* **44**, 671-681
78. Ronaldson, P. T., and Bendayan, R. (2008) HIV-1 viral envelope glycoprotein gp120 produces oxidative stress and regulates the functional expression of multidrug resistance protein-1 (Mrp1) in glial cells. *J Neurochem* **106**, 1298-1313
79. Pandhare, J., Dash, S., Jones, B., Villalta, F., and Dash, C. (2015) A Novel Role of Proline Oxidase in HIV-1 Envelope Glycoprotein Induced Neuronal Autophagy. *The Journal of biological chemistry*
80. Pang, S., and Curran, S. P. (2014) Adaptive capacity to bacterial diet modulates aging in C. elegans. *Cell Metab* **19**, 221-231
81. Zhang, L., Alfano, J. R., and Becker, D. F. (2015) Proline metabolism increases katG expression and oxidative stress resistance in *Escherichia coli*. *Journal of bacteriology* **197**, 431-440

82. Messner, K. R., and Imlay, J. A. (1999) The identification of primary sites of superoxide and hydrogen peroxide formation in the aerobic respiratory chain and sulfite reductase complex of Escherichia coli. *The Journal of biological chemistry* **274**, 10119-10128
83. Wadhawan, S., Gautam, S., and Sharma, A. (2014) Involvement of proline oxidase (PutA) in programmed cell death of Xanthomonas. *PloS one* **9**, e96423
84. Pistollato, F., Persano, L., Rampazzo, E., and Basso, G. (2010) L-Proline as a modulator of ectodermal differentiation in ES cells. Focus on "L-Proline induces differentiation of ES cells: a novel role for an amino acid in the regulation of pluripotent cells in culture. *Am. J .Physiol. Cell Physiol.* **298**, C979-981
85. Polyak, K., Xia, Y., Zweier, J. L., Kinzler, K. W., and Vogelstein, B. (1997) A model for p53-induced apoptosis. *Nature* **389**, 300-305
86. Chen, C., and Dickman, M. B. (2005) Proline suppresses apoptosis in the fungal pathogen *Colletotrichum trifolii*. *Proc. Natl. Acad. Sci. U.S.A* **102**, 3459-3464
87. Hu, C. A., Donald, S. P., Yu, J., Lin, W. W., Liu, Z., Steel, G., Obie, C., Valle, D., and Phang, J. M. (2007) Overexpression of proline oxidase induces proline-dependent and mitochondria-mediated apoptosis. *Mol Cell Biochem* **295**, 85-92
88. Elrod, H. A., and Sun, S. Y. (2008) PPARgamma and Apoptosis in Cancer. *PPAR Res* **2008**, 704165
89. Hare, P. D., and Cress, W. A. (1997) Metabolic implications of stress-induced proline accumulation in plants. *Plant Growth Regul* **21**, 79-102

CHAPTER 3

Proline Increases *katG* Expression and Oxidative Stress Resistance in *Escherichia coli*

Note: Part of this chapter has been published as the research article: “ Proline Metabolism Increases katG Expression and Oxidative Stress Resistance in *Escherichia coli*” Lu Zhang, James Alfano, Donald Becker. *Journal of Bacteriology*, 2014,197(3).

3.1 ABSTRACT

The oxidation of proline to glutamate in gram-negative bacteria is catalyzed by the proline utilization A (PutA) flavoenzyme, which contains fused proline dehydrogenase (PRODH) and Δ^1-pyrroline-5-carboxylate (P5C) dehydrogenase domains. The PRODH domain catalyzes the flavin-dependent oxidation of proline to Δ^1-pyrroline-5-carboxylate (P5C), a reaction that is coupled to the reduction of the electron transport chain, while the P5C dehydrogenase domain catalyzes the NAD^+-dependent formation of glutamate from P5C. Previous studies have suggested that aside from providing energy, proline metabolism may also influence oxidative stress response in bacteria. To explore this potential role and define the mechanism, we characterized the oxidative stress resistance of wild-type and *putA* mutant strains in *Escherichia coli*. Initial stress assays revealed that the *E. coli putA* mutant strain was significantly more sensitive to oxidative stress than the matching wild-type strain. Expression of PutA in the *putA* mutant strain restored oxidative stress resistance confirming that the loss of PutA activity was responsible for the oxidative stress phenotype of the *putA* mutant. Pre-treatment of wild-type *E. coli* cells with proline resulted in significantly higher survival rates in oxidative stress assays than cells without proline treatment. The mechanism of proline protection was then explored by using strains deficient in catalase and superoxide dismutase. *E. coli* strains that lack a functional *katG* gene failed to respond to proline despite exhibiting PutA expression. In wild-type cells, a > 3-fold increase in *katG* expression and activity was observed after 40 min incubation with proline.

Thus, proline metabolism leads to increased *katG* expression and oxidative stress tolerance in *E. coli*.

3.2 INTRODUCTION

The conversion of proline to glutamate is a four-electron oxidation process that is coordinated in two successive steps by the enzymes, proline dehydrogenase (PRODH) and Δ^1-pyrroline-5-carboxylate dehydrogenase (P5CDH) (Figure 3.1) (1,2). In gram-negative bacteria, PRODH and P5CDH are combined into a bifunctional enzyme known as proline utilization A (PutA) (3,4). The PRODH domain contains a non-covalently bound flavin adenine dinucleotide (FAD) cofactor and couples the two electron oxidation of proline to the reduction of ubiquinone in the cytoplasmic membrane (5). The product of the PRODH reaction, Δ^1-pyrroline-5-carboxylate (P5C), is subsequently hydrolyzed to glutamate-γ-semialdehyde (GSA), which is then oxidized to glutamate by the NAD^+-dependent P5CDH domain (6). In certain gram-negative bacteria such as *Escherichia coli*, PutA also has an N-terminus ribbon-helix-helix (RHH) DNA-binding domain (residues 1-47) (7). The RHH domain enables PutA to act as an autogenous transcriptional regulator of the *putA and putP* (high affinity proline transporter) genes (7). PutA represses *put* gene expression by binding to five conserved operator sites in the *put* regulatory region (8). Transcription of the *put* genes is activated by proline, which causes the reduction of the flavin cofactor and subsequent localization of PutA on the membrane (8-12).

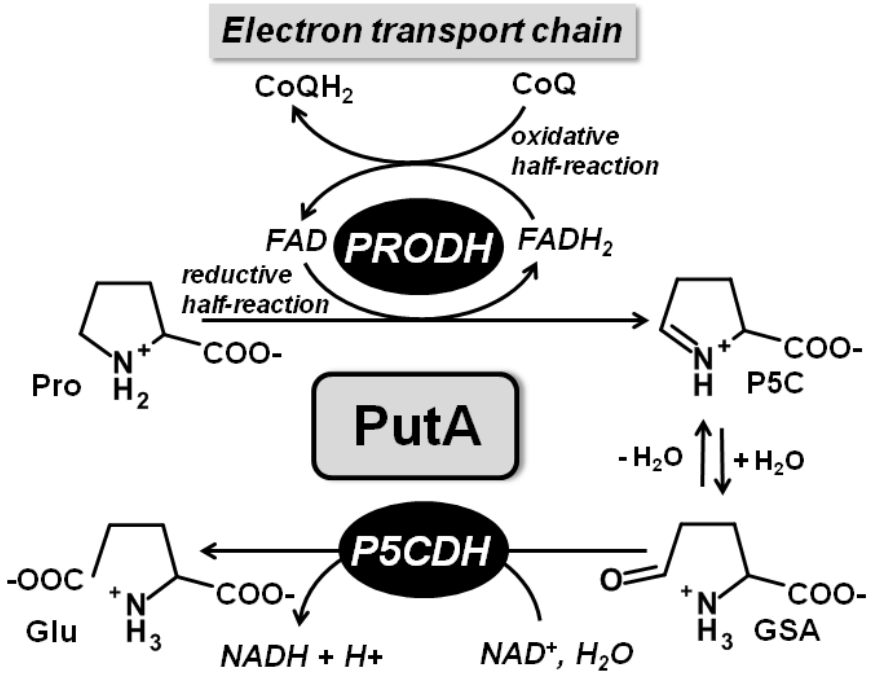

Figure 3.1 Reactions catalyzed by the PRODH and P5CDH domains of PutA. Reduction of ubiquinone (CoQ) in the electron transport chain is coupled to proline oxidation.

Proline has been shown to be an important carbon and nitrogen source supporting growth in varied nutrient conditions for *Escherichia coli*, *Pseudomonas putida*, *Bradyrhizobium japonicum*, and *Helicobacter pylori* (13-17). In *H. pylori*, L-proline is a preferred respiratory substrate in the gut (13,18). *H. pylori* can cause acute gastric inflammation that can progress from superficial gastritis to peptic ulceration, and gastric cancer (19). Proline levels are 10-fold higher in the gastric juice of patients infected with *H. pylori* than in noninfected individuals (13). Recently, a *H. pylori putA* mutant strain was shown to be less efficient in colonization of mice relative to the wild-type strain and the proline transporter, PutP, was found to be essential for gastric colonization of *H. pylori* (20). Altogether, these studies show that PutA and the proline catabolic pathway help promote the pathogenesis of *Helicobacter* species.

Besides being an important energy source in certain ecological niches, proline also provides protective benefits against abiotic and biotic stresses in a broad range of organisms (21-24). Proline is a well-known osmoprotectant and in *E. coli* proline has been described as a thermoprotectant by diminishing protein aggregation during heat stress (25-27). Proline has also been found to help combat oxidative stress, a property which has been well characterized in fungi and plants (22,23,28). The mechanism by which proline protects against oxidative stress is not fully known. However, in the fungal pathogen, *Colletotrichum trifolii,* proline was reported to increase catalase expression (28).

In a previous study, we examined the pathophysiological role of PutA in the mouse pathogen, *Helicobacter hepaticus.* We showed that a *H. hepaticus putA*

mutant strain caused significantly less inflammation in the livers of infected mice relative to mice inoculated with wild-type *H. hepaticus* (29). Unexpectedly, the *H. hepaticus putA* mutant strain was found to have lower catalase (*katA*) expression relative to the wild-type strain (29). The low catalase activity was proposed to contribute to the decreased pathogenesis of the *putA* mutant strain as *Helicobacter* species, which must effectively combat oxidative stress to successfully persist in the gastric mucosa (30-33). The rationale for lower catalase expression in *H. hepaticus putA* mutant cells relative to wild-type cells, however, was not apparent.

Here we further explore the role of proline metabolism in oxidative stress resistance in *E. coli*. We provide evidence that the mechanism by which proline enhances oxidative stress resistance involves upregulation of catalase, which is induced by proline-dependent ROS.

3.3 MATERIALS AND METHODS

3.3.1. Reagents, bacterial strains and culture conditions

β-mercaptoethanol, *o*-aminobenzaldehyde (*o*-AB), *o*-nitrophenyl-*β*-D-galactopyranoside, L-proline, and L-tetrahydro-2-furoic acid (L-THFA) were purchased from Sigma. All other chemicals were purchased from Thermo Fisher unless noted otherwise. PutA-pUC18 plasmid was described previously (8). *E. coli* strains used in this study are listed in Table 1. The MG1655 *ΔputA* strain was generated in this work by P1 transduction of the MG1655 wild-type strain (34). *E. coli* cultures were grown in Luria-Bertani (LB) broth (10 g tryptone, 5 g yeast extract, and 10 g NaCl per liter) or glucose minimal medium containing (0.5 g glucose, 0.1

g thiamine, 1 mM $MgSO_4$, 0.5 g NaCl, 1 g NH_4Cl, 3 g KH_2PO_4 and 6 g $Na_2HPO_4 \cdot 7H_2O$ per liter). Ampicillin and kanamycin were used as needed at 50 µg/ml. Cultures were grown at 37°C with shaking at 225 rpm. To perform measurements upon exponentially growing cells, overnight cultures were diluted 1,000-fold with fresh medium and grown to mid-logarithmic phase which corresponds to an optical density at 600 nm (OD_{600}) of 0.3.

Table 1. **Strains used in this study**

E. coli **K12 Strains**	**Relevant genotype**	**Ref**
MG1655	wild-type (F^-, *Δλ*$^-$, *rph-1*)	(35)
MG1655 *ΔputA*	As MG1655 plus *ΔputA758::kan*	This work
AL441	As MG1655 plus D(*lacZ1::cat*)1 *attl::*[pSJ501::*katG'-lacZ*$^+$ *cat*$^+$]	(36)
CSH4	wild-type (F^-, *lacZ1125*, *λ*$^-$, *trpA49*(Am), *relA1*, *rpsL150*(strR), *spoT1*)	(17)
JT31	As CSH4 plus *putA1::*Tn*5*	(17)
JT34	As CSH4 plus *putP3::*Tn*5*	(17)
BW25113	wild-type (F^-, *Δ*(*araD-araB*)*567*, *ΔlacZ4787*(*::rrnB-3*), *λ*$^-$, *rph-1*, *Δ*(*rhaD-rhaB*)*568*, *hsdR514*)	(37)
JW0999	As BW25113 plus *ΔputA758::kan*	(37)
JW1721	As BW25113 plus *ΔkatE731::kan*	(37)
JW3914	As BW25113 plus *ΔkatG729::kan*	(37)
JW3933	As BW25113 plus *ΔoxyR749::kan*	(37)
JW4024	As BW25113 plus *ΔsoxR757::kan*	(37)

3.3.2 Disk assay for oxidative stress sensitivity

Cells were grown in LB Broth to 0.3 OD_{600}. Aliquots (0.5 mL) from each culture were then mixed with 4.5 ml cooled down soft agar (glucose minimal medium, 0.8% agar and no antibiotics) and then poured immediately onto LB plates (no antibiotics). After the soft agar solidified, a round filter paper (d = 0.8 cm)

saturated with 10 µl of 6.6 M H_2O_2 was placed in the center of the plate. Plates were then incubated at 37°C overnight. The inhibitory circle diameter was measured from three different directions to calculate a mean value for the diameter of the inhibition zone.

3.3.3 Cell counting assay

Cells were grown in glucose minimal medium to 0.3 OD_{600} with (or without) 10 mM L-proline. Cells were then collected, diluted to 0.1 OD_{600} with fresh medium prior to 30 min treatment with 5 mM H_2O_2. After serial dilution, cells were spread onto LB plates and allowed to grow overnight at 37°C. Cell survival rates were calculated as colony forming units of H_2O_2 treated cells divided by those of untreated cells.

3.3.4 β-Galactosidase activity

To measure the effect of proline oxidation on *katG* expression, AL441 cells were grown in glucose minimal medium to 0.3 OD_{600} before treatment with 10 mM L-proline and L-THFA. Samples were collected at designated time points and β-galactosidase activities were measured as described (38). To determine the effect of H_2O_2 on *katG* expression, cells were cultured as described above and then treated with different concentrations of H_2O_2 for 30 min, followed by measurement of β-galactosidase activity. β-galactosidase activity assays were performed as previously described (38) and are reported in Miller units (34).

3.3.5 Catalase activity

MG1655 wild-type and *ΔputA* cells were grown in glucose minimal medium to 0.3 OD_{600} with (or without) 10 mM L-proline. Cells were then collected, centrifuged and lysed with bacterial extraction reagent (Pierce). Cell debris was removed by centrifugation, and catalase activity in the supernatant was measured with 20μM H_2O_2 by Amplex® Red Catalase Assay Kit (Life Technology) using a newly prepared H_2O_2 standard curve according to the manufacture's protocol and measuring absorbance at 568 nm with a powerwave XS microplate reader. Protein concentrations were determined with 660 nm Protein Assay (Pierce). One unit of catalase activity is defined as the decomposition of 1.0 μmole H_2O_2 per min at pH 7.0 at 25 °C.

3.3.6 H_2O_2 clearance assay

To determine the effect of proline oxidation on H_2O_2 scavenging, MG1655 wild-type and *ΔputA* cells were grown in glucose minimal medium to 0.3 OD_{600} with (or without) 10 mM L-proline. Cells were then pelleted, washed and resuspended in phosphate-buffered saline (PBS) to 0.1 OD_{600}. After addition of 5 μM H_2O_2, 0.45 mL aliquots were removed at different time intervals and H_2O_2 was measured immediately by Amplex® Red Hydrogen Peroxide/Peroxidase Assay Kit (Life Technology) at room temperature as previously described (39). Fluorescence measurements were made with an Agilent (Varian) Cary Eclipse fluorescence spectrophotometer with excitation at 545 nm and monitoring fluorescence emission at 590 nm.

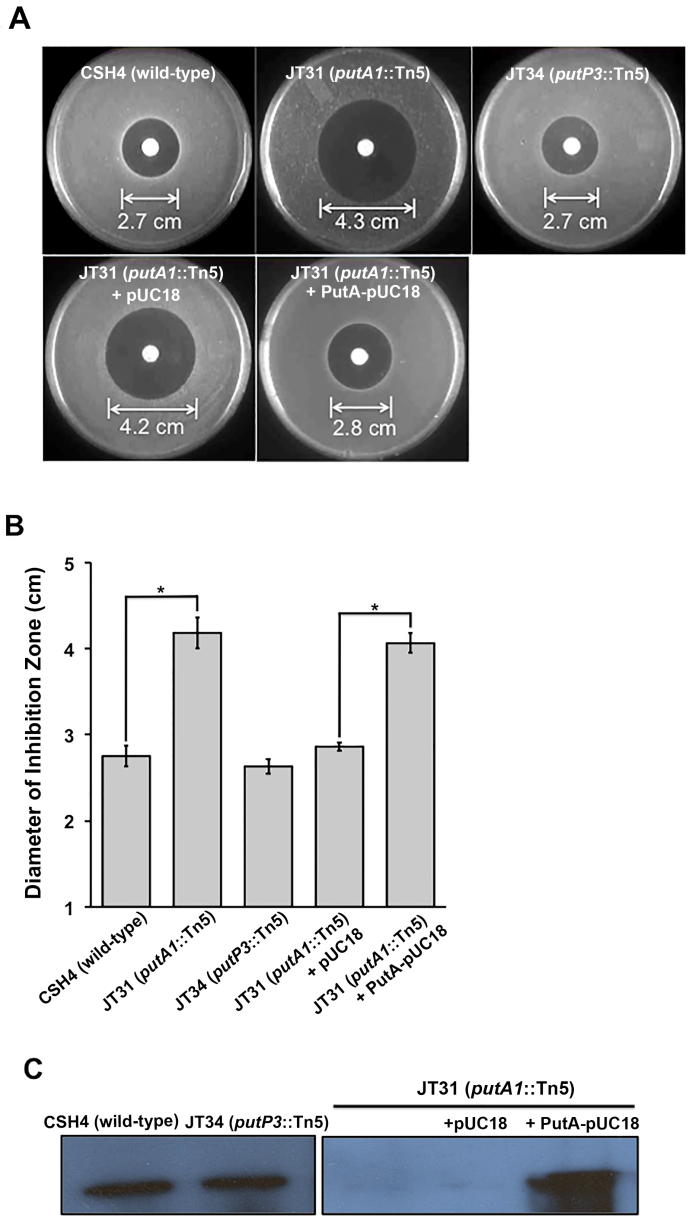

Figure 3.2 Depletion of PutA increases oxidative stress sensitivity. (A) Disk assays were performed with CSH4 (parental wild-type), JT31 (*putA1*::Tn5), JT34 (*putP3*::Tn5), JT31 transformed with empty pUC18 vector or pUC18 vector bearing wild-type PutA using filter paper saturated with 10 µl of 6.6 M H_2O_2. (B) Inhibition zone diameters from five replicates of the disk assays shown in (A) (*$P < 0.05$). (C) Western blot analysis of PutA expression in strains used for A and B.

3.3.7 Real-time PCR

MG1655 wild-type and *ΔputA* cells were grown in glucose minimal medium to 0.3 OD_{600}. At time zero (t = 0 min), 10 mM L-proline was added to the cultures. Immediately after, a sample of 0.5 mL was taken and mixed with 1 ml of RNAprotect Bacteria Reagent (Qiagen) for the time zero point. Additional samples were then withdrawn from the cultures at different time points. RNA was extracted using RNeasy Mini Kit (Qiagen) according to manufacturer's protocol. Genomic DNA was removed from the RNA preparations with RNase free DNase I (Fermentas). The cDNA was synthesized using the RevertAid^{TM} First Strand cDNA Synthesis Kit (Fermentas) with 100 ng of template RNA and random hexamer primers. The following primers were used to analyze expression of *katG*, *grxA*, *trxC*, and 16S rRNA: *katG* forward, 5'- AATCCAGTTCGAAGCGGTAG-3'; *katG* reverse, 5'-CACCAGCATTGTCGGTTTAC-3'; *grxA* forward, 5'-GATCTGGCT GAGAAATTGAG-3'; *grxA* reverse, 5'-GTTTACCTGCCTTTTGTTGT-3'; *trxC* forward, 5'- AATACCGTTTGTACCCATTG-3'; *trxC* reverse 5'-GCTTCGGTAT TCACTTTCAC-3'; 16S rRNA forward, 5'- GGATGATCAGCCACACTGGA-3'; 16S rRNA reverse, 5'- CCAAT ATTCCTCACTGCTGCC-3'. The 20 µL real-time PCR mixture contained 10 µL SsoFast EvaGreen Supermix (Biorad), 300 nM of primers and 50 ng cDNA. Thermal cycling was performed using iCycler iQ (Biorad) for 40 cycles in 3 steps: 95°C for 15 sec, 58°C for 30 sec and 65°C for 60 sec. Relative mRNA levels were calculated using the $2^{-\Delta\Delta CT}$ method and using 16s rRNA as the internal control. PCR products were also analyzed by agarose gel electrophoresis to confirm product size and specificity.

3.3.8 PutA western blotting

The expression of PutA was confirmed by western blot analysis as described previously using an antibody against a polypeptide containing PutA residues 1-47 (8).

3.3.9 Triphenyl tetrazolium chloride reduction (TTC) test

During the proline oxidation, TTC was reduced to red 1,3,5-triphenylformazan (TPF), which has a molar extinction coefficient of 13410 L $mol^{-1}cm^{-1}$ in ethanol. To confirm proline utilization in minimal media containing low glucose, MG1655 wild-type and *ΔputA* cells were grown in minimal media with 0.025% TTC to 0.3 OD_{600}, in the presence and absence of 10 mM proline. Cells were pelleted and washed, and TPF was extracted from pallet by 95% ethanol. The amount of TPF was determined by its absorbance at 485 nm.

3.3.10 H_2O_2 production assays

H_2O_2 produced and accumulated within cells passes through the membranes and equilibrates with the culture medium (53). To determine the effect of L-proline treatment on H_2O_2 production *in vivo*, BW25113 (Keio strain collection) wild-type and *ΔkatG* (strain JW3914) cells were grown to 0.3 OD_{600} in glucose minimal medium with (or without) 10 mM L-proline. Cells were then pelleted and the H_2O_2 content in the supernatant was measured immediately by

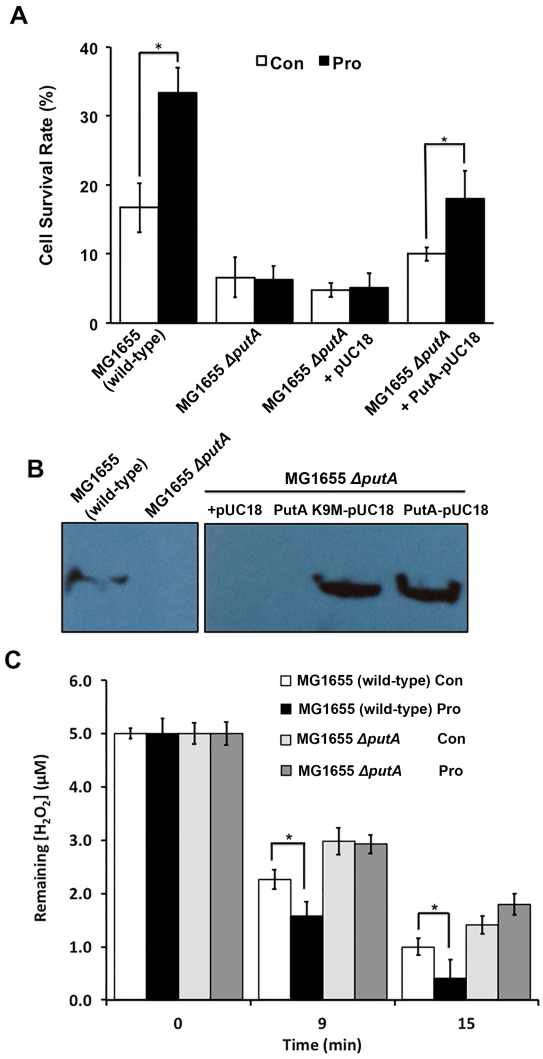

Figure 3.3 Proline enhances cell survival and H_2O_2 clearance. (A) Cell survival rates of MG1655 wild-type and *ΔputA* strains, and the *ΔputA* strain transformed with empty or PutA-pUC18 vectors in the absence (Con) and presence (Pro) of 10 mM proline in minimal medium. Cells were treated with 5 mM H_2O_2 for 30 min. (B) Western blot analysis of PutA expression in strains used for (A) and *ΔputA* strain transformed with PutA Lys9Met-pUC18 vector. (C) H_2O_2 clearance in MG1655 wild-type and *ΔputA* cells grown in minimal medium in the absence (Con) and presence (Pro). (*$P < 0.05$)

nm and monitoring fluorescence emission at 590 nm.

The kinetics of H_2O_2 formation from proline was determined using inverted membrane vesicles from the *ΔkatG* strain (JW3914). Inverted membrane vesicles were prepared as described (40) from JW3914 (*ΔkatG*) cells grown in minimal A medium (33 mM KH_2PO_4, 51 mM K_2HPO_4, 8 mM $(NH_4)_2SO_4$, 0.4 mM $MgSO_4$, 0.5 mM tryptophan, 10 mM L-proline, 8% glycerol and 0.05% glucose) to 0.7 OD_{600}. Assays were performed at room temperature with 50 µg/ml of membrane vesicles (or membrane protein) and 10 mM substrate (proline, glutamate, glycine and succinate) to estimate the rate of H_2O_2 production in the presence and absence of THFA and 1 µg/mL antimycin A. The assay buffer (pH 7.2) included 40 U/mL superoxide dismutase, 125 mM KCl, 4 mM KH_2PO_4, 14 mM NaCl, 20 mM HEPES-NaOH, 1 mM $MgCl_2$, 0.2% BSA, and 0.02 mM EDTA (41). H_2O_2 was quantified using the Amplex® Red Hydrogen Peroxide/Peroxidase Assay Kit with excitation at 555 nm and monitoring fluorescence emission at 581 nm as described (41) with the rate defined as pmol of H_2O_2 formed min^{-1} mg^{-1} of total membrane protein. To represent the intracellular H_2O_2 formation rate, extracellular H_2O_2 formation rate measured with membrane vesicle was normalized to cytosolic volume of cultured cells, by using the relationship that 1 ml of 1.0 OD bacteria comprises 0.47 µl of volume (42). Intracellular H_2O_2 formation rate µM min^{-1}= Measured H_2O_2 formation rate pmol mg^{-1} min^{-1} x total protein 20 mg/total cytosolic volume µl. Total cytosolic volume = 0.8 OD x 500 ml culture x 0.47 µl cytosolic volume. The effect of L-THFA on H_2O_2 production was determined using the same assay conditions above with

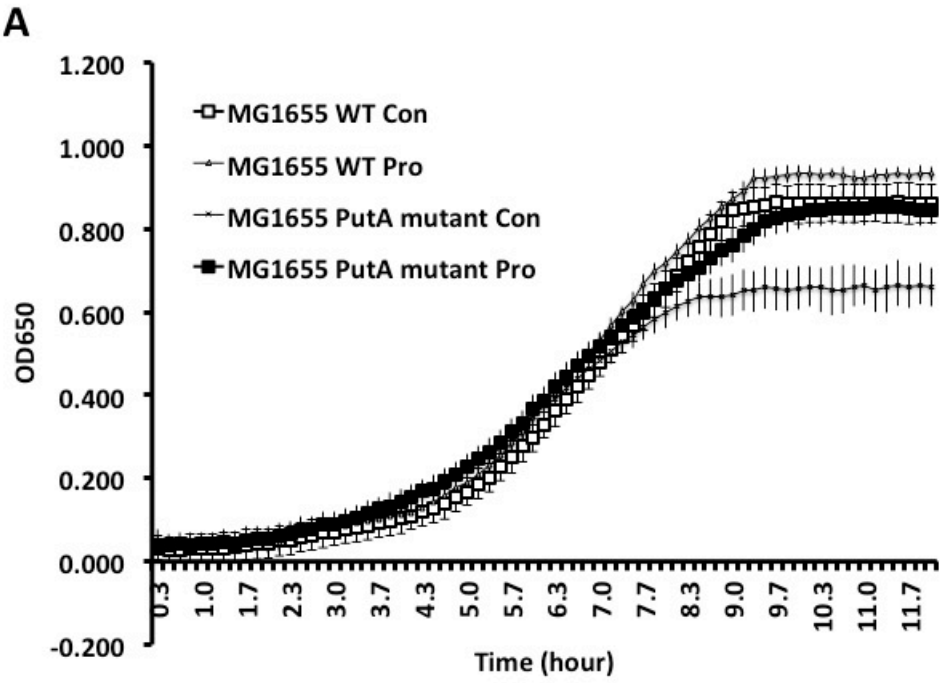

the

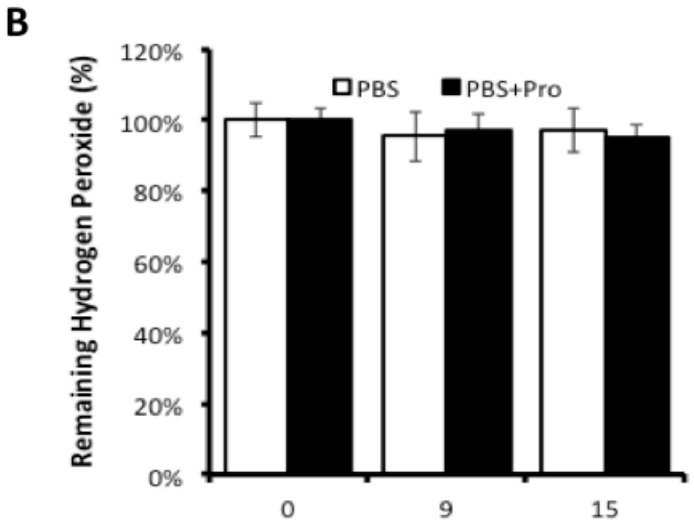

Figure 3.4 **Proline does not affect the growth curve of MG1655 wild-type and *ΔputA* strains or scavenge H_2O_2.** (A) The growth curve of MG1655 wild-type and *ΔputA* strains in the presence (Pro) and absence (Con) of 10 mM proline. (B) Proline itself does not scavenge H_2O_2 levels during a 30 min incubation of proline (10 mM) and H_2O_2 (5 μM) in medium without cells.

proline concentration fixed at 10 mM and varying L-THFA (1-10 mM). Background formation of H_2O_2 was determined in control cytosolic by quantifying P5C production using *o*-AB as previously described (43). The K_m value for proline with membrane vesicles as an electron acceptor is 1.5 mM (8).

3.3.11 Statistical analysis

The reported mean values and standard deviations are from three to five experiments. Data were analyzed by Student's *t*-tests with statistical significance considered to be a *P*-value < 0.05.

3.4 RESULTS

3.4.1 *E. coli putA* mutants have increased oxidative stress sensitivity.

Oxidative stress disk assays were performed with wild-type *E. coli* strain CSH4, the isogenic *putA* (JT31) and *putP* mutant (JT34) strains grown in LB broth to exponential phase (Figure 3.2A). The inhibition zone found for the JT31 strain is almost twice the size of the zones observed with CSH4 and JT34 strains (Figure 3.2A and B). This indicates JT31 cells have increased sensitivity to H_2O_2. The observed phenotype of the JT31 cells can be complemented by transformation with the pUC18 vector bearing the wild-type PutA (Figure 3.2), confirming that depletion of PutA contributes to the H_2O_2 sensitivity of JT31 cells. Expression levels of PutA in the different strains were confirmed by western blot analysis as shown in Figure 3.2C.

The above experiments were performed in LB broth, which is abundant in L- proline (9.5 mM) and contains low glucose (< 0.1 mM) necessitating *E. coli* to utilize amino acids for growth (44). It was previously reported that L-proline is significantly utilized by *E. coli* in LB broth (44). Thus, we hypothesized that proline catabolism may account for the differences in oxidative stress resistance observed between CSH4 and JT31 strains. Although CSH4 and JT31 are commonly used strains for proline studies (7,8,12), the CSH4 strain contains mutations in *relA* and *spoT*, which regulate (p)ppGpp levels and are important for bacterial survival under nutrient starvation, oxidative and osmotic stress conditions (45,46).

Thus, to further evaluate the effects of proline metabolism on oxidative stress sensitivity, a *ΔputA* strain was generated in the strain MG1655 by P1 transduction (Figure 3.3B). MG1655 wild-type and *ΔputA* strains exhibited similar growth profiles, and proline supplementation did not affect growth of either strain (Figure 3.4A).

To confirm proline utilization in MG1655 wild-type cells grown in minimal media in the presence of 0.05% glucose, proline oxidation indicator TTC was added to the minimal media. Proline utilization was measured by determining the accumulated TPF, the reduced product of TTC, in the cells. MG1655 wild-type cells accumulated 0.23 ± 0.01 μM OD^{-1} TPF when grown in the absence of proline. In the presence of proline, TPF level in wild-type cells reached 0.81 ± 0.027 μM OD^{-1}. On the other hand, proline supplementation had no effect on MG1655 *ΔputA* cells, their TPF levels are 0.19 ± 0.02 and 0.18 ± 0.01 μM OD^{-1}, in the absence and presence of proline, respectively. Therefore, MG1655 cells actively consume

proline during the growth even when a low amount of glucose presents in the media.

Figure 3.3A shows that proline supplementation promotes cell survival of the wild-type MG1655 strain by 2-fold after exposure to H_2O_2 whereas no protection is observed in the MG1655 *ΔputA* cells. To confirm that the lack of proline protection was due to the loss of PutA, MG1655 *ΔputA* cells were transformed with the PutA-pUC18 vector. PutA expression in the different strains was confirmed by western blot analysis as shown in Figure 3.3B. The MG1655 *ΔputA* cells transformed with the pUC18 vector carrying wild-type PutA showed increased survival with proline (Figure 3.3A), while the empty pUC18 vector had no effect. It was noticed that *ΔputA* cells were more sensitive to H_2O_2. One possible explanation is that the incapability of *ΔputA* cells to utilize endogenous proline impaired their ability to cope with oxidative stress. Consistent with this idea, complementing with PutA increased the survival rates of cells grown without proline by almost 2-fold. However, complemented *ΔputA* cells still have lower survival rate compared with wild-type cells in the presence or absence of proline. This may be due to the reason that the complementation did not fully restore the ability of *ΔputA* cells to metabolize proline, although a decent amount of PutA expression was detected by western-blot. Thus, PutA is required for the improved oxidative stress tolerance with proline of 10 mM proline.

Next, we questioned the mechanism by which proline enhances resistance to H_2O_2. Scavenging enzymes, like peroxidases and catalases, are a key defense mechanism against H_2O_2 (47). To test whether proline increased the scavenging

of H_2O_2, which is membrane permeable, extracellular H_2O_2 levels (Figure 3.3C) were measured in cultures of MG1655 wild-type and *ΔputA* cells grown to exponential phase in medium supplemented with and without proline. In wild-type cells, extracellular H_2O_2 (5 μM) was cleared at a significantly faster rate with proline than without proline (Figure 3.3C). In the MG1655 *ΔputA* strain, proline had no effect on the H_2O_2 clearance rate indicating that the faster clearance of H_2O_2 in wild-type cells with proline is dependent on PutA. Proline alone did not decrease H_2O_2 levels during a 30 min incubation of proline (10 mM) and H_2O_2 (5 μM) in medium without cells (Figure 3.4B). Therefore, proline oxidation rather than proline itself enhances H_2O_2 scanvanging ability in *E.coli*.

3.4.2 Proline metabolism upregulates *katG* expression and activity

The influence of proline on catalase activity was next evaluated as a possible means for the increased oxidative stress resistance and faster clearance of H_2O_2. Figure 3.5A shows that MG1655 wild-type cells exhibit 1.7-fold higher catalase activity with proline than cells without proline treatment. In the MG1655 *ΔputA* cells with no significant change in catalase activity was observed with proline.

E. coli has two catalases, hydroperoxidase I and hydroperoxidase II, which are encoded by *katG* and *katE*, respectively (48). The expression of *katE* is regulated by RpoS and up-regulated during stationary phase, whereas the expression of *katG* is regulated by OxyR and is induced by H_2O_2 during oxidative

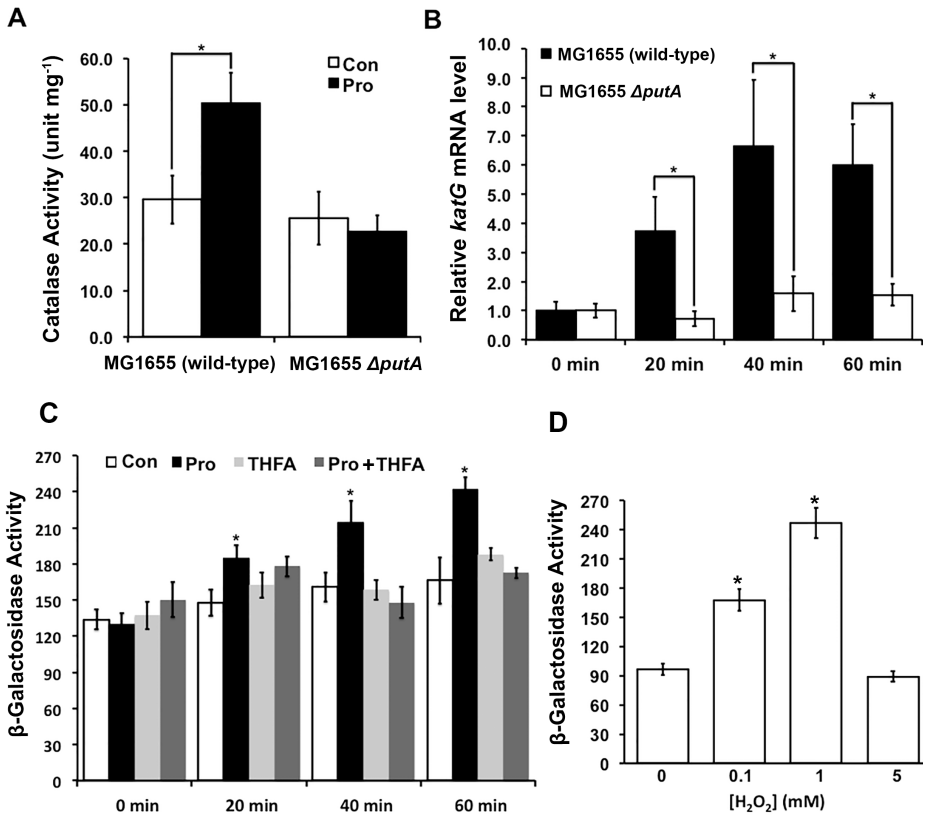

Figure 3.5 Catalase expression and activity are upregulated by proline. (A) Catalase activity of MG1655 wild-type and *ΔputA* cells grown with (Pro) and without (Con) 10 mM proline. (B) Time course of *katG* expression in MG1655 wild-type and *ΔputA* cells. Cells were harvested at the time indicated after 10 mM proline being added to and *katG* expression was measured by real-time PCR. 16S rRNA was used as the internal control. (C) Effect of proline on *katG'* promoter activity was determined by monitoring *katG'::lacZ* reporter construct activity in AL441 cells, which were treated with proline (10 mM) and THFA (10 mM) as indicated (0-60 min). β-galactosidase activity was measured. (D) Same as in (C) except AL441 cells were treated with increasing concentrations of H_2O_2 (30 min) prior to measuring β-galactosidase activity, reported as Miller units (U/OD_{600}). (*$P < 0.05$)

stress (48). Changes in expression of *katG* were quantified by real-time PCR in cells treated with proline for up to 60 min (Figure 3.5B). A 3.5-fold increase in *katG* expression was observed in wild-type MG1655 cells at 20 min and > 6- fold by 40 min. In the *ΔputA* cells, no increase in *katG* expression was observed in response to proline. Thus, proline induction of *katG* expression is dependent on PutA. Additional evidence for proline increasing *katG* expression was obtained using a *katG'::lacZ* expression reporter construct in MG1655 cells (strain AL441), in which the expression of *katG* is monitored by changes in β-galactosidase activity. Expression of *katG* was 1.5-fold higher in cells with proline relative to control cells without proline at 60 min (Figure 3.5C). Incubating cells with proline and THFA, a competitive inhibitor of PutA/PRODH activity (K_i = 1.6 mM) (5), blocked the observed increase in β-galactosidase activity suggesting PutA catalytic activity is critical for the effects of proline on *katG* expression (Figure 3.5C). The effect of proline metabolism on the *katG'::lacZ* reporter was then compared with the effect of adding H_2O_2 to the cell medium. Figure 3.5D shows that exposure of cells to 0.1 mM and 1 mM of H_2O_2 for 30 min results in 1.7- and 2.5-fold increases in *katG* expression, respectively. Thus, the level of increased *katG* expression by proline is similar to that observed with 0.1-1 mM H_2O_2. The different assay sensitivities may explain the higher *katG* up-regulation level obtained by real-time PCR in comparison with β-galactosidase assay, since 1 mM H_2O_2 treatment led to a 44-fold increase of *katG* expression according to previously reported microarray data (49), while we only observed 2.5-fold increase when using *katG:lacZ* fusion. Altogether, these results strongly suggest that proline metabolism promotes

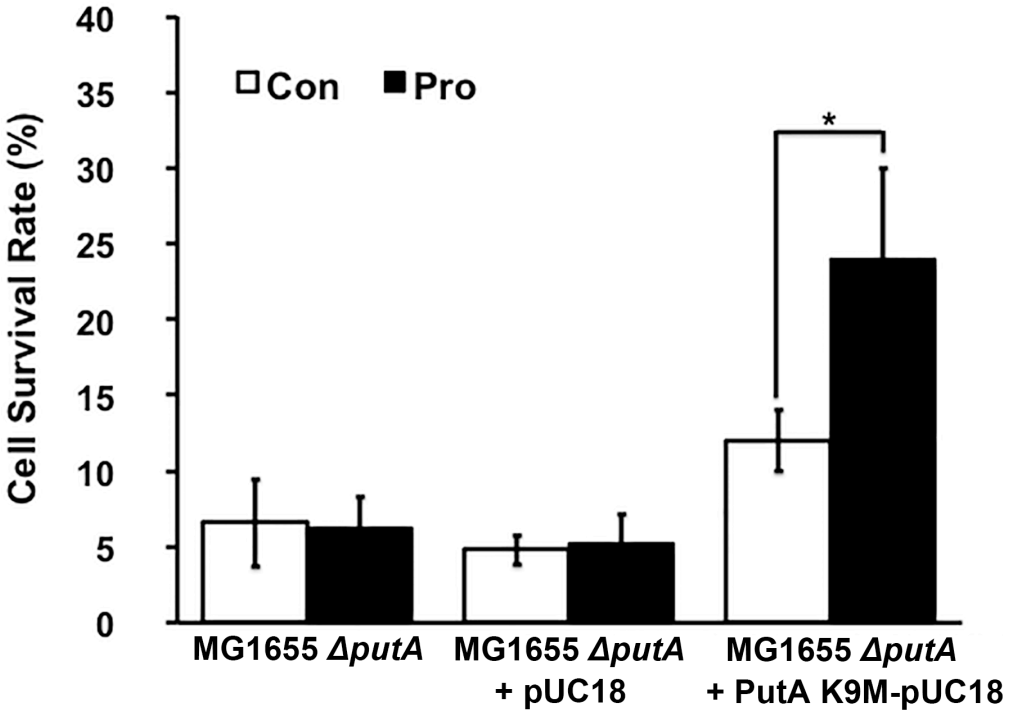

Figure 3.6 DNA binding is not required for proline dependent oxidative stress resistance. Survival rates of the MG1655 *ΔputA* cells and *ΔputA* cells transformed with empty or PutA K9M-pUC18 vector. PutA K9M is a mutant that does not bind DNA (*$P < 0.05$).

the expression of *katG* and catalase activity.

3.4.3 DNA binding function of PutA is not required for increased oxidative stress resistance

E. coli PutA contains a RHH DNA binding domain (residues 1-47) that enables PutA to act as transcriptional repressor of the *putA* and *putP* genes (7). Because PutA is a DNA binding protein, it is feasible that the effect of PutA on *katG* expression may be via direct PutA-DNA interactions. *E. coli* PutA-DNA binding involves a GTTGCA consensus motif (8), which is not found in the promoter region of *katG*. Nevertheless, to rule out the possibility that PutA regulates *katG* expression by DNA binding, we transformed the MG1655 *ΔputA* strain with the PutA mutant Lys9Met (K9M) (Figure 3.3B). Previously, Lys9 residue was determined to be critical for PutA-DNA interactions as the Lys9Met mutation abolished PutA-DNA binding (8). Figure 3.6 shows that *ΔputA* cells expressing the PutA mutant K9M respond to proline with a 2-fold increase in cell survival similar to that observed with wild-type PutA (Figure 3.3A). Expression of PutA K9M was confirmed by western blot analysis (Figure 3.3B). Therefore, the DNA binding function of PutA is not required for the proline dependent increase in oxidative stress resistance.

3.4.4 Proline metabolism activates the OxyR regulon

The effect of proline on cell survival was next tested using a panel of mutants from the *E. coli* Keio strain collection (37). The cell survival rates of

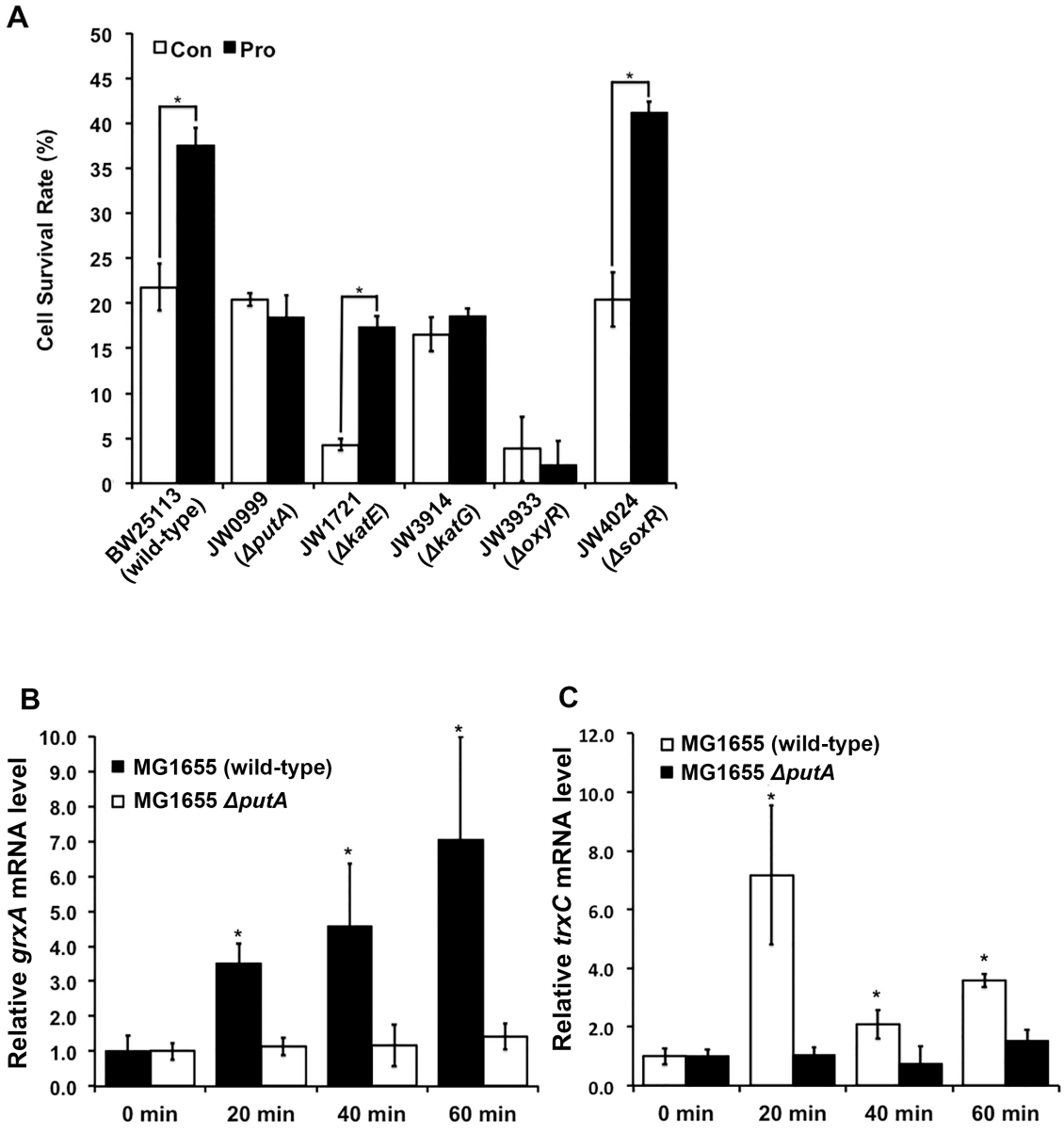

Figure 3.7 Proline protection involves the OxyR regulon. (A) Cell survival rates of the BW25113 wild-type strain and BW25113 *ΔputA, ΔkatE, ΔkatG, ΔoxyR,* and *ΔsoxR* mutants (**P* < 0.05). (B and C) Time course of *grxA* (B) and *trxC* (C) expression in MG1655 wild-type and *ΔputA* cells. Experiments were performed as described in Figure 3.4B using 16S rRNA as internal control (**P* < 0.05).

BW25113 wild-type and mutant strains after H_2O_2 stress treatment were tested in the absence and presence of proline (Figure 3.7A). As anticipated, proline increased the survival of BW25113 wild-type cells but not the *ΔputA* strain. Similar to the *ΔputA* strain, the survival rates of the *ΔkatG* and *ΔoxyR* cells were not increased by proline, suggesting that OxyR, which regulates *katG*, is involved in the protective mechanism of proline. In contrast, proline increased the survival rates of *ΔkatE* and *ΔsoxR* indicating that hydroperoxidase II and

SoxR which is a transcription factor activated in response to redox active metabolites (50), are not essential for the mechanism of proline protection. Besides H_2O_2 scavenging, activation of OxyR initiates other oxidative stress systems such as the sequestration of unincorporated iron by Dps and the repair of polypeptide cysteine oxidation by thioredoxins and glutaredoxins (47). Because OxyR appears to have a critical role in proline promoted oxidative stress resistance, the transcription levels of other antioxidant genes in the OxyR regulon were evaluated. Similar to *katG*, the expression levels of *grxA* (glutaredoxin 1) and *trxC* (thioredoxin 2) in MG1655 wild-type cells increased (~ 7-fold) in a time-dependent manner upon treatment with proline (Figure 3.7 B and C). In MG1655 *ΔputA* cells no changes in *grxA* or *trxC* transcription levels were observed. These results are consistent with proline metabolism activating OxyR.

3.4.5 Proline catabolism generates reactive oxygen species

Because of the above results, we suspected that proline respiration might generate H_2O_2 sufficient enough to activate OxyR. To test this, H_2O_2 levels in

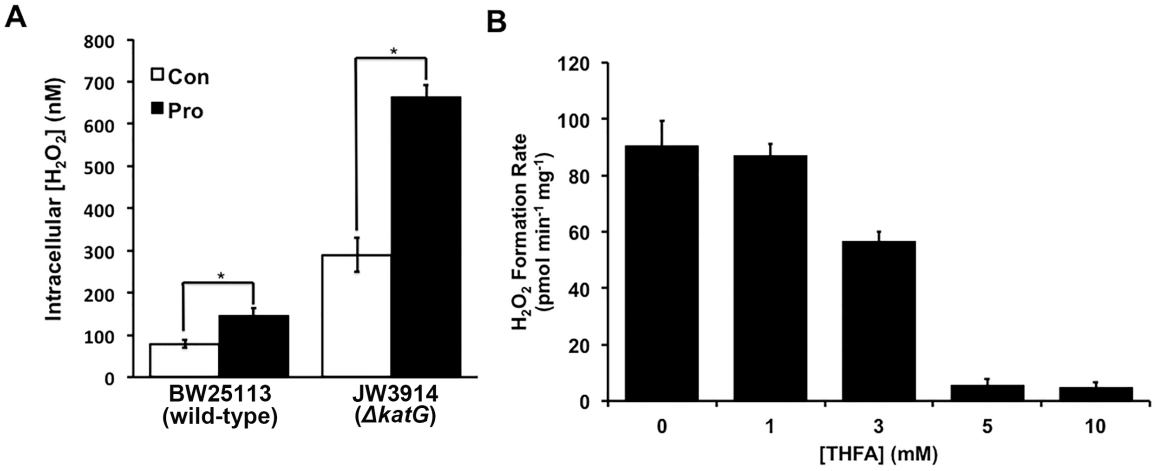

Figure 3.8 Proline metabolism generates H_2O_2. (A) BW25113 wild-type and *ΔkatG* (strain JW3914) cells were grown to exponential phase in minimal medium in the absence (Con) and presence of (Pro) of 10 mM L-proline. H_2O_2 content in medium was measured by Amplex® Red and converted to an estimate of the intracellular H_2O_2 concentration (*$P < 0.05$). (B) *In vitro* assays of H_2O_2 production uses inverted membrane vesicles from *ΔkatG* (strain JW3914) cells. Assays were performed with 50 µg/ml of membrane vesicles and 10 mM proline in the presence of varying concentrations of the PutA inhibitor THFA as indicated. H_2O_2 formation was estimated by the Amplex® Red assay (*$P < 0.05$).

BW25113 wild-type and *ΔkatG* strains were measured with and without proline. Without proline, the estimated intracellular concentration of H_2O_2 in *ΔkatG* cells was nearly 3-fold higher (289 ± 46 nM) than that of wild-type cells (79 ± 7 nM). In both strains, H_2O_2 levels were significantly higher in the presence of proline with a > 2-fold increase observed in the *ΔkatG* cells (663 ± 9 nM). In wild-type cells, intracellular H_2O_2 levels increased to 145 ± 8 nM with proline.

To further evaluate ROS production by proline oxidative metabolism, *in vitro* assays, membrane vesicles prepared from the BW25113 *ΔkatG* mutant strain are used. The rate of H_2O_2 formation with 10 mM proline was 91 ± 9 pmol min^{-1} mg^{-1} which is equivalent to 9.6 ± 0.9 μM min^{-1} when converted into an intracellular endogenous rate (Figure 3.8 B). With 10 mM proline, PutA activity in the membrane vesicle was 103 ± 6.5 nmol P5C min^{-1} mg^{-1}, indicating that the H_2O_2 production rate is ~0.1% of the PutA turnover rate. L-THFA was observed to inhibit H_2O_2 formation in a dose-dependent manner, with 5 mM THFA almost completely blocking H_2O_2 production (Fig. 3.8B). PutA activity was completely abolished with the concentration of THFA. With membrane vesicles as the electron acceptor, PutA has a K_m value of 1.5 mM proline. These results indicate that PutA/PRODH activity is required for H_2O_2 formation with proline.

3.4.6 Proline catabolism-mediated reactive oxygen species are produced at α-ketoglutarate dehydrogenase, glutamate dehydrogenase and cytochrome *bo*.

For PutA from *E. coli*, molecular oxygen is not a good electron acceptor,

therefore proline oxidation induced ROS is not generated by PutA itself (51). Instead, PutA most likely promotes the formation of endogenous H_2O_2 by passing electrons into the ubiquinone pool via the PRODH domain of PutA and the NADH pool via the activities of the P5CDH domain of PutA, glutamate dehydrogenase (GDH) and α-ketoglutarate dehydrogenase (aka, oxoglutarate dehydrogenase, OGDH) (Figure 3.9A). Increased electron flux through the respiratory chain in periplasmic membrane results in $O_2^{\cdot -}$ and subsequently H_2O_2 formation (Figure 3.9A). GDH and OGDH were found on the bacteria membrane vesicle by immunology study (52) and mass spectrometry (53), respectively. Therefore, in the *E. coli* membrane vesicle, both the PRODH and P5CDH domains of PutA, as well as OGDH and GDH are likely to be sources of proline-dependent ROS in assays with mitochondrial vesicles.

NAD^+ supplementation may induce the activities of all enzymes that consume NAD^+, which includes the P5CDH domain of PutA, OGDH and GDH (Figure 3.9B), thus elevating the amount of NADH and adding more fuel to the ETC and increasing H_2O_2 production. Consistent with this idea, addition of NAD^+ (0.2 mM) to *E. coli* membrane vesicles boost the production of H_2O_2 from 91 ± 9 pmol min^{-1} mg^{-1} to 2,524 ± 45 pmol min^{-1} mg^{-1} (Figure 3.9B). Treatment of the vesicles with 20 mM THFA, which is sufficient to completely inhibit PutA activity in membrane vesicles, dramatically reduced H_2O_2 production to 236 ± 3 pmol min^{-1} mg^{-1} (Figure 3.9 B). This result indicates that the basal H_2O_2 generation rate of NADH dehydrogenase and its downstream electron transporters is around 230 pmol min^{-1} mg^{-1} with saturating amounts of NAD^+. Thus, NADH provided by the P5CDH

domain of PutA, GDH and OGDH to the ETC can maximally generate 2.3 μmol of H_2O_2 per min. Because the H_2O_2 production rate using glutamate and proline has no difference (Figure 3.9 B), the P5CDH domain of PutA appears to have a minimal effect on ROS production. In contrast, when using succinate as a substrate, the H_2O_2 production rate is 25% lower than glutamate or proline used as a substrate (Figure 3.9 B), indicating that NADH provided via GDH and OGDH may account for 25% of proline-induced ROS production.

In the respiratory chain of *E. coli*, NADH dehydrogenase II, the primary site of ROS production, produces 133 molecules of H_2O_2 per min (54). Although ROS is generated at a slower rate, succinate dehydrogenase produces 13 molecules of H_2O_2 per min (55). Different from eukaryotes, *E. coli* uses cytochrome *bd* oxygen reductase or cytochrome *bo* oxygen reductase as terminal oxidases (Figure 3.9A). Cytochrome *bd* has a high affinity for molecular oxygen, predominates in *E. coli* under low oxygen conditions (56), and displays notable catalase activity (k_{cat} =130 s^{-1}) (57). In contrast, cytochrome *bo* oxygen reductase, has a low affinity for molecular oxygen and is the predominate enzyme during aerobic growth (56). Therefore, cytochrome *bo* terminal oxidase, instead of cytochrome *bd* oxygen reductase may contribute to ROS production in *E. coli* during aerobic exponential growth. In summary, NADH dehydrogenase, succinate dehydrogenase and cytochrome *bo* terminal oxidase are possible sources of proline-dependent ROS in the respiratory chain during aerobic growth.

Next, to answer which electron transporter in the respiratory chain is responsible for proline oxidation induced ROS, antimycin A was used. Antimycin

A is a compound that preferentially blocks electron transport between ubiquinone and cytochrome bd (58). With 1 μM of antimycin A, ~50% of electron flow between ubiquinone and cytochrome b is blocked and H_2O_2 production, due to ubisemiquinone autoxidation and reverse electron flow through NADH dehydrogenase, is increased by 2-3 fold (58). The application of 2 μM antimycin A along with 10 mM proline decreases both the PutA activity and H_2O_2 production rate, however, the H_2O_2 formation rate is still 0.1% of the PutA turnover rate, the same as that determined in the absence of antimycin A (Figure 3.9D). Since antimycin A has no effect on proline-dependent H_2O_2 formation, the source of proline-dependent H_2O_2 on respiratory chain is the most likely cytochrome *bo* terminal oxidase.

3.5 DISCUSSION

Proline is a multifaceted amino acid with important roles in carbon and nitrogen metabolism, protein synthesis, and protection against various environmental factors such as drought (59), metal toxicity (60,61), osmotic stress (26,27), ultraviolent irradiation (62), unfolded protein stress (25,63), and oxidative stress (22,28,64-66). In this study, we explored the role of proline metabolism in oxidative stress protection by characterizing the oxidative stress response of wild-type and *putA* mutant *E. coli* strains. Wild-type *E. coli* strains exhibited significantly higher resistance to H_2O_2 stress relative to the *putA* mutant strains in medium supplemented with proline. Complementation of the *putA* mutant strains with PutA restored oxidative stress protection to near that of the parent wild-type strain.

These results indicate that stress protection afforded by proline is a general phenotype in *E. coli*, and is dependent on PutA.

The addition of proline to the culture medium increased total catalase activity and led to significantly higher expression of *katG* in wild-type cells whereas no significant increase in catalase was observed with proline in *ΔputA* cells. Proline did not protect *ΔkatG* cells indicating that hydroperoxidase I is necessary for proline-enhanced protection against H_2O_2 stress in *E. coli*. The *katG* gene is regulated by the transcription factor OxyR (67), which is a critical regulator of cellular response to H_2O_2 and thiol redox changes. The OxyR regulon encodes response genes such as *katG*, *grxA* (glutaredoxin I), *trxC* (thioredoxin 2), and *ahpCF* (peroxidiredoxin AhpCF) that provide protection against reactive oxygen species (49). Consistent with hydroperoxidase I having a critical role in proline protection, proline did not improve the oxidative stress survival of the *oxyR* mutant strain. In addition, proline increased the expression of other genes in the OxyR regulon such as *grxA* and *trxC*. Whether proline broadly affects the OxyR regulon will require a more extensive profiling of gene expression changes. Altogether, our results indicate that proline catabolism activates OxyR, leading to increased expression of *katG*. In contrast to the *oxyR* mutant, proline enhanced the oxidative stress resistance of *soxR* mutant cells indicating that SoxR is not essential for proline protection.

The finding that proline increases transcription of genes in the OxyR regulon suggests that proline metabolism increases intracellular H_2O_2. OxyR reacts with H_2O_2 to form a disulfide bond between Cys199 and Cys208, which

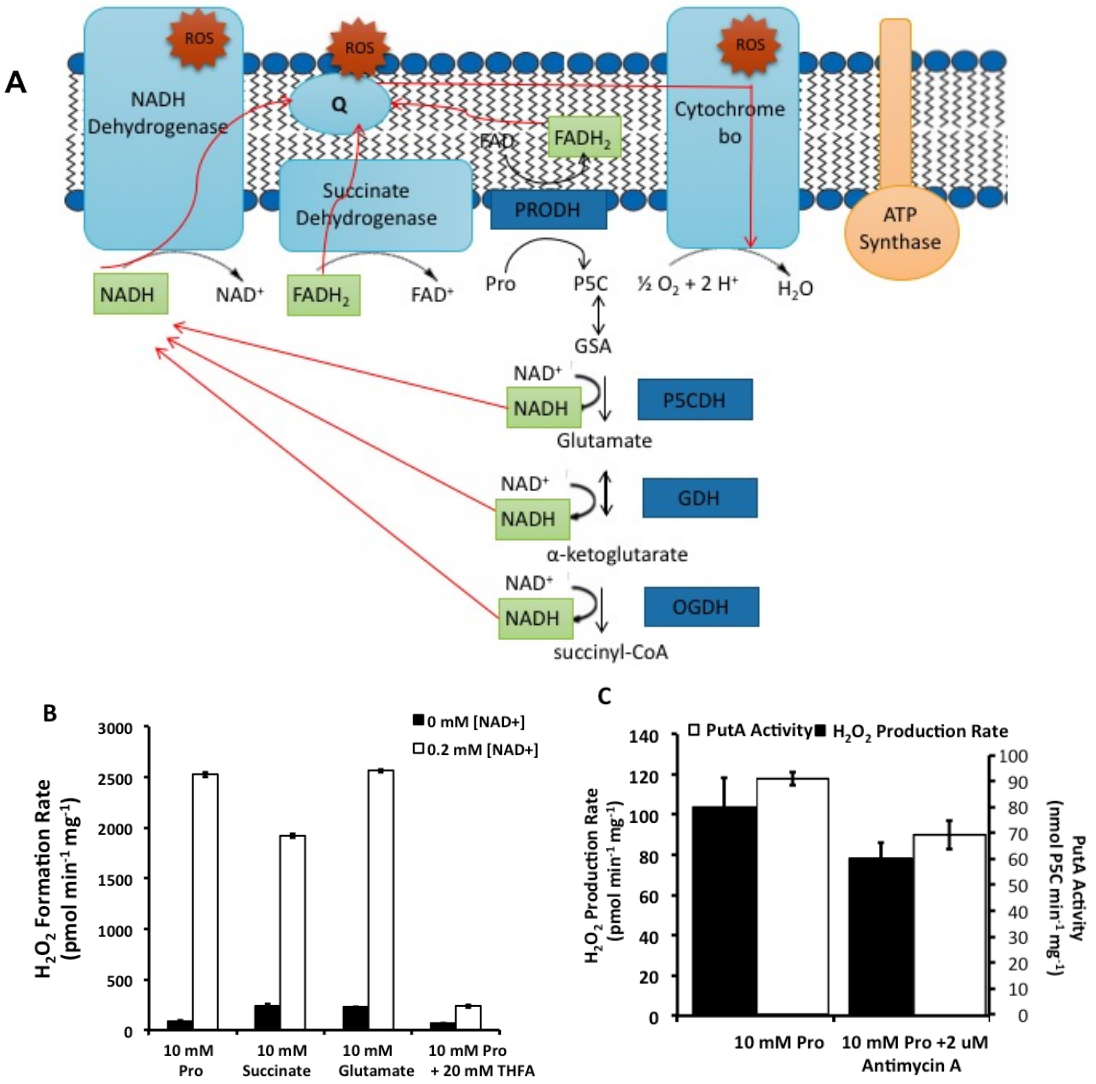

Figure 3.9 Proline catabolism-mediated reactive oxygen species are produced at oxoglutarate dehydrogenase and NADH dehydrogenase. (A). In *E. coli* membrane vesicles, $FADH_2$ provided by the PRODH domain of PutA and NADH provided by the P5CDH domain of PutA, GDH and OGDH fuel the ETC and ROS production. **(B)**. Rate of H_2O_2 production in response to different substrates and NAD^+ supplementation. (C). The effect of complex *bd* inhibitor Antimycin A on H_2O_2 production rate.

results in transcriptional activation of the OxyR regulon (68,69). Oxidation of OxyR and activation of the OxyR regulon have been reported to occur with 0.05-0.2 μM H_2O_2 (70,71). We observed a significant increase in endogenous H_2O_2 levels in *ΔkatG* cells with proline and, in wild-type cells, H_2O_2 levels were found to be > 0.1 μM with proline. Thus, it appears that proline oxidative metabolism can drive H_2O_2 concentrations to levels that are sufficient to induce OxyR. The rapid increase of *katG* transcription by proline treatment (20 min) is also consistent with the response time of the OxyR regulon to H_2O_2 stress (49).

Previous work has addressed metabolic sources of endogenous ROS in *E. coli* indicating that the respiratory chain contributes to the majority of endogenous H_2O_2 production (58). It was found, however, that H_2O_2 can also be significantly generated in *E. coli* by enzymes not associated with the respiratory chain (72). The oxidation of proline by PutA provides reducing equivalents directly to the respiratory pathway via ubiquinone (5). The PRODH domain of PutA contains a FAD cofactor that couples the oxidation of proline (reductive half-reaction) to the reduction of ubiquinone in the membrane (oxidative half-reaction). The rate limiting step in the proline:ubiquinone oxidoreductase reaction catalyzed by PutA is the oxidative step ($FADH_2$ oxidation by ubiquinone) (73). Production of H_2O_2 by proline oxidation would conceivably involve increased flux in the respiratory chain or aberrant electron transfer from $FADH_2$ to molecular oxygen generating superoxide anion radicals, a general feature of flavoenzymes. In a previous study, the reactivity of different PutA proteins with molecular oxygen was evaluated and PutA from *E. coli* was shown to have a turnover number of < 0.3 min^{-1} with oxygen (51).

Thus, we propose that endogenous H_2O_2 from proline metabolism is not generated directly by PutA, but rather by PRODH domain of PutA passing electrons into the ubiquinone pool and P5CDH domain of PutA, as well as GDH and OGDH producing NADH. Those reducing equivalents would lead to increased electron flux through the respiratory chain. Consistent with this, we observed that proline elevates respiration in wild-type *E.coli* cells by 4-fold using the redox indicator 2,3,5-triphenyl tetrazolium chloride. Superoxide that results from proline metabolism would be converted to H_2O_2 either non-enzymatically or enzymatically by superoxide dismutase. Our measurement of intracellular H_2O_2 in wild-type cells grown without proline is consistent with the physiological concentration of H_2O_2 (< 0.1 μM) reported previously for *E. coli* in the exponential growth phase (74). Two-fold increases in H_2O_2 production, which we observed with proline, have also been shown to significantly induce *katG* expression with intracellular H_2O_2 at 0.1-0.2 μM (58). Thus, increases in the endogenous levels of H_2O_2 as a byproduct of proline metabolism are likely to be enough to activate OxyR, which induces *katG* expression. Compared with the rate of H_2O_2 production by NADH dehydrogenase II, the main ROS producer on the respiratory chain of *E.coli*, the amount of H_2O_2 produced during proline oxidation is modest, and capable of serving as adaptive signal without causing detrimental effect on the cells.

We also studied the sources of proline-dependent ROS. Our results indicate that cytochrome *bo* terminal oxidase is the most likely source of proline-induced ROS in the respiratory chain. Among all the enzymes associated with proline oxidation, OGDH and GDH are the main suppliers of reducing equivalents

to the respiratory chain. This supports the unique role of proline oxidation in providing NADH for H_2O_2 production. Glycolysis and the TCA cycle also provide NADH to the respiratory chain, however, neither glucose nor glycine (which enters the TCA cycle via pyruvate) is able to induce H_2O_2 production or protect *E. coli* against oxidative stress (Data not shown).

The observation that proline metabolism can influence hydroperoxidase I activity, indicates that besides serving as an important growth substrate in nutritional deplete microenvironments, proline may offer a competitive advantage to bacteria in harsh oxidative environments. Bacteria often encounter oxidative stress from the host immune system such as the respiratory burst associated with phagocytic killing of microbes (75). Previously, pretreatment of *E. coli* cells with low amounts of H_2O_2 was shown to have a protective effect by 10-fold induction of hydroperoxidase I (76,77). Here, proline metabolism may also provide a preconditioning effect by generating H_2O_2 as a by-product and elevating hydroperoxidase I levels, thereby raising the overall stress tolerance of the cell. Various studies of proline metabolism in eukaryotes have shown that proline oxidation, which in eukaryotes occurs in the mitochondrion, generates ROS (22,66) which can mediate cell death (78), cell survival against oxidative stress (65), and lifespan (79). The results from this work further illustrate the fundamental importance of how H_2O_2 as a metabolic by-product, can enhance oxidative stress tolerance and appear to be an underlying feature of proline metabolism that is conserved between *E. coli* and mammals.

REFERENCES

1. Jeffery, C. J. (2004) Molecular mechanisms for multitasking: recent crystal structures of moonlighting proteins. *Curr Opin Struct Biol* **14**, 663-668
2. Krishnan, N., and Becker, D. F. (2005) Characterization of a bifunctional PutA homologue from *Bradyrhizobium japonicum* and identification of an active site residue that modulates proline reduction of the flavin adenine dinucleotide cofactor. *Biochemistry* **44**, 9130-9139
3. Tanner, J. J. (2008) Structural biology of proline catabolism. *Amino Acids* **35**, 719-730
4. Menzel, R., and Roth, J. (1981) Enzymatic properties of the purified *putA* protein from *Salmonella typhimurium*. *J. Biol. Chem.* **256**, 9762-9766
5. Moxley, M. A., Tanner, J. J., and Becker, D. F. (2011) Steady-state kinetic mechanism of the proline:ubiquinone oxidoreductase activity of proline utilization A (PutA) from Escherichia coli. *Arch Biochem Biophys* **516**, 113-120
6. Becker, D. F., and Thomas, E. A. (2001) Redox properties of the PutA protein from Escherichia coli and the influence of the flavin redox state on PutA-DNA interactions. *Biochemistry* **40**, 4714-4721
7. Gu, D., Zhou, Y., Kallhoff, V., Baban, B., Tanner, J. J., and Becker, D. F. (2004) Identification and characterization of the DNA-binding domain of the multifunctional PutA flavoenzyme. *J. Biol. Chem.* **279**, 31171-31176
8. Zhou, Y., Larson, J. D., Bottoms, C. A., Arturo, E. C., Henzl, M. T., Jenkins, J. L., Nix, J. C., Becker, D. F., and Tanner, J. J. (2008) Structural basis of the transcriptional regulation of the proline utilization regulon by multifunctional PutA. *J Mol Biol* **381**, 174-188
9. Zhou, Y., Zhu, W., Bellur, P. S., Rewinkel, D., and Becker, D. F. (2008) Direct linking of metabolism and gene expression in the proline utilization A protein from *Escherichia coli*. *Amino Acids* **35**, 711-718
10. Zhang, W., Zhou, Y., and Becker, D. F. (2004) Regulation of PutA-membrane associations by flavin adenine dinucleotide reduction. *Biochemistry* **43**, 13165-13174
11. Ostrovsky De Spicer, P., and Maloy, S. (1993) PutA protein, a membrane-associated flavin dehydrogenase, acts as a redox-dependent transcriptional regulator. *Proc. Natl. Acad. Sci. USA.* **90**, 4295-4298
12. Wood, J. (1987) Membrane association of proline dehydrogenase in *Escherichia coli* is redox dependent. *Proc. Natl. Acad. Sci. USA.* **84**, 373-377
13. Nagata, K., Nagata, Y., Sato, T., Fujino, M. A., Nakajima, K., and Tamura, T. (2003) L-Serine, D- and L-proline and alanine as respiratory substrates of Helicobacter pylori: correlation between in vitro and in vivo amino acid levels. *Microbiology* **149**, 2023-2030
14. Curtis, J., Shearer, G., and Kohl, D. H. (2004) Bacteriod proline catabolism affects N_2 fixation rate of drought-stressed soybeans. *Plant Physiol.* **136**, 3313-3318

15. Kohl, D. H., Schubert, K. R., Carter, M. B., Hagedorn, C. H., and Shearer, G. (1988) Proline metabolism in N_2-fixing root nodules: Energy transfer and regulation of purine synthesis. *Proc. Natl. Acad. Sci. USA* **85**, 2036-2040
16. Vílchez, S., Manzanera, M., and Ramos, J. (2000) Control of expression of divergent *Pseudomonas putida put* promoters for proline catabolism. *Appl. Environ. Microbiol* **66**, 5221-5225
17. Wood, J. M. (1981) Genetics of L-proline utilization in *Eschericia coli*. *J. Bacteriol.* **146**, 895-901
18. van Amsterdam, K., and van der Ende, A. (2004) Nutrients released by gastric epithelial cells enhance *Helicobacter pylori* growth. *Helicobacter* **9**, 614-621
19. Kelly, D. J. (1998) The physiology and metabolism of the human gastric pathogen Helicobacter pylori. *Adv Microb Physiol* **40**, 137-189
20. Nakajima, K., Natsu, S., Mizote, T., Nagata, Y., Aoyania, K., Fukuda, Y., and Nagata, K. (2008) Possible involvement of putA gene in *Helicobacter pylori* colonization in the stomach and motility. *Biomed Res-Tokyo* **29**, 9-18
21. Sharma, S., Villamor, J. G., and Verslues, P. E. (2011) Essential role of tissue-specific proline synthesis and catabolism in growth and redox balance at low water potential. *Plant Physiol* **157**, 292-304
22. Szabados, L., and Savoure, A. (2010) Proline: a multifunctional amino acid. *Trends in Plant Science* **15**, 89-97
23. Cecchini, N. M., Monteoliva, M. I., and Alvarez, M. E. (2011) Proline dehydrogenase contributes to pathogen defense in Arabidopsis. *Plant Physiol* **155**, 1947-1959
24. Morita, Y., Nakamori, S., and Takagi, H. (2003) L-proline accumulation and freeze tolerance of Saccharomyces cerevisiae are caused by a mutation in the PRO1 gene encoding gamma-glutamyl kinase. *Appl Environ Microbiol* **69**, 212-219
25. Chattopadhyay, M. K., Kern, R., Mistou, M. Y., Dandekar, A. M., Uratsu, S. L., and Richarme, G. (2004) The chemical chaperone proline relieves the thermosensitivity of a *dnaK* deletion mutant at 42 degrees C. *J. Bacteriol.* **186**, 8149-8152
26. Csonka, L. N. (1981) Proline over-production results in enhanced osmotolerance in *Salmonella typhimurium*. *Mol. Gen. Genet.* **182**, 82-86
27. Wood, J. M. (1988) Proline porters effect the utilization of proline as a nutrient of osmoprotectant for bacteria. *J. Membr. Biol.* **106**, 183-202
28. Chen, C., and Dickman, M. B. (2005) Proline suppresses apoptosis in the fungal pathogen of *Colletotrichum trifolii*. *Proc. Natl. Acad. Sci. U S A* **102**, 3459-3464
29. Krishnan, N., Doster, A. R., Duhamel, G. E., and Becker, D. F. (2008) Characterization of a *Helicobacter hepaticus putA* mutant strain in host colonization and oxidative stress. *Infect Immun* **76**, 3037-3044
30. Wang, G., Alamuri, P., and Maier, R. J. (2006) The diverse antioxidant systems of *Helicobacter pylori*. *Mol Microbiol* **61**, 847-860

31. Wang, G., Hong, Y., Olczak, A., Maier, S. E., and Maier, R. J. (2006) Dual Roles of *Helicobacter pylori* NapA in inducing and combating oxidative stress. *Infect Immun* **74**, 6839-6846
32. Sato, D., Yanaka, A., Shibahara, T., Matsui, H., Nakahara, A., Yanagawa, T., Warabi, E., Ishii, T., and Hyodo, I. (2007) Peroxiredoxin I protects gastric mucosa from oxidative injury induced by *H. pylori* infection. *J Gastroenterol Hepatol*
33. Kim, H. (2005) Oxidative stress in *Helicobacter pylori*-induced gastric cell injury. *Inflammopharmacology* **13**, 63-74
34. Miller, J. H. (1972) *Experiments in molecular genetics*, Cold Spring Harbor Laboratory, Cold Spring Harbor, N.Y.
35. Guyer, M. S., Reed, R. R., Steitz, J. A., and Low, K. B. (1981) Identification of a sex-factor-affinity site in E. coli as gamma delta. *Cold Spring Harb Symp Quant Biol* **45 Pt 1**, 135-140
36. Liu, Y., and Imlay, J. A. (2013) Cell death from antibiotics without the involvement of reactive oxygen species. *Science* **339**, 1210-1213
37. Baba, T., Ara, T., Hasegawa, M., Takai, Y., Okumura, Y., Baba, M., Datsenko, K. A., Tomita, M., Wanner, B. L., and Mori, H. (2006) Construction of Escherichia coli K-12 in-frame, single-gene knockout mutants: the Keio collection. *Mol Syst Biol* **2**, 2006 0008
38. Zhu, W., Haile, A. M., Singh, R. K., Larson, J. D., Smithen, D., Chan, J. Y., Tanner, J. J., and Becker, D. F. (2013) Involvement of the beta3-alpha3 loop of the proline dehydrogenase domain in allosteric regulation of membrane association of proline utilization A. *Biochemistry* **52**, 4482-4491
39. Seaver, L. C., and Imlay, J. A. (2001) Alkyl hydroperoxide reductase is the primary scavenger of endogenous hydrogen peroxide in Escherichia coli. *J Bacteriol* **183**, 7173-7181
40. Abrahamson, J. L., Baker, L. G., Stephenson, J. T., and Wood, J. M. (1983) Proline dehydrogenase from Escherichia coli K12. Properties of the membrane-associated enzyme. *Eur J Biochem* **134**, 77-82
41. Starkov, A. A. (2010) Measurement of mitochondrial ROS production. *Methods Mol Biol* **648**, 245-255
42. Imlay, J. A., and Fridovich, I. (1991) Assay of metabolic superoxide production in Escherichia coli. *The Journal of biological chemistry* **266**, 6957-6965
43. Srivastava, D., Schuermann, J. P., White, T. A., Krishnan, N., Sanyal, N., Hura, G. L., Tan, A., Henzl, M. T., Becker, D. F., and Tanner, J. J. (2010) Crystal structure of the bifunctional proline utilization A flavoenzyme from Bradyrhizobium japonicum. *Proceedings of the National Academy of Sciences of the United States of America* **107**, 2878-2883
44. Sezonov, G., Joseleau-Petit, D., and D'Ari, R. (2007) Escherichia coli physiology in Luria-Bertani broth. *J Bacteriol* **189**, 8746-8749
45. Braeken, K., Fauvart, M., Vercruysse, M., Beullens, S., Lambrichts, I., and Michiels, J. (2008) Pleiotropic effects of a rel mutation on stress survival of Rhizobium etli CNPAF512. *BMC Microbiol* **8**, 219

46. Magnusson, L. U., Farewell, A., and Nystrom, T. (2005) ppGpp: a global regulator in Escherichia coli. *Trends Microbiol* **13**, 236-242
47. Imlay, J. A. (2008) Cellular defenses against superoxide and hydrogen peroxide. *Annu Rev Biochem* **77**, 755-776
48. Switala, J., O'Neil, J. O., and Loewen, P. C. (1999) Catalase HPII from Escherichia coli exhibits enhanced resistance to denaturation. *Biochemistry* **38**, 3895-3901
49. Zheng, M., Wang, X., Templeton, L. J., Smulski, D. R., LaRossa, R. A., and Storz, G. (2001) DNA microarray-mediated transcriptional profiling of the Escherichia coli response to hydrogen peroxide. *J Bacteriol* **183**, 4562-4570
50. Singh, A. K., Shin, J. H., Lee, K. L., Imlay, J. A., and Roe, J. H. (2013) Comparative study of SoxR activation by redox-active compounds. *Molecular microbiology* **90**, 983-996
51. Krishnan, N., and Becker, D. F. (2006) Oxygen reactivity of PutA from Helicobacter species and proline-linked oxidative stress. *J Bacteriol* **188**, 1227-1235
52. Atassi, M. Z., Van Oss, C. J., and Absolom, D. R. (1984) *Molecular immunology : a textbook*, M. Dekker, New York
53. Toyofuku, M., Roschitzki, B., Riedel, K., and Eberl, L. (2012) Identification of proteins associated with the Pseudomonas aeruginosa biofilm extracellular matrix. *J Proteome Res* **11**, 4906-4915
54. Messner, K. R., and Imlay, J. A. (1999) The identification of primary sites of superoxide and hydrogen peroxide formation in the aerobic respiratory chain and sulfite reductase complex of Escherichia coli. *The Journal of biological chemistry* **274**, 10119-10128
55. Messner, K. R., and Imlay, J. A. (2002) Mechanism of superoxide and hydrogen peroxide formation by fumarate reductase, succinate dehydrogenase, and aspartate oxidase. *The Journal of biological chemistry* **277**, 42563-42571
56. Trumpower, B. L., and Gennis, R. B. (1994) Energy transduction by cytochrome complexes in mitochondrial and bacterial respiration: the enzymology of coupling electron transfer reactions to transmembrane proton translocation. *Annu Rev Biochem* **63**, 675-716
57. Borisov, V. B., Forte, E., Davletshin, A., Mastronicola, D., Sarti, P., and Giuffre, A. (2013) Cytochrome bd oxidase from Escherichia coli displays high catalase activity: an additional defense against oxidative stress. *FEBS Lett* **587**, 2214-2218
58. Gonzalez-Flecha, B., and Demple, B. (1995) Metabolic sources of hydrogen peroxide in aerobically growing Escherichia coli. *The Journal of biological chemistry* **270**, 13681-13687
59. Barnett, N. M., and Naylor, A. W. (1966) Amino Acid and protein metabolism in bermuda grass during water stress. *Plant Physiol* **41**, 1222-1230
60. Chen, C. T., Chen, L., Lin, C. C., and Kao, C. H. (2001) Regulation of proline accumulation in detached rice leaves exposed to excess copper. *Plant Sci* **160**, 283-290

61. Tripathi, B. N., Mehta, S. K., Amar, A., and Gaur, J. P. (2006) Oxidative stress in Scenedesmus sp. during short- and long-term exposure to Cu2+ and Zn2+. *Chemosphere* **62**, 538-544
62. Saradhi, P. P., Alia, Arora, S., and Prasad, K. V. (1995) Proline accumulates in plants exposed to UV radiation and protects them against UV induced peroxidation. *Biochemical and biophysical research communications* **209**, 1-5
63. Liang, X., Dickman, M. B., and Becker, D. F. (2014) Proline Biosynthesis is Required for Endoplasmic Reticulum Stress Tolerance in Saccharomyces cerevisiae. *The Journal of biological chemistry*
64. Krishnan, N., Dickman, M. B., and Becker, D. F. (2008) Proline modulates the intracellular redox environment and protects mammalian cells against oxidative stress. *Free radical biology & medicine* **44**, 671-681
65. Natarajan, S. K., Zhu, W., Liang, X., Zhang, L., Demers, A. J., Zimmerman, M. C., Simpson, M. A., and Becker, D. F. (2012) Proline dehydrogenase is essential for proline protection against hydrogen peroxide-induced cell death. *Free radical biology & medicine* **53**, 1181-1191
66. Liang, X., Zhang, L., Natarajan, S. K., and Becker, D. F. (2013) Proline mechanisms of stress survival. *Antioxidants & redox signaling* **19**, 998-1011
67. Visick, J. E., and Clarke, S. (1997) RpoS- and OxyR-independent induction of HPI catalase at stationary phase in Escherichia coli and identification of rpoS mutations in common laboratory strains. *J Bacteriol* **179**, 4158-4163
68. Lee, C., Lee, S. M., Mukhopadhyay, P., Kim, S. J., Lee, S. C., Ahn, W. S., Yu, M. H., Storz, G., and Ryu, S. E. (2004) Redox regulation of OxyR requires specific disulfide bond formation involving a rapid kinetic reaction path. *Nat Struct Mol Biol* **11**, 1179-1185
69. Zheng, M., Aslund, F., and Storz, G. (1998) Activation of the OxyR transcription factor by reversible disulfide bond formation. *Science* **279**, 1718-1721
70. Gonzalez-Flecha, B., and Demple, B. (1997) Homeostatic regulation of intracellular hydrogen peroxide concentration in aerobically growing Escherichia coli. *J Bacteriol* **179**, 382-388
71. Aslund, F., Zheng, M., Beckwith, J., and Storz, G. (1999) Regulation of the OxyR transcription factor by hydrogen peroxide and the cellular thiol-disulfide status. *Proceedings of the National Academy of Sciences of the United States of America* **96**, 6161-6165
72. Seaver, L. C., and Imlay, J. A. (2004) Are respiratory enzymes the primary sources of intracellular hydrogen peroxide? *The Journal of biological chemistry* **279**, 48742-48750
73. Moxley, M. A., and Becker, D. F. (2012) Rapid reaction kinetics of proline dehydrogenase in the multifunctional proline utilization a protein. *Biochemistry* **51**, 511-520
74. Seaver, L. C., and Imlay, J. A. (2001) Hydrogen peroxide fluxes and compartmentalization inside growing Escherichia coli. *J Bacteriol* **183**, 7182-7189

75. Jiang, F., Zhang, Y., and Dusting, G. J. (2011) NADPH oxidase-mediated redox signaling: roles in cellular stress response, stress tolerance, and tissue repair. *Pharmacological reviews* **63**, 218-242
76. Imlay, J. A., and Linn, S. (1986) Bimodal pattern of killing of DNA-repair-defective or anoxically grown Escherichia coli by hydrogen peroxide. *J Bacteriol* **166**, 519-527
77. Imlay, J. A., and Linn, S. (1987) Mutagenesis and stress responses induced in Escherichia coli by hydrogen peroxide. *J Bacteriol* **169**, 2967-2976
78. Liu, W., Le, A., Hancock, C., Lane, A. N., Dang, C. V., Fan, T. W., and Phang, J. M. (2012) Reprogramming of proline and glutamine metabolism contributes to the proliferative and metabolic responses regulated by oncogenic transcription factor c-MYC. *Proceedings of the National Academy of Sciences of the United States of America* **109**, 8983-8988
79. Zarse, K., Schmeisser, S., Groth, M., Priebe, S., Beuster, G., Kuhlow, D., Guthke, R., Platzer, M., Kahn, C. R., and Ristow, M. (2012) Impaired insulin/IGF1 signaling extends life span by promoting mitochondrial L-proline catabolism to induce a transient ROS signal. *Cell metabolism* **15**, 451-465

CHAPTER 4

Proline Oxidation and ROS Production in Mammalian Mitochondria

4.1 ABSTRACT

Besides serving as an energy source and building block of proteins, proline and its oxidation in human cells play an important role in regulating cell apoptosis, proliferation, autophagy and defense against oxidative stress. All of these functions of proline catabolism appear to be associated with reactive oxygen species (ROS). Previously, we have shown that proline catabolism protects human cell lines from H_2O_2 stress by maintaining ATP levels and activating the Akt pathway. However, it is unclear whether proline-induced ROS is involved in this protection. Recently, proline-dependent ROS was shown to serve as an adaptive signal to H_2O_2 stress in *E. coli*. We hypothesize that the generation of ROS by proline catabolism is a conserved feature in different organisms that potentially influences various cell signaling pathways such as the OxyR regulon in *E. coli*, Nrf2 in worm, and Akt in human cell lines. In this chapter, proline catabolism is studied in mitochondria isolated from mammalian cells to evaluate ROS production as a function of proline and PRODH activity. ROS generation from proline was observed in mitochondria isolated from a human cell line and pig kidney, suggesting proline-induced ROS is common to mammalian cells. In addition, we found mitochondria using proline as a substrate have a lower efficiency (low respiration and high ROS production) than those using succinate as a substrate. Our data suggest that the amount of ROS generated by proline oxidation is sufficient to serve as an adaptive signal to oxidative stress and does not exceed a threshold that would induce adverse effects.

4.2 INTRODUCTION

Proline oxidation and ROS signaling have been shown to play a vital role in mammalian cell proliferation, apoptosis and survival (1-3). The various cellular responses to proline oxidation are thought to be due to different amounts of ROS. Constitutively expressed PRODH is associated with a lower amount of ROS production and is associated with protective effects, such as pro-survival autophagy in neurons encountering cytotoxic HIV envelope protein gp120 (4). Overexpression of PRODH, such as induction by p53, usually results in deleterious effects, such as cell apoptosis (5).

Previously, our lab has shown that proline treatment is capable of protecting human embryonic kidney 293 (HEK293) cells against H_2O_2 stress by diminishing the amount of ROS in the cell (6). Later, the beneficial effect of proline on WM35 (human melanoma cell lines) and PC3 (human prostate cancer cell line) cells against H_2O_2 stress was shown to rely on PRODH activity, since knockdown of PRODH abolished the protective effect of proline supplementation (7). Proline oxidation was observed to facilitate cell survival by providing ATP and activating the Akt signaling pathway, which promotes tumor cell survival, proliferation and metastasis (7). Although no evidence was reported in these experiments for transient ROS being generated from proline oxidation, ROS was still implicated as proline treatment induced phosphorylation of Akt at major regulatory sites Ser-473 and Thr-308 (7), which mimics Akt activation by H_2O_2 (8-9). Studies in *E. coli* (10) and *C. elegans* daf-2 mutant (11) have both indicated that ROS is generated during proline oxidation resulting in the upregulation of antioxidant enzymes via

OxyR and p38 MAPK/Nrf2, respectively. Therefore, it is plausible that proline oxidation generates H_2O_2 that is sufficient to activate Akt and other pathways helping to maintain redox homeostasis and promote cell survival.

Previous studies have shown evidence for proline-dependent ROS formation in various mammalian cell lines using a fluorescence probe against superoxide anion or hydrogen peroxide, however, little is known about the actual sites of ROS formation during proline oxidation. So far, the sources of proline-dependent ROS in mammalian cells were reported to be PRODH itself and/or the electron transport chain (ETC) of mitochondria. In support of the former source, partially purified human PRODH exhibited production of superoxide ($O_2^{\bullet-}$) during catalytic turnover with proline and molecular oxygen (6), suggesting that PRODH can react with molecular oxygen as an electron acceptor and directly produce ROS. However, the activity of the partially purified PRODH with molecular oxygen was similar (~ 0.1 U/mg) to that with the artificial electron acceptor, 2,6-dichlorophenolindophenol, indicating human PRODH is not a genuine flavoenzyme oxidase (6). Evidence for sites of proline-dependent ROS production in the ETC was obtained from assays using isolated mouse liver mitochondria and ZR75-30 (human breast cancer cell) mitochondria. In these experiments it was concluded that complex III (12) of mouse liver mitochondria and complex I/α-ketoglutarate dehydrogenase (13) of breast cancer cell mitochondria were the sites of ROS generation during proline oxidation.

To further examine potential sites of ROS formation in mitochondria during proline oxidation, we explored sources of ROS in isolated human mitochondria

and pig mitochondria. In this study, we found that in comparison with proline and glutamine co-treatment, WM35 cells with proline treatment alone have a higher survival rate under oxidative stress but a lower maximal oxygen consumption rate, which suggests a higher possibility of ROS production. Consistently, proline treatment induces H_2O_2 production in both whole cells and isolated mitochondria of the CRL2429 (human skin fibroblast) cell line. Proline-mediated H_2O_2 production can be diminished by L-THFA, a competitive inhibitor of PRODH. We also found proline induces superoxide production in isolated pig mitochondria, suggesting superoxide/hydrogen peroxide from proline catabolism is a common feature shared in different mammalian cells. In addition, mitochondria using proline substrate was found to have a higher ratio of ROS production (ROS production/ oxygen consumption) relative to succinate.

4.3 MATERIAL AND METHODS

4.3.1 Materials and growth conditions

All chemicals, enzymes and regents were purchased from Fisher scientific and Sigma-Aldrich, Inc. unless stated otherwise. CRL2429 (human skin fibroblast cell) cell line was purchased from ATCC. WM35 cells were provided by Dr. Adam Richardson and Dr. Jeffrey Smith at the Sanford-Burnham Medical Research Institute, La Jolla, CA. Pig kidney was generously provided by Dr. Brett White, Animal Science Department at the University of Nebraska-Lincoln. WM35 cells and CRL2429 cells were grown in Dulbecco's Modified Eagle's Medium (DMEM) and Iscove's Modified Dulbecco's Medium (IMDM), respectively, and

supplemented with 10% fetal bovine serum (FBS) and 0.25 µg/ml of antibiotic-antimycotic solution (Invitrogen) at 37 °C in 5% CO2 environment. IMDM media was obtained from Thermo Scientific contains 0.35 mM of proline.

4.3.2 Mitochondria isolation

For CRL2429 cells, once cells reached 80% confluence they were scraped off the petri dish and washed twice with ice cold PBS via centrifugation. The cell pellets were resuspended in 5 mM Tris buffer containing 0.25 M sucrose and 1 mM EDTA, pH 7.4. Resuspended cells were hand homogenized using a Dounce homogenizer with 25x up-and-down strokes on ice. The cellular lysates were centrifuged at 150 × g for 10 min at 4 °C and then the supernatants were centrifuged at 17,000 × g for 15 min at 4 °C to pellet the mitochondria. Total protein concentrations were quantified using the Pierce 660 nm protein assay. For isolation of mitochondria from pig kidney, connective tissue and blood vessels were removed from the kidney tissue. The kidney tissue was then cut into 1cm x 1cm pieces and extensively washed with ice cold PBS to remove blood. After that, the kidney tissue was disrupted with Polytron tissue grinder at 500 rpm for 1 min in 5 mM Tris buffer with 0.25 M sucrose and 1 mM EDTA, pH 7.4. Mitochondria were then pelleted with the aforementioned procedures. The presence of human and pig PRODH in isolated human and pig mitochondria were confirmed by western blot against human PRODH and mass spectrometry, respectively.

4.3.3 Western blot

Antibodies recognizing VDAC/Porin were from Sigma. Polyclonal antibodies against PRODH, were custom-made by Proteintech. Horse radish peroxidase (HRP)-labeled anti-mouse, anti-goat and anti-rabbit secondary antibodies were from GE Healthcare. Isolated mitochondria were lysed using M-PER (Pierce) and the proteins of the mitochondrial lysates were resolved by SDS-PAGE. Proteins were transferred to a PVDF membrane and visualized by immunoblotting.

4.3.4 Stress and cell viability

For stress treatments, WM35 and CRL2429 cells were grown to 80% confluence. Cells were then treated with and without 5 mM proline, 10 mM pipecolate or proline plus 4 mM glutamine for 12 hr in cultural media containing 10% FBS. The media was then changed and cells were incubated for 3 hr with and without H_2O_2 stress (0.1 mM or 1 mM, 3 h) in serum free medium. After stress treatment, cells were washed with PBS and cell viability was quantified using the tetrazolium compound [3-(4,5-dimethylthiazol-2-yl)-5-(3-carboxymethoxyphenyl)-2-(4-sulfophenyl)-2H-tetrazolium] (MTS) (Promega). Cell survival rates were determined relative to the control groups.

4.3.5 ROS measurement

H_2O_2 produced by mitochondria and whole CRL2429 cells was measured at room temperature with 50 µg/ml of mitochondria or 13,000 cells/mL and different amounts of substrate. The assay buffer (pH 7.2) included 40 U/mL superoxide

dismutase, 125 mM KCl, 4 mM KH_2PO_4, 14 mM NaCl, 20 mM HEPES-NaOH, 1 mM $MgCl_2$, 0.2% BSA, and 0.02 mM EDTA (14). H_2O_2 was quantified using the Amplex® Red Hydrogen Peroxide/Peroxidase Assay Kit with excitation at 555 nm and monitoring fluorescence emission at 581 nm as described (14) with the rate defined as pmol of H_2O_2 formed min^{-1} mg^{-1} of mitochondria. Superoxide production was detected by measuring the H_2O_2 production rate in the absence of SOD, which is subtracted from the H_2O_2 production rate in the presence of SOD. The effect of L-THFA or antimycin A on H_2O_2 production was determined using the same assay conditions as mentioned above. Background formation of H_2O_2 was determined in control assays without substrate. For the calculation of intracellular levels of H_2O_2 in CRL2429 cells, the cytosolic volume of CRL2429 was estimated to be 940 μm^3 (15).

4.3.6 Measurement of oxygen consumption

The oxygen consumption of isolated mitochondria was measured using a Clark-type electrode. Air-saturated 50 mM phosphate buffer, pH 7.4 (0.5 ml) was introduced into the electrode chamber (capacity of 1 ml) and incubated until a steady baseline was obtained. 50 mg of mitochondria was suspended in 0.5 ml buffer and then added to the incubation chamber using a Hamilton syringe. Oxygen consumption with different substrates was then recorded. All of the measurements were carried out at 25 °C. The oxygen consumption rate (OCR) in intact WM35 cells was measured using a Seahorse XF extracellular Flux analyzer

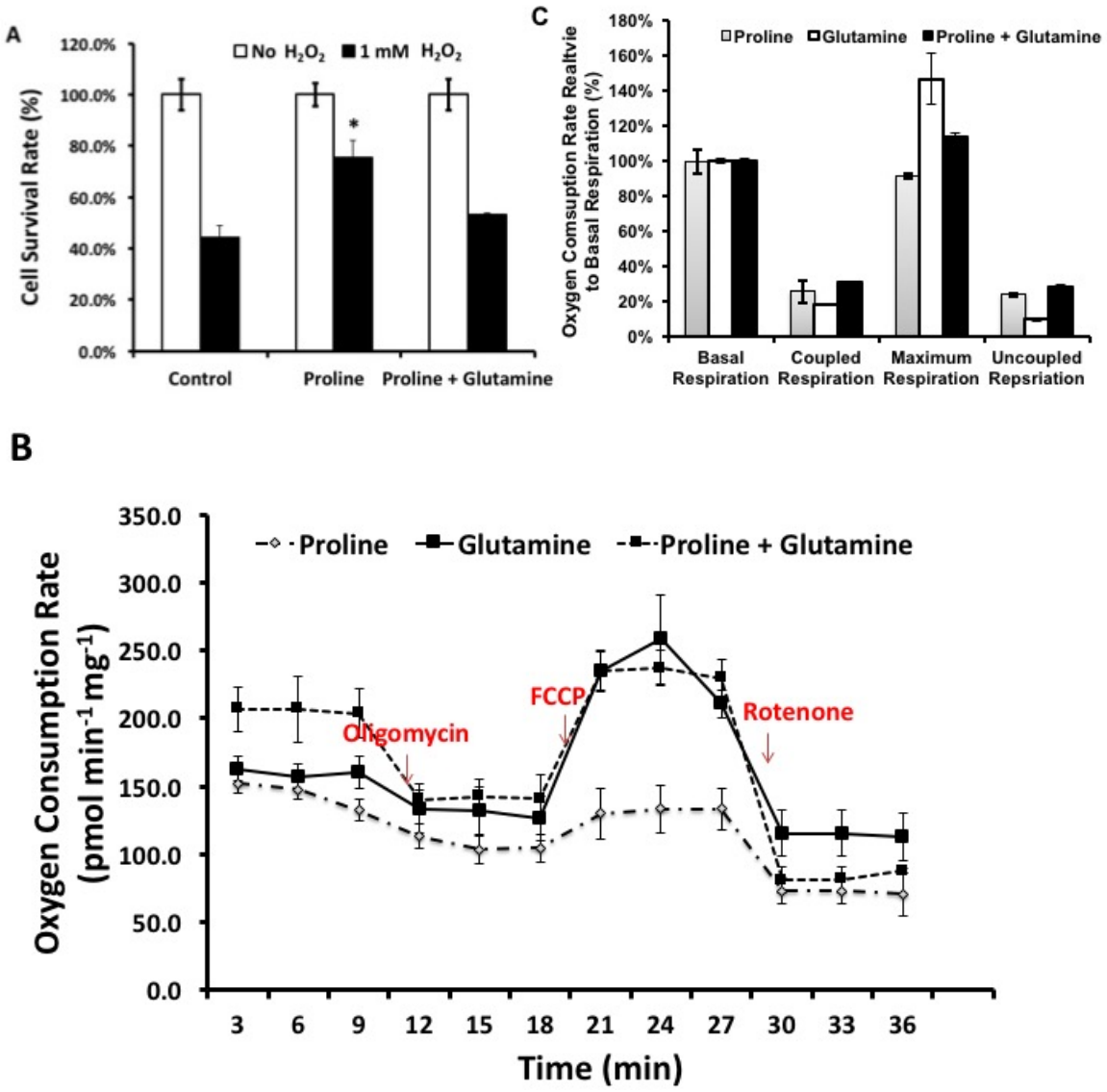

Figure 4.1 **Oxygen consumption and cell survival rate of WM35 cells treated with proline or/and glutamine.** (A) Cell survival rate of cells under 1 mM H_2O_2 with and without treatment of 5 mM proline, or co-treatment of 5 mM proline and 4 mM glutamine. (B, C). Oxygen consumption rate of cells using 5 mM proline, or 5 mM proline plus 4 mM glutamine as substrate.

(Seahorse). 20,000 cells were seeded in a 96-well culture plate in high glucose DMEM media. The cells were then treated with 5 mM proline or 5 mM glutamine for 3 hr before the assay and for the duration of the experiment. Selective inhibitors were injected at the indicated time points during the measurement to achieve the final concentration of 1 μM oligomycin, 2 μM carbonyl cyanide-4-phenylhydrazone (FCCP), and 2 μM rotenone. The baseline OCR was defined as the average of the values measured from time points 1 to 3 during the experiments, and normalized by the total protein concentration. The maximum OCR is the average values from time points 7 to 9, which is after addition of FCCP. The spare OCR is the average values from time points 10 to 12. The coupled OCR is the basal OCR minus the average values from time points 4 to 6. After the analysis the cells were stained with Trypan Blue (Invitrogen) to confirm cell viability.

4.3.7 Measurement of PRODH activity

PRODH activity in the mitochondria was confirmed by quantifying P5C production through adding *o*-aminobenzaldehyde (*o*-AB) (4 mM final concentration) and following the formation of the *o*-AB-P5C yellow complex at 443 nm (ε = 2,900 M^{-1} cm^{-1}) as previously described (16).

4.3.8 Statistic analysis

Data were collected with 3-5 replicates and are expressed as mean ± standard deviation. Statistical significant analysis was tested by Student's t-test, with a *P* value of <0.05 considered to be statistically significant.

4.4 RESULTS

4.4.1 WM35 Cells with proline supplementation have a lower maximum oxygen consumption rate

Previously, 5 mM proline supplementation has been shown to increase the survival rate of HEK293 cells from 39% to 77% after H_2O_2 treatment (0.5 mM, 3 hr) (6). Whereas, 5 mM glutamine showed less ability to protect cells from oxidative stress, with a 45% cell survival rate after H_2O_2 treatment (6). Our study in WM35 cells had a similar result. Without amino acid supplementation, cells had 49% survival rate after H_2O_2 treatment (1 mM, 3 hr) (Figure 4.1A). Treatment with 5 mM proline increased the cell survival rate to 73% , whereas 5 mM proline and 4 mM glutamine co-treatment modestly increased cell survival rate to 53% (Figure 4.1A). Since both proline and glutamine enter the tricarboxylic acid cycle via glutamate and α-ketoglutarate, oxidation of proline and glutamine are likely to provide similar amounts of ATP. To test this hypothesis, we measured the bioenergetic profile of intact WM35 cells (Figure 4.1 B). The coupled respiration is calculated by subtracting the residual respiration, which is the OCR after the addition of oligomycin, an F1Fo-ATPase inhibitor, from the basal respiration. It represents the rate of mitochondria oxygen consumption used for ATP generation via F1Fo-ATPase (17). Proline treatment alone and proline/glutamine co-treatment resulted in no significant difference in coupled respiration (Figure 4.1 C). This is consistent with our hypothesis that supplementation with proline and proline/glutamine has minimal difference in ATP production.

Different amount of ROS production during proline oxidation and proline/

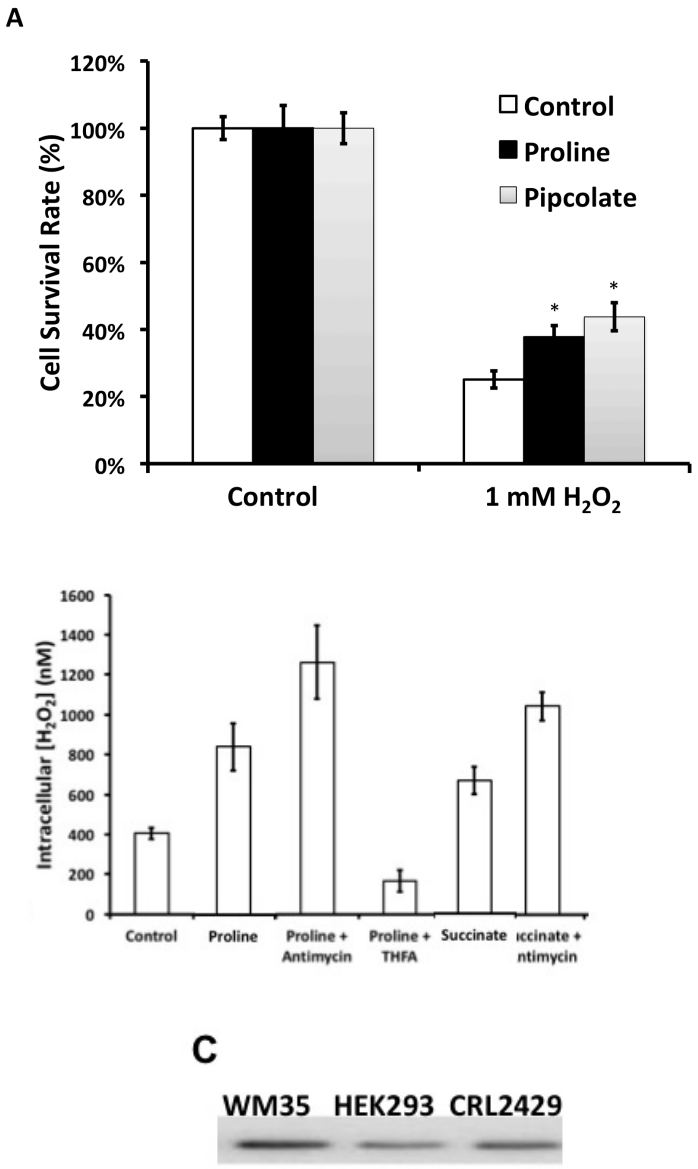

Figure 4.2. **Proline induces ROS production and resistance to H_2O_2 stress in CRL2429 cells.** (A). Cell survival rate of CRL2429 cells after H_2O_2 treatment (1 mM, 3 hr) in the presence and absence of 5 mM proline or pipcolate. (B). Intracellular H_2O_2 level in CRL2429 cells with and without 10 mM succinate, 5 mM proline, 2 μg/mL antimycin A and 3 mM THFA. (C). Western blot analysis of human PRODH in WM35, EHK293 and CRL2429 cells.

glutamine catabolism may be another possible explanation for the difference in proline and proline/glutamine mediated protection against H_2O_2 stress. Proton leak, which is mediated by electron flow via complexes I, III, and IV, has been suggested to have physiological function as heat production and prevention of ROS formation (18). Proton leak (uncoupled respiration) can be calculated by subtracting the rate of respiration after the addition of rotenone, a complex I inhibitor that suppresses mitochondrial respiration, from the rate of respiration after addition of FCCP, which uncouples mitochondrial ATP generation from oxygen consumption (17). Proton leak with proline supplementation (35 ± 5.1 pmol O_2 consumption min^{-1} mg^{-1}) is significantly lower than that of proline/ glutamine supplementation (58 ± 2.5 pmol O_2 consumption min^{-1} mg^{-1}) (Figure 4.1C). This implies proline treatment may induce more ROS generation.

Interestingly, maximum respiration with proline/glutamine treatment is much higher than that of proline treatment (Figure 4.1C). Maximal respiration is the rate of OCR after the addition of FCCP (17). Maximum respiration represents the maximum capacity of electron transport by the cell under assay condition (18). Decreased maximum respiration usually indicates lower efficiency of electron transport, which can be caused by proton leak or reverse electron flow (18). In mitochondria isolated from Parkinson's disease subjects, proton leak at Complex I resulted in a loss of maximum respiration (19). Promoting reverse electron flow by application of antimycin A, which inhibits the electron flow from going through Complex III, resulted in decreased maximum respiration (20). Since we observed a lower amount of proton leak with proline supplementation, reversed electron flow

may be the contributor of the decreased maximum respiration. Reverse electron flow has been linked to ROS production (21).

In summary, the oxygen consumption profile of WM35 cells suggested cells with proline treatment have lower proton leak and maximum respiration, indicating possible higher production of ROS during proline oxidation. Higher ROS signaling may explain the higher survival rate of cells grown with proline alone under H_2O_2 stress.

4.4.2 Proline induces H_2O_2 production in CRL2429 cells

In order to measure the mitochondria ROS production, we switched to CRL2429, which is a skin fibroblast cell line and is well suited isolation of mitochondria. The expression of human PRODH in CRL2429 cells was confirmed by western blot (Figure 4.2 C). We then measured the cell survival rate of CRL2429 under oxidative stress. After H_2O_2 treatment (1 mM, 3 hr), treatment with 5 mM proline or 5 mM pipecolate resulted in 1.7-and 2-fold increases of cell survival rate, compared with that of cells without proline supplementation (Control) (Figure 4.2.A). Pipecolate, oxidized by pipecolate oxidase, is not a substrate or inhibitor of PRODH. It was found previously in HEK293 cells (6) and WM35 cells (unpublished data) that pipecolate treatment protects cells against H_2O_2 stress similarly to proline. The ability of pipecolate to protect against oxidative stress was contributed to its antioxidant property (6). Thus, our data showed that CRL2429 cells, similar to WM35 and HEK293 cells, could be protected from H_2O_2 stress by proline and pipcolate supplementation.

Next, the intracellular concentration of H_2O_2 formation was measured using CRL2429 cells, with the estimated cell cytosolic volume as 940 μm^3 (15). Because SOD was added to the assay buffer, the level of H_2O_2 accounts for both $O_2^{\bullet-}$ and H_2O_2. In the absence of amino acid supplementation, the basal level intracellular H_2O_2 was 400 nM in CRL2429 cells (Figure 4.2.B). Succinate, a commonly used positive control for the measurement of mitochondrial H_2O_2 production, increased the intracellular H_2O_2 production to 660 nM. Proline treatment also elevated H_2O_2 production to 825 nM, indicating that half of intracellular H_2O_2 (~425 nM) was produced by proline oxidation. From the measurements in rat liver, *in vivo* intracellular H_2O_2 concentrations was estimated to be on the order of 0.2 μM (27). In addition, the intracellular H_2O_2 concentration used for signaling in mammalian cells was estimated to be 0.5-0.7 μM (27). Therefore, with proline supplementation, intracellular H_2O_2 concentration is sufficient to induce cellular signaling pathways in CRL2429 cells.

Using L-THFA as a competitive inhibitor along with proline treatment significantly decreased the intracellular level H_2O_2 formation (50 nM) (Figure 4.2.B). It is unclear why intracellular H_2O_2 level after L-THFA treatment is lower than that of control. But L-THFA may also inhibit the usage of both intracellular and extracellular proline. Since previous research has shown that proline-dependent ROS was produced at complex III (12), we use antimycin A to test whether proline-induced ROS is also produced at the same complex in CRL2429 cells. Antimycin A binds to the oxidized ubiquinone (Qi site) of Complex III, inhibiting electron transfer from reduced heme b_L of Complex III to oxygen via semiquinone

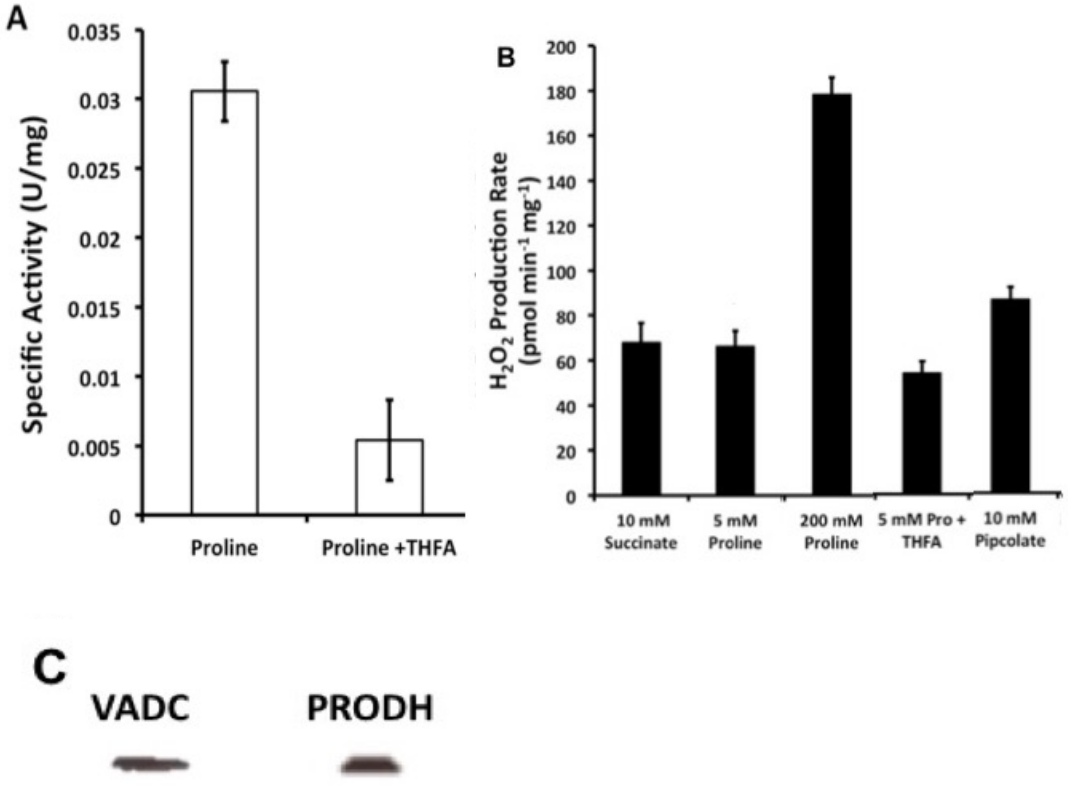

Figure 4.3 Proline induces ROS production in isolated mitochondria from CRL2429 cells. (A). The specific activity of PRODH in isolated mitochondria using 240 mM proline as substrate, in the presence and absence of 10 mM THFA. (B). H_2O_2 production rate of isolated mitochondria using succinate, proline and pipcolate as substrate, in the presence and absence of 10 mM THFA. (C). Western blot analysis of human PRODH and VADC in isolated mitochondria.

(Qo site) (22). Application of antimycin A nearly doubled intracellular H_2O_2 concentration when using proline as substrate (Figure 4.2.B). In cell level, antimycin A has been used as a ROS generator and was shown to induce mammalian cell apoptosis (28). This may be contributed to the ability of antimycin A in inducing mitochondrial swelling and loss of membrane potential, as well as the apoptosis signaling (23). The succinate induced ROS production is known to be mainly contributed by complex II (29). Because antimycin A treatment increases the intracellular H_2O_2 concentration by the same level using proline and succinate as substrate, we suspect that the effect of antimycin A on H_2O_2 levels that we observed is due largely to its effect on mitochondrial membrane potential.

4.4.3 Proline induces H_2O_2 production in isolated mitochondria from CRL2429

After confirming proline-dependent H_2O_2 production in CRL2429 cells, we then tested ROS production in isolated mitochondria from CRL2429. The existence of PRODH in isolated mitochondria was confirmed by western blot against PRODH, with VADC serving as a mitochondrial marker (Figure 4.3C). The specific activity of PRODH in isolated mitochondria was determined by following the production of P5C when using proline as a substrate. With saturated proline (200 mM), the specific activity of mitochondrial PRODH is 0.03 U/mg (Figure 4.3A). 80% of the activity can be inhibited by application of 10 mM L-THFA. In addition, the existence of PRODH in the isolated mitochondria was confirmed by co-

treatment of mitochondria with proline and 10 mM THFA. Those data suggest isolated mitochondria from CRL2429 cells contain active PRODH.

The H_2O_2 production rate of isolated mitochondria using proline as substrate (65 pmol min^{-1} mg^{-1}) is similar to that using succinate as substrate (67 pmol min^{-1} mg^{-1}) (Figure 4.3B). Using pipcolate as substrate, a higher rate of H_2O_2 formation (91 pmol min^{-1} mg^{-1}) was observed. Figure 4.3B also shows that the H_2O_2 production rate increases in response to increased amount of proline (200 mM) as substrate. 10 mM of L-THFA inhibits the H_2O_2 production rate by 23%.

4.4.4 Proline induced the production of $O_2^{\bullet-}$ and H_2O_2 in isolated pig mitochondria

The existence of pig PRODH in isolated mitochondria was confirmed by mass spectrometry. Since the sequencing information for domestic pig (*Sus scrofa domesticus*) is unavailable, trypsin digested solubilized pig mitochondria were sequenced against *Sus Scorfa* (wild boar) PRODH, resulting in 32% sequence coverage. The activity of pig PRODH in pig kidney mitochondria was 35 ± 4 mU/mg in the presence of 240 mM of proline (Figure 4.4.A). Co-treatment of mitochondria with proline and 10 mM THFA resulted in 70% decreased PRODH activity (Figure 4.4A). Therefore, isolated pig kidney mitochondria contain active PRODH.

We then measured the superoxide and hydrogen peroxide production in isolated mitochondria from pig kidney. The rate of $O_2^{\bullet-}$ production and H_2O_2 production induced by 10 mM proline were 26 ± 2.2 pmol min^{-1} mg^{-1} and 0.94 ±

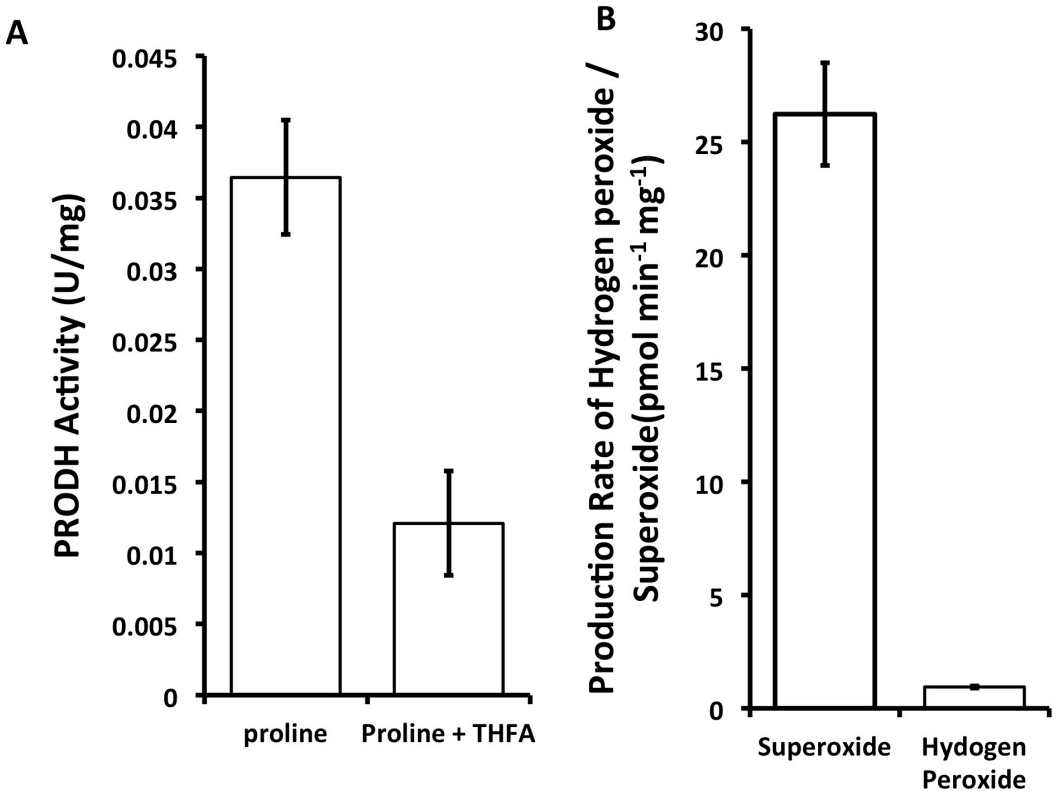

Figure 4.5. **PRODH activity and proline induced superoxide and hydrogen peroxide formation in isolated pig kidney mitochondria.** (A). PRODH activity of pig mitochondria was measured by determining the formation of P5C-oAB complex using 240 mM proline in the presence and absence of 10 mM THFA. (B). Formation of superoxide and hydrogen peroxide induced by 10 mM proline in pig mitochondria.

0.05 pmol min^{-1} mg^{-1}, respectively (Figure 4.4B). This is consistent with the previous idea that proline-oxidation mediated ROS is primarily in the form of $O_2^{\bullet-}$, as overexpressed SOD can diminish the ROS produced by overexpressed PRODH (25).

4.4.5 Proline induced H_2O_2 is regulated independent of proline induced oxygen consumption

Pig PRODH has not been purified yet and its reactivity with molecular oxygen remains to be determined. We would like to test whether proline mediated $O_2^{\bullet-}$ and H_2O_2 is mediated by the oxygen reactivity of pig PRODH. Therefore, we compared the oxygen consumption of pig kidney mitochondria with proline and succinate as substrate (Figure 4.5A). With 10 mM succinate as substrate, the oxygen consumption rate of pig mitochondria is 22 nmol min^{-1} mg^{-1}. Using 10 mM proline as substrate, the oxygen consumption rate of pig mitochondria is 4 nmol min^{-1} mg^{-1}. The mitochondria oxygen consumption rate with proline as substrate not only represents the total mitochondria respiration induced by proline, but also represents the rate of oxygen reactivity of pig PRODH. We then measured the ROS production rate of mitochondria using either substrate. The level of H_2O_2 accounts for both $O_2^{\bullet-}$ and H_2O_2, since SOD was added to the assay buffer. With the same amount of proline and succinate, similar rates of H_2O_2 production were observed (Figure 4.5B). Proline and succinate generate H_2O_2 at a rate of 26.2 pmol min^{-1} mg^{-1} and 25.4 pmol min^{-1} mg^{-1}, respectively. The results show that proline generates more ROS per oxygen in isolated pig mitochondria relative to

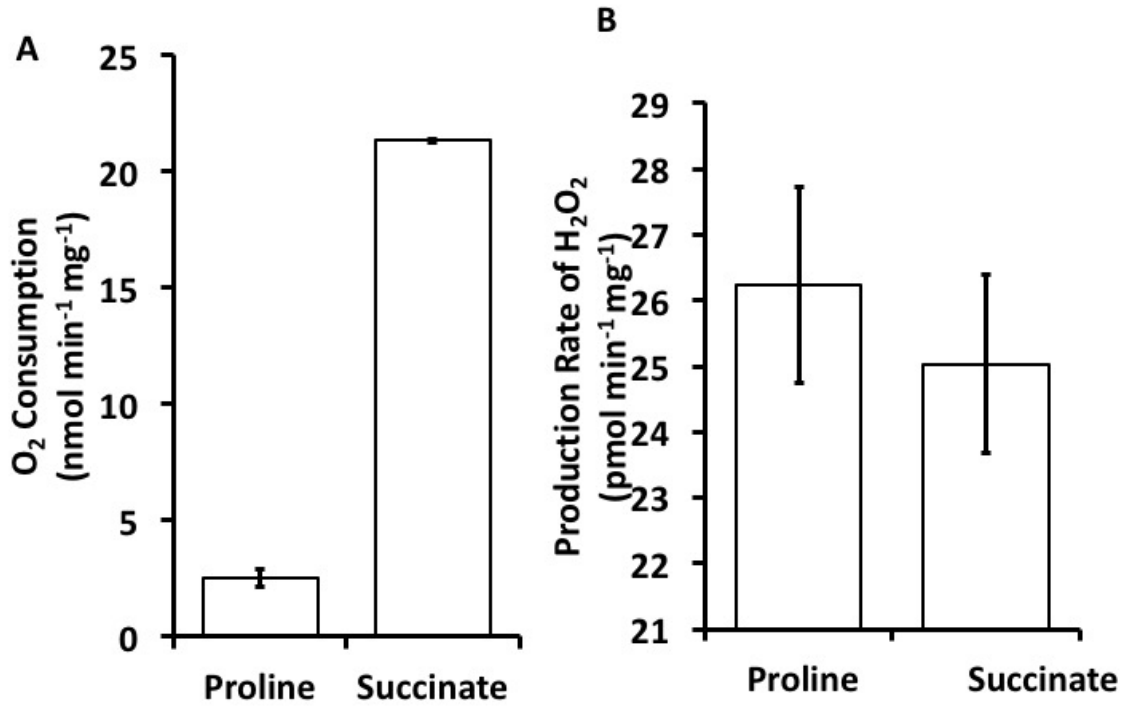

Figure 4.5 Proline oxidation induced H_2O_2 formation is not correlated with proline-induced oxygen consumption. (A). Oxygen consumption of isolated pig mitochondria using 10 mM proline and succinate as substrates. (B). H_2O_2 production rates of isolated pig kidney mitochondria using 10 mM proline and 10 mM succinate as substrates in the presence of SOD.

succinate.

4.5 DISCUSSION

Proline-dependent ROS ($O_2^{\bullet-}$ and H_2O_2) production is critical to the effect of PRODH in regulating cell proliferation, apoptosis and survival under oxidative stress (1-3). In WM35 cells, proline-mediated protection against oxidative stress requires proline oxidation, which provides ATP and activates Akt signaling pathways (7). It is still unclear whether proline-dependent ROS plays a role in regulating oxidative stress resistance in WM35 cells. However, it has been reported that proline-induced ROS is required for the survival of mammalian cells under oxidative stress (3), and the activation of Akt (phosphorylation at Thr308 and Ser473) responds to oxidative stress. This leads to the hypothesis that proline-induced ROS is sufficient to activate Akt pathway.

In comparison with glutamine and glutamine/proline co-treatment, the oxygen consumption profile of WM35 cells suggests cells with proline treatment have lower proton leak and maximum respiration relative to glutamine, suggesting possible higher production of ROS during proline oxidation, because decreased maximum respiration is commonly linked to increased reverse electron flow (18), a well-known source of ROS generation. Interestingly, we also observed a higher survival rate of WM35 cell under H_2O_2 stress grown with proline alone. In addition, pipecolate, which shows better protection for CRL2429 cells from oxidative stress, induces more ROS formation than proline. These data highlight the possibility of proline-induced ROS serving as a signaling molecule in regulating the survival of

cells under oxidative stress as higher ROS signaling may explain the higher cell survival rate.

By using CRL2429 cells, we observed proline treatment doubles the intracellular H_2O_2 concentration, reaching ~800 nM. In mammalian cells with a fully functional antioxidant system, as low as 50-60 μM extracellular H_2O_2 is sufficient to induce oxidative stress (32), as treatment with 60 μM of H_2O_2 was found to induce aldehydic DNA lesions (33). Thus, the amount of ROS formed during proline oxidation is insufficient to cause deleterious effect. On the other hand, treating chicken B cell line DT40 with 10μM of H_2O_2 for 30 min reuslted in significantly increased phosphorylation of Akt (34). In addition, extracellular application of 0.1 μM of H_2O_2 was shown to increase the phosphorylation of Ser473 by 1.7-fold (30). This suggests proline-induced H_2O_2 is sufficient to induce the activation of Akt pathway. Future study is required to test whether proline oxidation induced Akt pathway can be abolished by the application of antioxidant or overexpression of MnSOD.

We also found that proline and succinate generate similar amount of ROS in CRL2429 cells, and in isolated mitochondria from CRL2429 cells and pig kidney. To the best of our knowledge, unlike proline, oxidation of succinate does not protect mammalian cells against oxidative stress. Therefore, although ROS generated by proline oxidation is sufficient to induce pro-survival signaling pathways, proline oxidation-mediated oxidative stress protection can not be completely explained by proline-dependent ROS. Furthermore, application of antimycin A elevates the amount of H_2O_2 generated by proline oxidation and

succinate oxidation by ~2-fold. Phang et al. (5) also observed increased proline oxidation-mediated ROS production by antimycin A treatment. Based on the observation, Phang et al. (5) claimed complex III is the production site of proline-dependent ROS. However, since antimycin A induces the production of proline-dependent ROS and succinate-dependent ROS, we are not able to draw the conclusion that Complex III is the source of proline-mediated ROS. Instead, decreased mitochondrial membrane potential may be the reason for antimycin A induced production of ROS.

We also observed that mitochondria (or cells) consuming proline have a relatively low oxygen comsuption rate than those consuming glutamine and succinate. On the other hand, H_2O_2 production rates of mitochondria consuming proline and succinate as substrates are similar. Those data indicate that mitochondria oxidizing proline has lower respiration efficiency, suggesting the unique role of proline catabolism in generating signaling ROS. The low respiration efficiency found in mitochondria using proline may have two explanations: 1). Proline oxidation impairs mitochondrial membrane integrity and decreases mitochondrial membrane potential; 2).Proline oxidation regulates mitochondrial matrix calcium signaling, thereby regulating oxidative metabolism and respiration in mitochondria.

In summary, we observed proline oxidation induced production of mitochondrial of ROS in both human cells and pig tissue, indicating ROS formation induced by proline oxidation is a common phenomenon in mammalian cells. Although the ROS produced by proline oxidation is sufficient to activate Akt

pathways, we suspect partial proline-mediated protection against oxidative stress is mediated by proline-dependent ROS. In addition, oxygen consumption of proline in mitochondria is lower than succinate.

References:

1. Phang, J. M., Liu, W., and Zabirnyk, O. (2010) Proline metabolism and microenvironmental stress. *Annu Rev Nutr* **30**, 441-463
2. Phang, J. M., Donald, S. P., Pandhare, J., and Liu, Y. (2008) The metabolism of proline, a stress substrate, modulates carcinogenic pathways. *Amino Acids* **35**, 681-690
3. Phang, J. M., Liu, W., Hancock, C., and Christian, K. J. (2012) The proline regulatory axis and cancer. *Front Oncol* **2**, 60
4. Pandhare, J., Dash, S., Jones, B., Villalta, F., and Dash, C. (2015) A Novel Role of Proline Oxidase in HIV-1 Envelope Glycoprotein Induced Neuronal Autophagy. *The Journal of biological chemistry*
5. Liu, Y. M., Borchert, G. L., Donald, S. P., Diwan, B. A., Anver, M., and Phang, J. M. (2009) Proline Oxidase Functions as a Mitochondrial Tumor Suppressor in Human Cancers. *Cancer Research* **69**, 6414-6422
6. Krishnan, N., Dickman, M. B., and Becker, D. F. (2008) Proline modulates the intracellular redox environment and protects mammalian cells against oxidative stress. *Free Radic. Biol. Med.* **44**, 671-681
7. Kumar Natarajan, S., Zhu, W., Liang, X., Zhang, L., Demers, A. J., Zimmerman, M. C., Simpson, M. A., and Becker, D. F. (2012) Proline dehydrogenase is essential for proline protection against hydrogen peroxide-induced cell death. *Free Radic Biol Med* 53(5):1181-1191
8. Dossumbekova, A., Berdyshev, E. V., Gorshkova, I., Shao, Z., Li, C., Long, P., Joshi, A., Natarajan, V., and Vanden Hoek, T. L. (2008) Akt activates NOS3 and separately restores barrier integrity in H2O2-stressed human cardiac microvascular endothelium. *American journal of physiology. Heart and circulatory physiology* **295**, H2417-2426
9. Wang, R., Peng, L., Zhao, J., Zhang, L., Guo, C., Zheng, W., and Chen, H. (2015) Gardenamide A Protects RGC-5 Cells from H(2)O(2)-Induced Oxidative Stress Insults by Activating PI3K/Akt/eNOS Signaling Pathway. *International journal of molecular sciences* **16**, 22350-22367
10. Zhang, L., Alfano, J. R., and Becker, D. F. (2015) Proline metabolism increases katG expression and oxidative stress resistance in *Escherichia coli*. *Journal of bacteriology* **197**, 431-440
11. Zarse, K., Schmeisser, S., Groth, M., Priebe, S., Beuster, G., Kuhlow, D., Guthke, R., Platzer, M., Kahn, C. R., and Ristow, M. (2012) Impaired insulin/IGF1 signaling extends life span by promoting mitochondrial L-proline catabolism to induce a transient ROS signal. *Cell metabolism* **15**, 451-465
12. Liu, W., Le, A., Hancock, C., Lane, A. N., Dang, C. V., Fan, T. W., and Phang, J. M. (2012) Reprogramming of proline and glutamine metabolism contributes to the proliferative and metabolic responses regulated by oncogenic transcription factor c-MYC. *Proceedings of the National Academy of Sciences of the United States of America* **109**, 8983-8988

13. Goncalves, R. L., Rothschild, D. E., Quinlan, C. L., Scott, G. K., Benz, C. C., and Brand, M. D. (2014) Sources of superoxide/H2O2 during mitochondrial proline oxidation. *Redox biology* **2**, 901-909
14. Starkov, A. A. (2010) Measurement of mitochondrial ROS production. *Methods Mol Biol* **648**, 245-255
15. Fujioka, A., Terai, K., Itoh, R. E., Aoki, K., Nakamura, T., Kuroda, S., Nishida, E., and Matsuda, M. (2006) Dynamics of the Ras/ERK MAPK cascade as monitored by fluorescent probes. *The Journal of biological chemistry* **281**, 8917-8926
16. Srivastava, D., Schuermann, J. P., White, T. A., Krishnan, N., Sanyal, N., Hura, G. L., Tan, A., Henzl, M. T., Becker, D. F., and Tanner, J. J. (2010) Crystal structure of the bifunctional proline utilization A flavoenzyme from Bradyrhizobium japonicum. *Proceedings of the National Academy of Sciences of the United States of America* **107**, 2878-2883
17. Zhang, J., Khvorostov, I., Hong, J. S., Oktay, Y., Vergnes, L., Nuebel, E., Wahjudi, P. N., Setoguchi, K., Wang, G., Do, A., Jung, H. J., McCaffery, J. M., Kurland, I. J., Reue, K., Lee, W. N., Koehler, C. M., and Teitell, M. A. (2011) UCP2 regulates energy metabolism and differentiation potential of human pluripotent stem cells. *The EMBO journal* **30**, 4860-4873
18. Brand, M. D., and Nicholls, D. G. (2011) Assessing mitochondrial dysfunction in cells. *The Biochemical journal* **435**, 297-312
19. Esteves, A. R., Lu, J., Rodova, M., Onyango, I., Lezi, E., Dubinsky, R., Lyons, K. E., Pahwa, R., Burns, J. M., Cardoso, S. M., and Swerdlow, R. H. (2010) Mitochondrial respiration and respiration-associated proteins in cell lines created through Parkinson's subject mitochondrial transfer. *J Neurochem* **113**, 674-682
20. Belskie, K. M., Van Buiten, C. B., Ramanathan, R., and Mancini, R. A. (2015) Reverse electron transport effects on NADH formation and metmyoglobin reduction. *Meat science* **105**, 89-92
21. Selivanov, V. A., Votyakova, T. V., Pivtoraiko, V. N., Zeak, J., Sukhomlin, T., Trucco, M., Roca, J., and Cascante, M. (2011) Reactive oxygen species production by forward and reverse electron fluxes in the mitochondrial respiratory chain. *PLoS computational biology* **7**, e1001115
22. Drose, S., and Brandt, U. (2008) The mechanism of mitochondrial superoxide production by the cytochrome bc1 complex. *The Journal of biological chemistry* **283**, 21649-21654
23. Tzung, S. P., Kim, K. M., Basanez, G., Giedt, C. D., Simon, J., Zimmerberg, J., Zhang, K. Y., and Hockenbery, D. M. (2001) Antimycin A mimics a cell-death-inducing Bcl-2 homology domain 3. *Nature cell biology* **3**, 183-191
24. Barja, G. (2007) Mitochondrial oxygen consumption and reactive oxygen species production are independently modulated: implications for aging studies. *Rejuvenation research* **10**, 215-224
25. White, T. A., Krishnan, N., Becker, D. F., and Tanner, J. J. (2007) Structure and kinetics of monofunctional proline dehydrogenase from Thermus thermophilus. *The Journal of biological chemistry* **282**, 14316-14327

26. Liu, W., Zabirnyk, O., Wang, H., Shiao, Y. H., Nickerson, M. L., Khalil, S., Anderson, L. M., Perantoni, A. O., and Phang, J. M. (2010) miR-23b*targets proline oxidase, a novel tumor suppressor protein in renal cancer. *Oncogene* **29**, 4914-4924
27. Stone, J. R., and S. Yang. (2006). Hydrogen peroxide: a signaling messenger. *Antioxid Redox Signa*l **8**, 243-70.

28. Park, W. H., Han, Y. W., Kim, S. H., and Kim S. Z. (2007) An ROS generator, antimycin A, inhibits the growth of HeLa cells via apoptosis. *J. Cell. Biochem.* **102**, 98–109

29. Quinlan, C.L., Orr, A.L., Perevoshchikova, I.V., Treberg, J.R., Ackrell B.A., Brand M.D.. (2012) Mitochondrial complex II can generate reactive oxygen species at high rates in both the forward and reverse reactions. *J Biol Chem*. **287(32),** 27255-64.

30. Iwakami, S., Misu, H., Takeda, T., Sugimori, M., Matsugo, S., Kaneko, S., Takamura, T. (2011) Concentration-dependent dual effects of hydrogen peroxide on insulin signal transduction in H4IIEC hepatocytes. *PloS One*. **6(11),** e27401

31. Chen, J., Zhang, Y., Wang, C., Lu, W., Jin, J. B., and Hua, X. (2011) Proline induces calcium-mediated oxidative burst and salicylic acid signaling. *Amino Acids* **40**, 1473-1484

32. Huang, B.J., Sikesb, H.D. (2014) Quantifying intracellular hydrogen peroxide perturbations in terms of concentration. *Redox Biology* **2**, 955-962

33. Nakamura, J., Purvis, E.R., Sweberg, J.A. (2003) Micromolar concentrations of hydrogen peroxide induce oxidative DNA lesions more efficiently than millimolar concentrations in mammalian cells. *Nucleic Acids Res*. **31(6)**, 1790–1795.

34. Ding, Y., Takano, T., Gao, S., Han, W., Noda, C., Yanagi, S., and Yamamura, H. (200) Syk is required for the activation of Akt survival pathway in B cells exposed to oxidative stress. *J Biol Chem*. **275(40),** 30873-77.

CHAPTER 5

Purification and Characterization of Human Proline Dehydrogenase 1 (Mitochondrial Isoform 1)

5.1 ABSTRACT

The *Homo sapiens* PRODH1, a mitochondrial enzyme, catalyzes the conversion of L-proline to Δ^1-pyrroline-5-carboxylate, which is the first step of proline oxidation. Human PRODH1 plays a vital role in ATP production, regulating cell survival and apoptosis, and missense mutations in the *PRODH1* gene are associated with schizophrenia. Human PRODH1 contains all the components of the $(\beta\alpha)_8$ catalytic core, which is conserved in monofunctional PRODHs and bifunctional PutAs, except sheet β2. Full-length recombinant human PRODH1 that lacks only its mitochondrial targeting signal peptide (PRODH1 ΔMTS) was expressed and purified from *Escherichia coli.* The kinetic parameters of human PRODH1 ΔMTS using an artificial electron acceptor for the oxidative half-reaction were estimated to be K_m = 6.6 mM proline and k_{cat} = 0.75 s^{-1}. With ubiquinone-1 (CoQ_1) as an electron acceptor, human PRODH1 ΔMTS exhibited a K_m = 3.3 ± 0.6 mM proline and k_{cat} = 0.35 ± 0.01 s^{-1}. The oxygen reactivity of human PRODH1 ΔMTS is low, with estimated k_{cat} = 0.06 min^{-1} and K_m = 7.7 mM proline, indicating human PRODH1 does not significantly react with molecular oxygen during turnover with proline. Human PRODH1 exhibited optimal activity at pH 7.9 and L-tetrahydro-2-furoic acid was determined to be a competitive inhibitor with a K_{ic} of 3.4 mM.

5.2 INTRODUCTION

Homo sapiens PRODH1, located on chromosome 22a11.21, encodes proline dehydrogenase (aka, oxidase) 1 (EC 1.5.99.8) that catalyzes the first step of proline degradation by oxidizing L-proline to Δ^1-pyrroline-5-carboxylate (P5C) (1). There are two isoforms of human PRODH1: human PRODH1, mitochondrial isoform 1 (NP_057419) and human PRODH1, mitochondria isoform 2 (NP_0011821155) (2). The former has 600 amino acids, containing the mitochondrial target sequence (1-48 residues). The latter is a splice variant of isoform 1, with a length of 492 amino acids, lacking an N-terminal region of 1-118 residues. The expression of human PRODH1 isoform 2 has been linked to an increased risk of autism (3), although the reason for this linkage remains unknown. Human PRODH1 isoform 2 was found in mitochondria (2), but it is unclear how this isoform is transported into the mitochondria in the absence of mitochondrial target sequence. The localization of human PRODH1 isoform 1 was suggested to be on the matrix side of the inner mitochondrial membrane in kidney, liver, and brain (4).

Most functional studies of human PRODH1 have been on isoform 1. Phang's group has shown that human PRODH1 isoform 1 is a tumor suppressor, negatively regulated by the oncogenic transcription factor c-MYC (5). Human PRODH1 is also regulated by p53 and has a role in programmed cell death. Overexpression of human PRODH1 results in tumor cell apoptosis (6-8). In paired tumor and normal tissues (kidney, liver, colon and rectum, etc) from patients, immunohistochemical staining of human PRODH1 revealed that 56 of 92 pairs had

decreased expression of human PRODH1 in tumor tissues compared with that of normal tissue (9). Constitutive expression of human PRODH1 is beneficial to cell survival under oxidative stress or cytotoxic conditions by providing ATP, Akt activation (10), and promoting pro-survival autophagy (11). In the brain, proline is the precursor of the neurotransmitter glutamate. Therefore, proline catabolism may be involved in neurological diseases. Deficiencies in human PRODH1 are linked to schizophrenia, a psychiatric disorder affecting about 1% of the population (12). Human PRODH1 missense mutations Arg185Trp and Gly521Arg are associated with increased susceptibility of schizophrenia (12). Hyperprolinemia type I is another disease caused by a deficiency in human PRODH1 (13). The plasma proline level in people with hyperprolinemia type I is 3-10 times higher than the normal level (13).

To further explore the function of human PRODH1 in tumor progression and neurological disease, it is necessary to understand the relationship between the activity and polymorphisms of PRODH. These types of studies are dependent on having purified active human PRODH1. Previously our lab partially purified full-length human PRODH1 but the yield was poor (<0.1 mg/L of culture) and was not sufficient for detailed enzymological and structural studies (14). The semi-purified recombinant PRODH was reported to have a specific activity of 0.1 U/mg and a K_m value for proline of about 15 mM using the proline: DCPIP oxidoreductase assay (14). By monitoring P5C formation and cytochrome c reduction, the proline:O_2 activity of recombinant PRODH was determined to be 0.09 U/mg (14). A second purification of human PRODH1 was reported more recently but was only

successful by deleting one third of the protein. This truncated form of human PRODH1 (residues 176-572) was purified in high yield (10 mg/L of culture) and using the proline: DCPIP oxidoreductase assay, the specific activity was reported to be 0.032 U/mg with a K_m of 470 mM proline (15). Although the specific activity of truncated human PRODH1 was similar to that of full-length semi-purified human PRODH1, the K_m of for proline was considerably much higher. Because human plasma proline concentration is around 0.2-0.3 mM (16), the K_m value for the truncated form of PRODH1 is likely not physiologically relevant.

In this study, we designed, expressed and purified human PRODH1 in which the mitochondrial target sequence was deleted (PRODH1 ΔMTS). The recombinant human PRODH1 (ΔMTS) was characterized by steady-state kinetics including pH activity profile and inhibition by the proline analog L-tetrahydro-2-furoic acid.

5.3 MATERIALS AND METHODS

5.3.1 Chemicals

All chemicals, enzymes and buffers were purchased from Fisher Scientific Inc., Fermentas and Sigma-Aldrich, Inc. unless otherwise noted. Nanopure water was used in all experiments.

5.3.2 Human PRODH 1 construct

The *PRODH1* gene was obtained from a previously made PRODH1-pFlag-CMV3 construct. *PRODH* 1, mitochondria isoform 1 precursor was subcloned

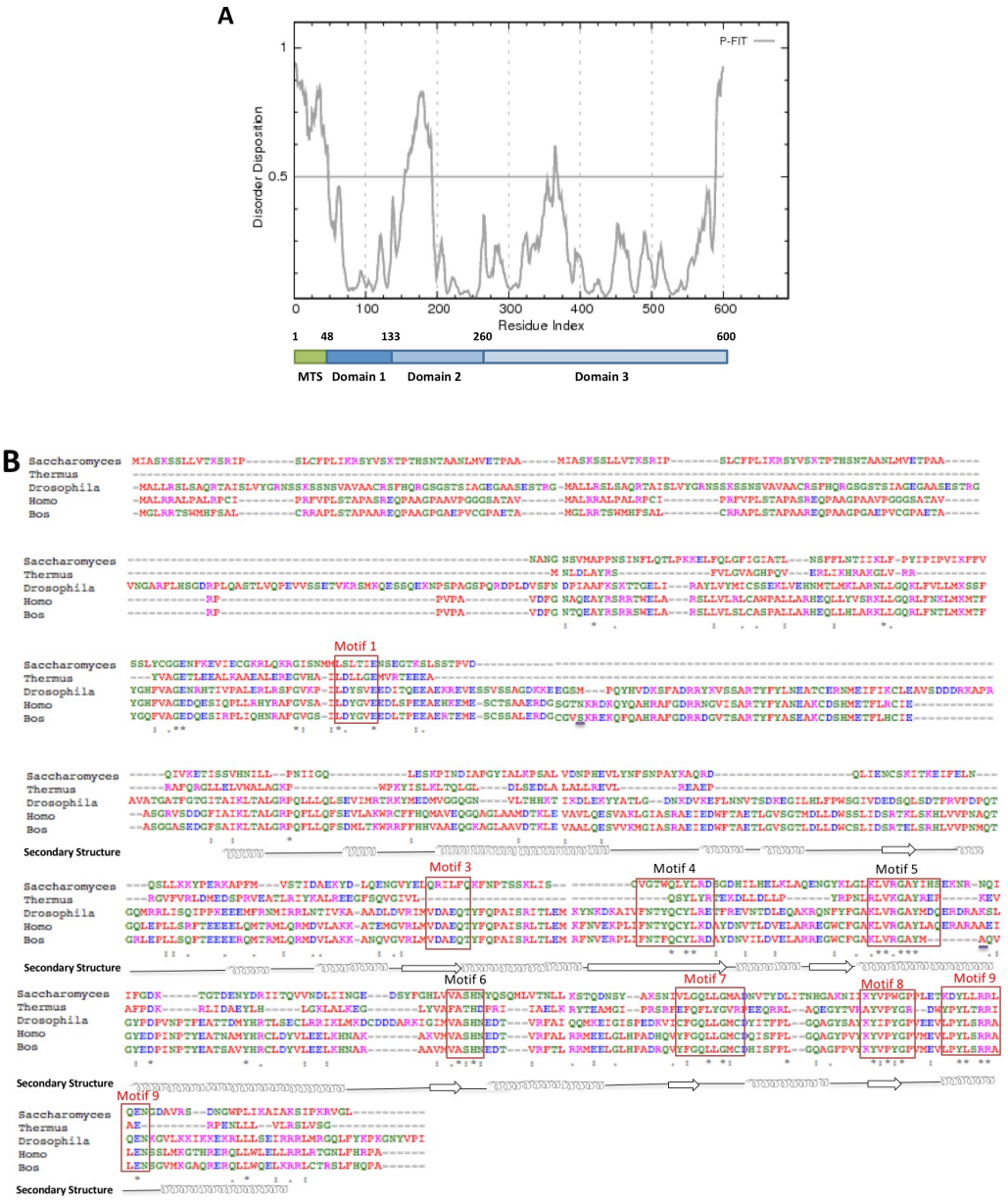

Figure 5.1 Analysis of the protein sequence of full-length Human PRODH 1. (A) Regions human PRODH1 has the tendency to be structurally disordered and domain scheme of human PRODH1 (bottom). (B) Multiple alignment of protein sequences of PRODHs from different organisms. Secondary structure analysis was done for domain 3 (260-600 residues) of human PRODH1. Red boxes: conserved motifs involved in FAD (black letters) and proline binding (red letters).

without the Flag tag into the EcoRV and XhoI sites of pET32a. Analysis of the primary structure of Human PRODH1 by Target P and MitoProt suggested the N-terminal 48 residues comprised a mitochondrial signaling peptide (MSP). The predicted MSP was removed by site-directed mutagenesis by through inserting a BamHI site upstream of residue 49 using primer 5'-CGAAATGGATC CCCGGTTCGGGCCGTG-3' and 5'-CGAATACTCGAGCTAGCAGGGCGATG-3'. After BamHI and XhoI digestion, PRODH 1ΔMTS was cloned into pET28a to make pET28a-human PRODH 1ΔMTS which encodes a N-terminal 6xHis tag fusion human PRODH 1 lacking MTS (His-human PRODH 1ΔMTS). Double digested PRODH 1ΔMTS was also cloned into pGEX-4t-1 (GE Health) to make pGEX-4t-1-human PRODH 1ΔMTS which codes an N-terminal glutathione S-transferase (GST) tag fusion human PRODH 1 lacking MTS (GST-human PRODH 1ΔMTS). The PRODH1 constructs were confirmed by nucleic acid sequencing (Eurofins Scientific). Two mutations (N175I & A454V) were found in the PRODH1-pFlag-CMV3 construct.

5.3.3 Expression and purification of human PRODH1 ΔMTS

His-human PRODH1 ΔMTS construct was transformed into *E. coli* strain BL21 (DE3) pLysS and then plated onto Luria-Bertani (LB) agar containing chloramphenicol (34 μg/ml) and kanamycin (50 μg/ml). Resulting colonies were inoculated and grown in 5 ml of LB broth with the appropriate antibiotics. 1 ml per Liter of the LB culture was then inoculated to 4 Liter of LB media containing the desired antibiotics. The cultures were incubated at 30°C with shaking (250 rpm)

until OD_{600} of 1.0 at which point His-human PRODH1 ΔMTS expression was induced with 0.2 mM IPTG for 10 hr at 18°C. The overnight cultures were centrifuged at 6000 rpm for 10 min at 4 °C. The resulting pellets were resuspended in a final 400 ml volume of binding buffer (50 mM NaH_2PO_4, 5 mM imidazole, 0.5 M NaCl, 10% glycerol, pH 8.0) supplemented with protease inhibitors (3 mM ε-amino-N-caproic acid, 0.3 mM phenyl methyl sulfonyl chloride, 1.2 μM leupeptin, 48 μM N-*p*-tosyl-L-phenyl alanine chloromethyl ketone, 78 μM N-α-tosyl-L-lysine chloromethylketone) and 0.1% Triton X-100. The cell suspension was disrupted by sonication at 4 °C for a total of 5 min (5 sec pulse on, 15 sec pulse off, 50% power). The cell extract was centrifuged at 16000 rpm (4 °C) for 20 min. The supernatant (100 ml) was passed through a 0.45 μm filter (VWR) and applied to a Ni-NTA superflow (Qiagen) resin (40 ml bed volume in a 2.8 cm × 30 cm column) equilibrated with binding buffer. Wash buffer (0.4 L, Binding buffer, 20 mM imidazole,) was then applied to the column followed by elution buffer (His-human PRODH 1ΔMTS 500 mM imidazole, 0.5 M NaCl, 10% glycerol, pH 8.0). Eluted protein was then dialyzed into Storage Buffer (50 mM NaH_2PO_4, 0.5 M NaCl, 10% glycerol, 0.5mM Tris (3-hydroxypropyl) phosphine, pH 8.0,) and concentrated using an Amicon 30-kDa cutoff filter (Millipore).

GST-human PRODH1 ΔMTS construct was expressed and purified from BL21(DE3) pLysS, which was grown in LB media containing chloramphenicol (34 μg/ml) and Ampicillin (100 μg/ml) until OD_{600} of 0.5. The expression of GST-human PRODH 1ΔMTS was induced by 0.1 mM IPTG for 1 hr at 30°C. Cells were pelleted using the procedures as described above. The cells were resuspended in PBS

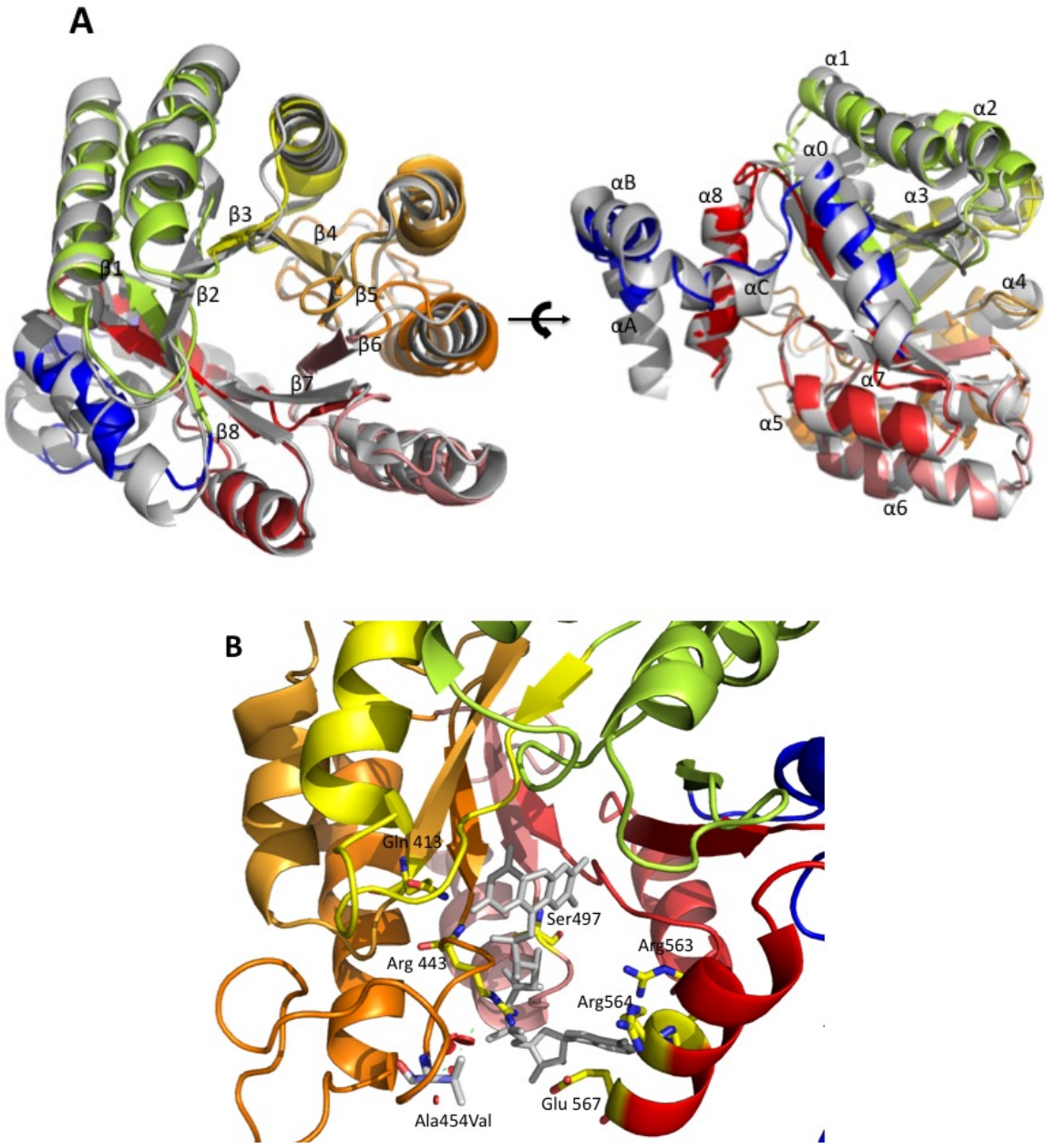

Figure 5.2 3D-structure model of domain 3 of human PRODH 1. (A). Structure alignment of TtPRODH (grey; PDB:2EKG) and domain 3 of human PRODH1 with indicated $(\alpha\beta)_8$-barriel domain. (B). Flavin and conserved residue proposed to be important for enzyme activity are shown in sticks. Mutated residue of Ala454Val is also shown in sticks.

containing protease inhibitors, 1% Triton X-100 and 0.5 mM Tris (3-hydroxypropyl) phosphine (THP). Cells were then lysed by sonication and cell debris was pelleted by centrifugation. After passing through a 0.45 μm filter, the lysate supernatant was loaded onto a glutathione sepharose column (GE Healthcare) equilibrated with PBS, at a flow rate of 0.1 ml/min. After 10 volumes of washing with PBS, the protein was eluted with reduced glutathione (GSH) elution buffer (20 mM Tris, 200 mM NaCl, 10 mM GSH, pH 8.0). The eluted protein was digested with thrombin (10 Unit per mg of protein) at 4 °C overnight to remove the N-terminal-GST tag. After removing thrombin by a HiTrap Benzamidine column (GE Healthcare), the protein was extensively (2,000-fold) dialyzed against PBS (0.5 mM THP) to remove GSH. Then un-cleaved protein was removed by glutathione sepharose column and protein was dialyzed against 20 mM Tris, 0.2 M NaCl, 10% glycerol, 0.5 mM THP, pH8.0. Protein concentration was measured by Pierce protein A660 nm assay buffer.

5.3.4 Steady-state kinetic measurements

Measurements were made with a Cary® 50 UV-Vis spectrophotometer (Varian, Inc). For the measurement of human PRODH 1ΔMTS activity, dichlorophenolindo-phenol (DCPIP) and CoQ_1(100 μM) were used as terminal electron acceptors with varying proline (0-200 mM) as previously described (17). The DCPIP assay mixture contained 20 mM Tris, 0.27 mM phenazine methosulfate and 75 μM DCPIP, pH 8.0. The rate of DCPIP reduction was monitored by the absorbance at 600 nm (ε = 16100 cm^{-1} M^{-1}). When using CoQ_1

as the electron acceptor, PRODH activity was measured by the production of the yellow dihydroquinazolinium complex, which is formed between P5C and *o*-aminobenzaldehyde (o-AB). P5C formation was monitored by the absorbance at 443 nm (ε = 2900 $M^{-1}cm^{-1}$) (18). The PRODH1-CoQ_1 assay mixture contained 50 mM potassium phosphate buffer, 4 mM *o*-AB and 100 µM CoQ_1, pH 8.0. One unit of PRODH activity is defined as the amount of enzyme that transfers electrons from 1 µmol of proline to the electron acceptor per min at 25°C. The parameters K_m and V were obtained by fitting the data to the Michaelis-Menten equation using Prism Software.

Inhibition of PRODH activity by L-tetrahydro-2-furoic acid (THFA) was examined by steady-state inhibition kinetic measurements using proline as the variable substrate (0-200 mM) and DCPIP as the electron acceptor. L-THFA concentration was varied from 0 – 6 mM. The inhibition constant (K_I) for L-THFA was estimated by Lineweaver-Burk plot analysis (18).

The pH profile of PRODH1 activity was determined using a mixed buffer system from pH 6.0–10.0 comprised of 20 mM each HEPES, MES, MOPS and TAB (80 mM total). The kinetic measurements were performed at different pH values by varying proline (0-200 mM) and using DCPIP as the electron acceptor. The pH profiles of the kinetic parameters for PRODH1 were analyzed for the effect of pH on enzyme−ligand complexes by plotting k_{cat}, k_{cat}/K_m, and K_m vs pH. Kinetic data were fit to the equation $P_{obs} = P_{lim}/(1+10^{(pKa-pH)})$ (eq1), where P_{obs} and P_{lim} represent the observed and limited parameter values, respectively, and pK_a is the acidic-dissociation equilibrium constant, representing the ionization

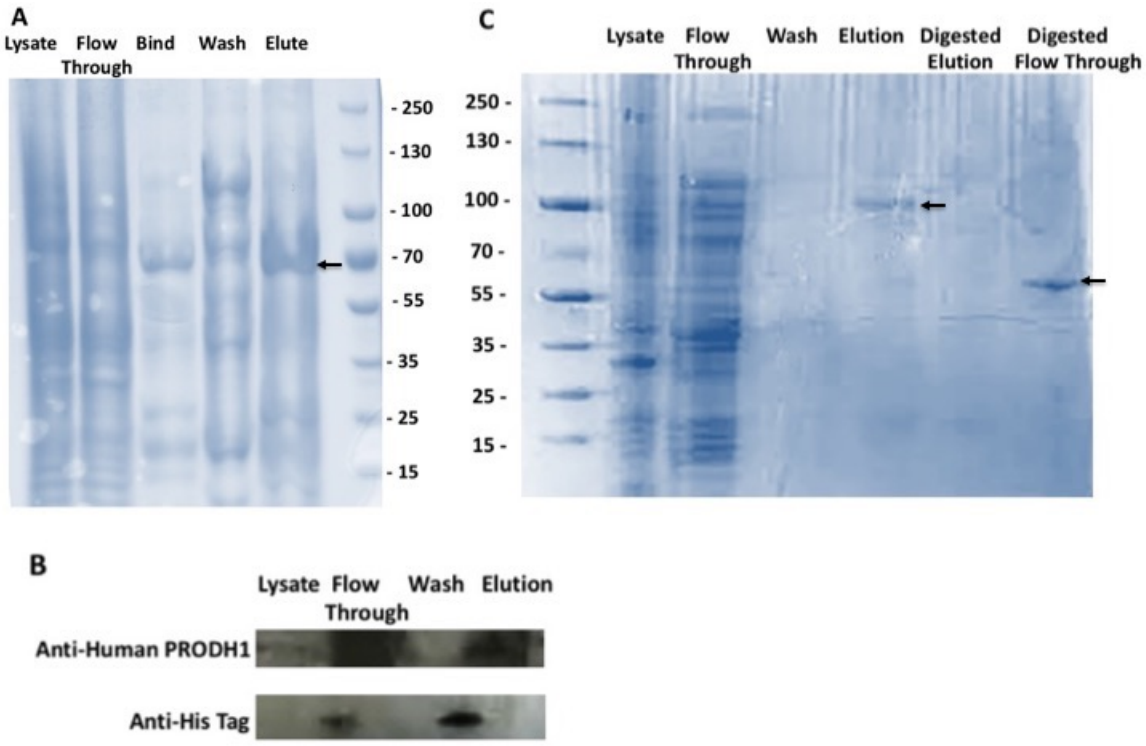

***Figure 5.3*. SDS-PAGE analysis of His-Human PRODH 1 ΔMTS and GST-human PRODH 1 ΔMTS.** (A). SDS-PAGE electrophoresis of samples from purification of His-Human PRODH1 ΔMTS (indicated with arrow). (B). Western blot analysis of samples from purification of His-Human PRODH 1 ΔMTS using anti-human PRODH antibody and anti-His antibody. (C). SDS-PAGE electrophoresis of samples from purification of GST-Human PRODH1 ΔMTS (indicated with arrow), with digested flow through representing protein with cleaved his-tag (indicated with arrow) and digested elution representing protein with un-cleaved his-tag (not shown on the gel).

that contributes to the pH dependent curve of the reaction velocity (19).

5.3.5 Proline:O_2 reactivity

Proline:O_2 activity was measured in air-saturated 50 mM potassium phosphate buffer (pH 7.5) at 25°C, using various amounts of proline (0 - 200 mM) as substrate. The assay buffer included 40 U/mL superoxide dismutase, 125 mM KCl, 4 mM KH_2PO_4, 14 mM NaCl, 20 mM HEPES, 1 mM $MgCl_2$, 0.2% BSA, and 0.02 mM EDTA (20). Rates of the proline:O_2 activity were determined by following the production of H_2O_2, which was quantified using the Amplex® Red Hydrogen Peroxide/Peroxidase Assay Kit (20). H_2O_2 was measured by monitoring the fluorescence emission at 581 nm (555nm excitation wavelength) with a Cary® Eclipse Fluorescence Spectrophotometer. One unit of proline:O_2 activity is defined as the amount of PRODH that generates 1 µmol of H_2O_2 per min at 25°C. The effect of L-THFA on proline:O_2 activity was determined using the same assay conditions as described above.

5.3.6 UV-Visible spectroscopy

The UV-visible spectra were recorded from 300–700 nm on a Cary 100 spectrophotometer. GST-human PRODH1 ΔMTS (6.7 µM) was incubated with increasing concentration of flavin to reach a final concentration of 7 µM. The absorbance spectrum was measured after addition of flavin and incubation period of 5 min. The GST-human PRODH1 ΔMTS (6.7 µM) and flavin (7 µM) mixture were then titrated with proline range (0 – 10 mM). The absorbance spectrum was

recorded at each proline concentration after incubating the enzyme with proline for 5 min.

5.3.7 Statistical analysis

The reported mean values and standard deviations are from three to five replicates. Data were analyzed by Student's *t*-tests with statistical significance considered to be a *P*-value < 0.05.

5.4 RESULTS

5.4.1 Design of human PRODH1 ΔMTS

Human PRODH1 is predicted to harbor a mitochondria targeting sequence of residues 1-48. (MTS, 1-48). Secondary structure analysis also defines three domains in PRODH1 of residues 48-133 (domain 1), 134-260 (domain 2), and 261-600 (domain 3). (Figure 5.1A). Domain 3 is predicted to be the catalytic domain of human PRODH1 as it contains highly conserved active sites residues such as Arg563 and Arg564 (motif 9) which are known to be critical for proline binding in *E. coli* PutA (4). The association of human PROH1 with the inner mitochondrial membrane suggests that it may contain hydrophobic regions that are prone to be distorted in the absence of membrane. The distorted regions would likely diminish the solubility of recombinant human PRODH1. Indeed, RONN (regional order neural network) analysis of human PRODH1 indicates (Figure 5.1A) three regions of high distortion probability which are located at MTS, the first part of domain 2 (175-200 residues) and at the end of domain 3 (590-600 residues). Previously, truncation off prone-distorted regions was shown to improve the solubility of

recombinant human PRODH1, however, the enzyme kinetic properties appear to be significantly impacted (15). Therefore, in this study, we chose to remove only the MTS region and develop alternative strategies to improve solubility human PRODH1 by using 0.1-1% Tween-100 during purification and expressing human PRODH1 as a GST-tag fusion protein.

5.4.2 Homology modeling of human PRODH1 catalytic domain

It has been reported that PRODHs share nine motifs that contribute conserved residues in the active site important for FAD and substrate binding (4). Multiple alignment of the protein sequence of PRODHs from *Homo Sapiens*, *Saccharomyces cerevisiae*, *Drosophila melanogaster*, *Thermus thermophilus* and *Bos Taurus* indicates that human PRODH1 contains 8 out of the 9 motifs (Figure 5.1B), with motifs 4–6 involved in FAD binding and motifs 1, 3, 7-9 responsible for substrate recognition (4). For instance, Gln413 of motif 4 and Arg443 of motif 5 may be important for hydrogen binding to the FAD O2 and N5, respectively (Figure 5.2B). Also, arginine residues (Arg563 and Arg564) of motif 9 were proposed to form ion pairs with the carboxyl group of the substrate proline (Figure 5.2B) (4). Nucleotide sequencing indicated that there are two mutations found in our human PRODH1 construct, Asn175Ile and Ala454Val. These mutations, Asn175 and Ala454 are not conserved in PRODHs and are not anticipated to impact the activity of human PRODH1.

Secondary structure analysis of human PRODH1 domain 3 revealed 11 α-helixes and 7 β-sheets (Figure 5.1B). Crystal structure of monofunctional PRODH

from *T. thermophilus* and the PRODH domain of *E. coli* PutA established that PRODHs adopt a distorted $(\beta\alpha)_8$-barrel (4). The typical $(\beta\alpha)_8$-barrel consists of an eight parallel β-sheet forming a barrel (21). Each β-sheet is followed by one α-helix, surrounding the β-sheet barrel (21). The catalytic face of $(\beta\alpha)_8$-barrel is comprised of the C-terminal ends of the β strands and the loops that link β strands with the subsequent α helices (21).

The amino acid sequence of human PRODH1 domain 3 shares 35.2% sequence similarly with catalytic domain of *T. thermophilus* PRODH. Therefore, we are able to obtain a homology structure of the human PRODH1 catalytic domain by SWISS-MODEL based on the structure of *T. thermophilus* PRODH (PDB:2EKG). Figure 5.2A indicates that human PRODH1 contains all the components of the $(\beta\alpha)_8$-barrel, except sheet β2. Similar to other PRODHs, human PRODH1 has the helix α8 on top of the barrel, whereas typical $(\beta\alpha)_8$-barrel has that helix alongside sheet β8 (4). In addition, helix 8 contains the two arginine residues of motif 9 that are critical for substrate binding (22) (Figure 5.2B). In Figure 5.2B, FAD of PRODHs was placed at the C-terminal ends β strands, where it has been shown to bind in the active site (4).

5.4.3 Purification of human PRODH1 ΔMTS

Tallarita et al. made an attempt to purify human PRODH1 by deleting residues 1-48 (MTS), but this deletion was reported to have extremely low protein expression (<0.1 mg/L of culture) (15). In our case, expression of His-human PRODH1 ΔMTS resulted in a low amount of soluble protein as well (<0.5 mg/L of

culture), whereas expression of GST-human PRODH1 ΔMTS led to a significantly increased amount of soluble protein (~3 mg/L of culture). SDS-PAGE analysis showed a major protein band of about 65-kDa (Figure 5.3A and Figure 5.3C), consistent with the predicted molecular weight of human PRODH1 ΔMTS (63.3 kD). The expression of human PRODH1 ΔMTS was confirmed by Western blot analysis (Figure 5.3 B) and mass spectrometry. Unfortunately, SDS-PAGE (Figure 5.3A) also showed that His-human PRODH1 ΔMTS was not fully purified. Attempts to cleave the histidine tag of His-human PRODH1 ΔMTS were not successful as only 10% of the His-tag PRODH1 ΔMTS appeared to be cleavable by thrombin (10 U/ mg protein with overnight incubation). The inability to effectively cleave the His tag may be due to the N-terminus of PRODH1 being buried. It was observed that His-human PRODH1 ΔMTS binds weakly to the Ni-NTA column as the protein eluted at low imidazole concentrations (10-20 mM), which suggests the N-terminal His tag may have limited solvent accessibility. Purification of GST-human PRODH1 ΔMTS resulted in a single band with apparent molecular weight of 97 kDa (Figure 5.3C). Approximately 90% of histidine tag was estimated to be cleaved by overnight treatment with thrombin (Figure 5.3C). The kinetics studies in this chapter were mainly performed with GST-human PRODH1 ΔMTS except for the pH activity profile and THFA inhibition.

The UV-visible spectra of purified His-PRODH1 and His-GST-human PRODH1 ΔMTS showed very little FAD is present as maxima absorption features for flavin at 355 and 451 nm and a shoulder at 478 nm were not

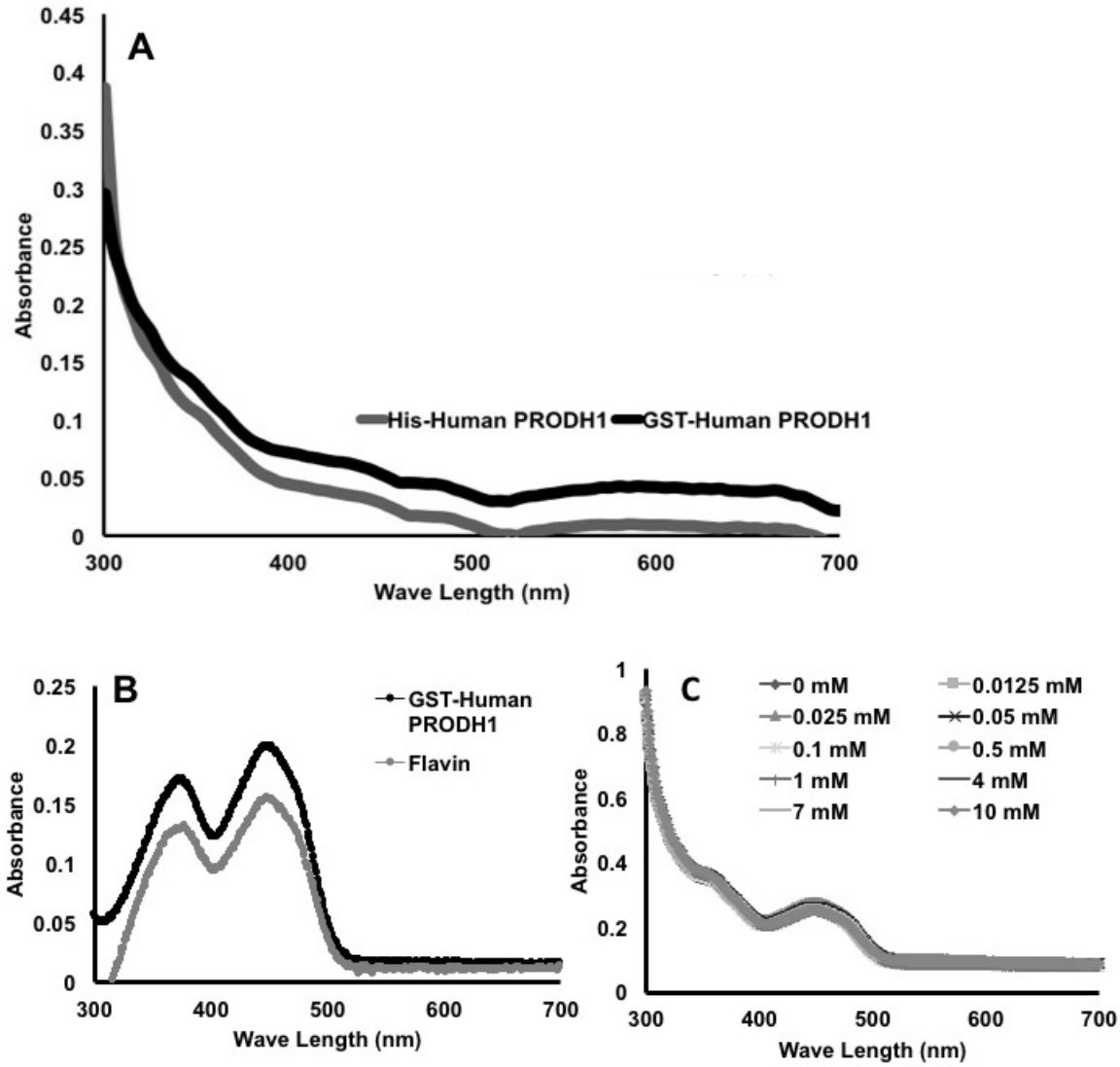

Figure 5.4. **UV-visible spectra of purified PRODH1 proteins.** (A) UV-visible spectra of purified His-human PRODH1 and His-GST-human PRODH1. Spectra indicate very little FAD is present in the purified proteins. (B) UV-visible spectrum of uncleaved His-GST-human PRODH ΔMTS (6.7 μM) after incubation with FAD (7 μM) and with spectrum of free FAD (7 μM) for comparison. (C) Spectra of GST-human PRODH 1 ΔMTS with FAD after each addition of proline (0-10 mM).

Table 1. Kinetic parameters using L-proline as substrate

	H. Sapiens PRODH	*T. thermophilus* PRODH[a]	*E. coli* PutAb	*S.cerevisiae* Put1p[c]	*H. pylori* PutA[d]
proline:DCPIP assay					
***Km* (mM)**	6.6	27	100	36	146
***Vmax* (U/mg)**	0.68	20.5	5	4.2	3.6
***kcat* (s^{-1})**	0.75	13	12	27	8
***kcat/Km* (s^{-1} M^{-1})**	113	481	122	750	56
***KI* for THFA (mM)**	3.4	1.0	0.2	5.3	0.35
proline:O_2 assay					
***Km* (mM)**	7.7	1.3	ND	50	150
***Vmax* (mU/mg)**	0.95	335	< 2	144	230
***kcat* (min^{-1})**	0.06	12.7	<0.3	0.8	31
DCPIP/O_2 activity ratio	750	61	> 2500	2025	16

- a. Data obtained from Whit et al. (18).
- b. Data obtained from Zhu et al. (23) and Krishnan and Becker (25).
- c. Data obtained from Wanduragala et al. (19).
- d. Data obtained from Krishnan and Becker (25).

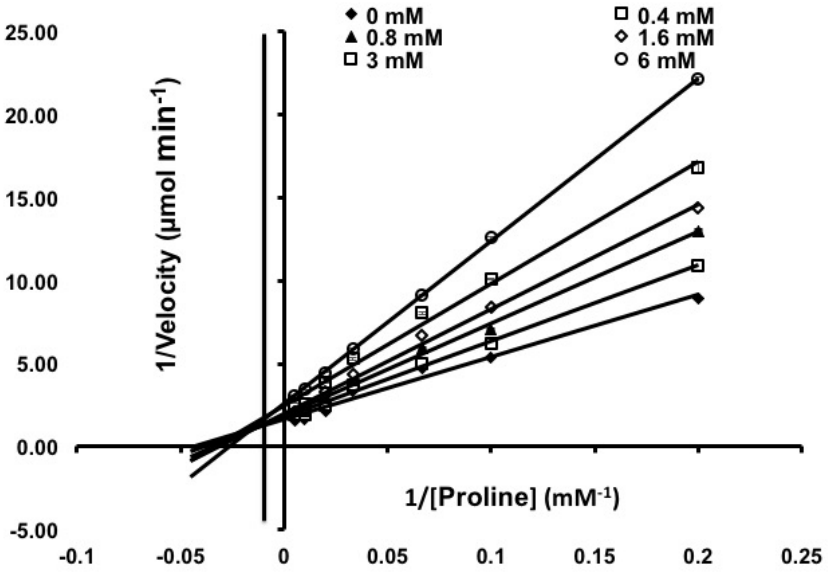

Figure 5.5 Inhibition of human PRODH1 ΔMTS (semi-purified N-terminal histidine tagged form) activity by L-THFA (0-6 mM).

observed, indicating that these proteins were largely purified in apoforms (Figure 5.4A). His-GST-human PRODH1 was then incubated with increasing amounts of FAD in an attempt to generate a flavin bound protein species. Figure 5.4B shows that the flavin spectrum in the presence of His-GST-human PRODH1 is very similar to that of free flavin as no shoulder at 478 nm was observed which is typical of protein bound FAD. To test whether the FAD could be reduced with proline, which would provide evidence of a His-GST-human PRODH1 bound FAD, the GST-tagged human PRODH1 ΔMTS was incubated with increasing concentrations of proline under aerobic conditions. Figure 5.4C shows no significant reduction of the FAD was observed with proline indicating that FAD was not bound to the His-GST-tagged human PRODH1 ΔMTS protein.

5.4.4 Steady-state kinetics

The kinetic parameters for human PRODH1 ΔMTS using the proline:DCPIP oxidoreductase assay were estimated to be K_m = 6.6 ± 0.6 mM proline, V = 0.66 U/mg and k_{cat} = 0.75 ± 0.008 s^{-1} (Table 1). The corresponding values for other monofunctional PRODHs from *T. thermophilus* and *S. cerevisiae*, as well as bifunctional PutAs such as *E. coli* and *Helicobacter pylori* are listed in Table 1. The K_m parameter of human PRODH1 ΔMTS is 20-fold higher than human plasma proline concentration (0.2-0.3 mM)(16), and 4-5 and 15-20 times lower than those of the monofunctional PRODHs and the PutAs, respectively. This is consistent with a previous observation that monofunctional PRODHs have lower K_m values for proline than bifunctional PutA enzymes (19). Compared with previous studies of

human PRODH, our estimated K_m value is similar to Krishnan et al. data (K_m =15 mM) (14), and 2 orders of magnitude lower than that reported by Tallarita et al. (K_m = 0.47 M) (15). The specific activity of human PRODH1 ΔMTS determined here (0.68 U/mg) is 7- and 20-fold higher than that reported previously by Krishnan et al. (0.1 U/mg) (14) and Tallarita et al. (0.032 U/mg) (15), for full-length and truncated human PRODH1, respectively. The turnover rate of truncated human PRODH 176-572 (44.6 kD) is estimated to be 0.023 s^{-1}, which is > 30-fold lower than that of human PRODH1 ΔMTS (0.75 s^{-1}). Therefore, human PRODH1 ΔMTS has significantly higher activity than that obtained previously with other purified human PRODHs. However, the turnover number of human PRODH1 ΔMTS is 10-20 times lower than that of PutAs and PRODHs. The k_{cat}/K_m for human PRODH1 is similar to bifunctional PutAs but is significantly lower than that reported for PRODHs from *T. thermophilus* and *S. cerevisiae.* The k_{cat}/K_m for human PRODH1 is the first time this kinetic parameter has been reported for human PRODH1.

The inhibition of human PRODH1 activity with L-THFA, an isostructural analog of proline, was next investigated. Figure 5.5A shows a Lineweaver Burk plot of the inhibition of human PRODH1 ΔMTS activity by L-THFA. The plot shows that L-THFA acts as a competitive inhibitor of human PRODH1 ΔMTS with K_I of 3.4 ± 0.4 mM. The K_I of human PRODH1 ΔMTS for L-THFA is similar to that of monofunctional PRODHs (K_I = 1 – 5.3 mM) but higher than bifunctional PutAs (K_I = 0.2 – 0.3 mM) (Table 1).

Since deprotonating of the proline amine group is a crucial step in PRODH reaction, and pK_a reflects the ionization of a group on the enzyme or substrate, we

then measure the pH activity profile of human PRODH1. The pH-activity profile of human PRODH1 ΔMTS was measured by following proline:DCPIP oxidoreductase activity over the pH range 6–9.5 and the pH dependence of the kinetic parameters k_{cat}, K_m, and k_{cat}/K_m of PRODH was determined (Figure 5.6). The k_{cat} and k_{cat}/K_m of the enzyme followed a bell-shape curve, with the pH optimum at 7.9, which is relatively lower than that of Put1p ($pH_{optimum}$ = 8.6) (19). The values of pK_a were estimated to be 6.2 ± 0.16 and 6.1 ± 0.08 for k_{cat} and k_{cat}/K_m, respectively. Human PRODH1 also has lower pK_a, compared with *E.coli* PutA (pK_a of 7.4 (k_{cat}/K_m) and pK_a of 7.3 (k_{cat}). The K_m values for proline for human PRODH1 appear to be insensitive to pH alteration.

Human PRODH1 ΔMTS activity was also characterized using CoQ_1 as an electron acceptor and proline as a substrate (Figure 5.6A). By holding CoQ_1 fixed, the kinetic parameters for proline were estimated to be k_{cat} = 0.35 ± 0.01 s^{-1} and K_m = 3.3 ± 0.6 mM proline. Adding flavin to the assay increased k_{cat} by 2-fold (k_{cat} = 0.75 ± 0.01 s^{-1}) but the K_m remained the same. The k_{cat}/K_m for Human PRODH1 ΔMTS using CoQ_1 as an electron acceptor was 227 M^{-1} s^{-1} which is about 2-fold higher than that determined by the DCPIP assays. When compared with Put1p (k_{cat}/K_m = 750 M^{-1} s^{-1}), however, the activity of human PRODH1 ΔMTS is about 3-fold lower (19).

5.4.5 Reactivity of human PRODH1 ΔMTS with molecular oxygen

We next characterized the reactivity of human PRODH1 ΔMTS with oxygen by following the production of production of H_2O_2 in air-saturated buffer during turnover with proline. SOD is included in these assays so that any

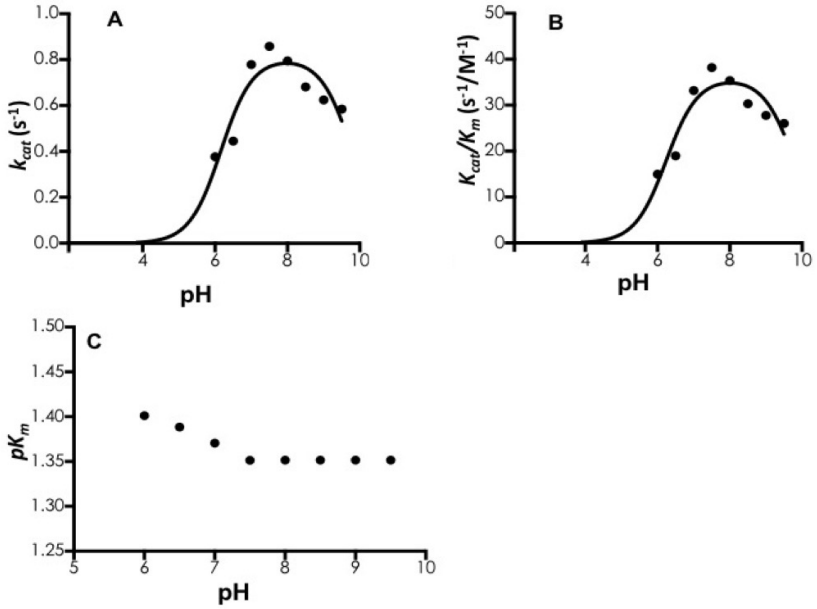

Figure 5.6 p**H profiles of steady-state kinetic parameters of human PRODH1 ΔMTS (semi-purified N-terminal histidine tagged form).** Measurements were performed in a 80 mM mixed buffer from pH 6−9.5 at 25 °C. (A) Plot of kcat vs pH, (B) plot of kcat/ Km vs pH, and (C) plot of pKm for proline vs pH for human PRODH1 ΔMTS.

superoxide anion generated during catalytic turnover in the PRODH1 active site is quickly converted into H_2O_2. The H_2O_2 production rate of the reaction increases with proline reaching a maximum rate around 15 mM proline (Figure 5.6.B). Addition of THFA (10 mM) significantly attenuated H_2O_2 production consistent with H_2O_2 being generated by human PRODH1 ΔMTS activity. The kinetic parameters for human PRODH1 ΔMTS oxidase activity (proline:O_2 assay) were k_{cat} = 0.06 min^{-1} and K_m = 7.7 mM (Table 1). Clearly proline:O_2 activity is significantly lower than proline:DCPIP or proline:CoQ_1 activity. When comparing the activity ratio of DCPIP versus O_2 as an electron acceptor, the ratio for human PRODH1 ΔMTS is 10-50 fold higher than that of *T. thermophilus* PRODH and *H. pylori* PutA, but 3 times lower than that of Put1p and *E. coli* PutA (Table 1). These results show that O_2 is highly unfavored as a electron acceptor for human PRODH1 ΔMTS, indicating that CoQ is the physiological electron acceptor and that proline-dependent ROS is derived from the ubiquinone pool and the mitochondrial respiratory electron transport chain.

5.5 DISCUSSIONS

Multiple PRODH missense mutations have been identified in patients with hyperprolinemia type I or schizophrenia. Five of these mutations were shown by assays of cell lysates to result in reduced human PRODH1 activity when expressed in CHO cells (12-13). Purification of a soluble and active human PRODH1 is a crucial step to understand the structure–function relationships of this enzyme. In this study, we were able to purify a soluble and active GST-human

PRODH1 enzyme which lacked the N-terminal mitochondria targeting sequence. To the best of our knowledge, GST- human PRODH1 ΔMTS is the first purified human PRODH1 that is active, soluble and contains all three domains. However, why our enzyme preparation resulted in a low amount of bound FAD in human PRODH1 ΔMTS, namely the apoform, remains unknown and will require further attempts to improve flavin incorporation.

Human PRODH1 contains 8 out of 9 motifs that contain conserved residues responsible for proline and flavin binding (Figure 5.1B). The catalytic domain of human PRODH1 is predicted to share 35% sequence similarity with that of *T. thermophilus* PRODH, which represents the minimalist PRODH enzyme and has provided the only structure thus far of a monofunctional PRODH enzyme. The sequence similarity of human PRODH1 with *T. thermophilus* PRODH highly suggests that human PRODH1 shares the active site structure and $(\beta\alpha)_8$ catalytic core of that in bacterial monofunctional PRODHs. Monofunctional PRODHs and PRODH domains of bifunctional PutAs share a distorted $(\beta\alpha)_8$-barrel (4). The secondary structure analysis (Figure 5.1B) and homology modeling (Figure 5.2) of the human PRODH1catlytical domain (domain 3) indicate it contains all the components of $(\beta\alpha)_8$-barrel except sheet β2. Whether the β2 sheet is actually missing in human PRODH1 will require a crystal structure of the enzyme. In addition, human PRODH1 has two additional domains that are not present in *T. thermophilus* PRODH. A crystal structure would also help with determining the function of these domains. These domains, however, appear to be important for activity as deletion of the domains in the truncated PRODH1 reported previously,

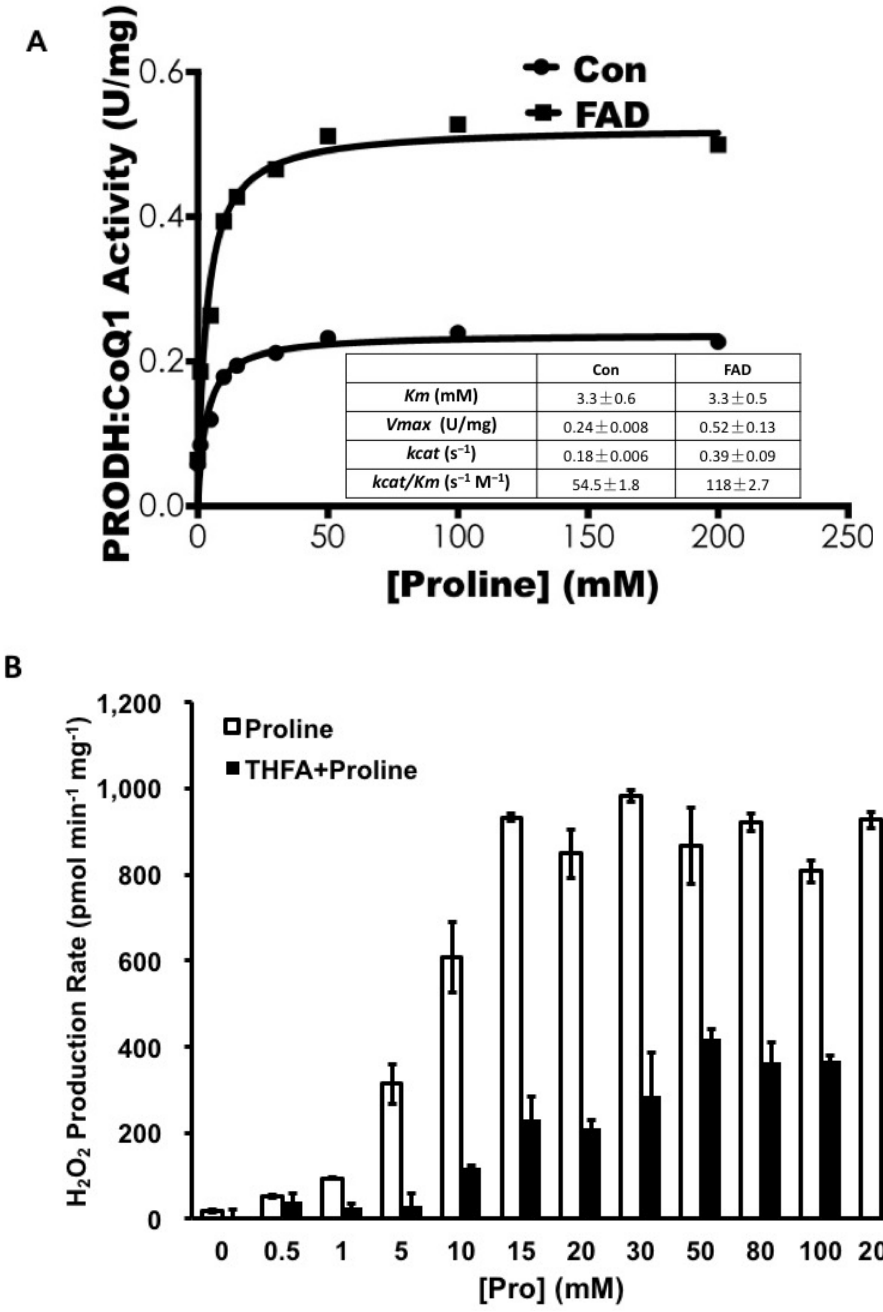

Figure 5.7 Oxidative half-reaction of human PRODH1 ΔMTS using CoQ1 and oxygen as electron acceptors. (A). Activity of human PRODH1 ΔMTS (33 nM) using CoQ1 (100 μM) as electron acceptor in the presence and absence of 2 μM FAD. (B). Oxygen reactivity of human PRODH1 ΔMTS was measured by following the production of H_2O_2 in the presence and absence of 10 mM THFA.

resulting in lower activity than what we found here for the full-length enzyme (15).

Human PRODH1 was shown to highly prefer DCPIP or its physiological electron acceptor CoQ over molecular oxygen. This result demonstrates that human PRODH1 is a flavoenzyme dehydrogenase and that the prevalent use of proline oxidase in the literature is a misnomer. Clearly, proline oxidation–induced superoxide/hydrogen peroxide production is critical to the ability of human PRODH1 to function in mediating cellular signaling and processes (6-8). The main source of proline-derived ROS, however, is not at the flavin active site, but rather from the ubiquinone pool and electron transport events in the respiratory chain of the mitochondrion. Those results are consistent with our data of fibroblast cells and isolated mitochondria (Chapter 4) and from a recent study of isolated mitochondria from human breast cells examining superoxide/hydrogen peroxide production by proline oxidation (24). A previous study of oxygen reactivity in PutAs identified a tyrosine residue (Tyr437 in *E. coli* PutA) of motif 5 having a role limiting solvent accessibility to the active site and therefore limiting reactivity with molecular oxygen (25). *H. pylori* PutA, which exhibits significant reactivity with molecular oxygen, has an asparagine residue (Asn291) at the same position in motif 5 suggesting the active site of *H. pylori* PutA is more exposed to solvent. The sequence of alignment shown in Figure 5.1B shows human PRODH1 has a tyrosine residue (Tyr452) in motif 5. This may explain the low reactivity of human PRODH1 with oxygen similar to that proposed for *E. coli* PutA. However, several monofunctional PRODHs, including *T. thermophilus* PRODH and Put1p all share the tyrosine residue at motif. Put1p fails to react with oxygen but *T. thermophilus*

PRODH has high reactivity of oxygen (Table 1). It has also been proposed that the flexibility of α8 helix of PRODH may determine its O_2 reactivity (4). Structure determination of human PRODH1 will be beneficial to understanding the difference of oxygen reactivity between human and *T. thermophilus* PRODH1 enzymes.

REFERENCES:

1. Pandhare, J., Donald, S. P., Cooper, S. K., and Phang, J. M. (2009) Regulation and function of proline oxidase under nutrient stress. *Journal of cellular biochemistry* **107**, 759-768
2. Suntsova, M., Gogvadze, E. V., Salozhin, S., Gaifullin, N., Eroshkin, F., Dmitriev, S. E., Martynova, N., Kulikov, K., Malakhova, G., Tukhbatova, G., Bolshakov, A. P., Ghilarov, D., Garazha, A., Aliper, A., Cantor, C. R., Solokhin, Y., Roumiantsev, S., Balaban, P., Zhavoronkov, A., and Buzdin, A. (2013) Human-specific endogenous retroviral insert serves as an enhancer for the schizophrenia-linked gene PRODH. *Proceedings of the National Academy of Sciences of the United States of America* **110**, 19472-19477
3. Corominas, R., Yang, X., Lin, G. N., Kang, S., Shen, Y., Ghamsari, L., Broly, M., Rodriguez, M., Tam, S., Trigg, S. A., Fan, C., Yi, S., Tasan, M., Lemmens, I., Kuang, X., Zhao, N., Malhotra, D., Michaelson, J. J., Vacic, V., Calderwood, M. A., Roth, F. P., Tavernier, J., Horvath, S., Salehi-Ashtiani, K., Korkin, D., Sebat, J., Hill, D. E., Hao, T., Vidal, M., and Iakoucheva, L. M. (2014) Protein interaction network of alternatively spliced isoforms from brain links genetic risk factors for autism. *Nature communications* **5**, 3650
4. Tanner, J. J. (2008) Structural biology of proline catabolism. *Amino Acids* **35**, 719-730
5. Liu, W., Le, A., Hancock, C., Lane, A. N., Dang, C. V., Fan, T. W., and Phang, J. M. (2012) Reprogramming of proline and glutamine metabolism contributes to the proliferative and metabolic responses regulated by oncogenic transcription factor c-MYC. *Proceedings of the National Academy of Sciences of the United States of America* **109**, 8983-8988
6. Phang, J. M., Liu, W., and Zabirnyk, O. (2010) Proline metabolism and microenvironmental stress. *Annu Rev Nutr* **30**, 441-463
7. Phang, J. M., Donald, S. P., Pandhare, J., and Liu, Y. (2008) The metabolism of proline, a stress substrate, modulates carcinogenic pathways. *Amino Acids* **35**, 681-690
8. Phang, J. M., Liu, W., Hancock, C., and Christian, K. J. (2012) The proline regulatory axis and cancer. *Front Oncol* **2**, 60
9. Liu, Y. M., Borchert, G. L., Donald, S. P., Diwan, B. A., Anver, M., and Phang, J. M. (2009) Proline Oxidase Functions as a Mitochondrial Tumor Suppressor in Human Cancers. *Cancer Research* **69**, 6414-6422
10. Kumar Natarajan, S., Zhu, W., Liang, X., Zhang, L., Demers, A. J., Zimmerman, M. C., Simpson, M. A., and Becker, D. F. (2012) Proline dehydrogenase is essential for proline protection against hydrogen peroxide-induced cell death. *Free Radic Biol Med*
11. Pandhare, J., Dash, S., Jones, B., Villalta, F., and Dash, C. (2015) A Novel Role of Proline Oxidase in HIV-1 Envelope Glycoprotein Induced Neuronal Autophagy. *The Journal of biological chemistry*
12. Ghasemvand, F., Omidinia, E., Salehi, Z., and Rahmanzadeh, S. (2015) Relationship between polymorphisms in the proline dehydrogenase gene

and schizophrenia risk. *Genetics and molecular research : GMR* **14**, 11681-11691

13. Mitsubuchi, H., Nakamura, K., Matsumoto, S., and Endo, F. (2014) Biochemical and clinical features of hereditary hyperprolinemia. *Pediatrics international : official journal of the Japan Pediatric Society* **56**, 492-496
14. Krishnan, N., Dickman, M. B., and Becker, D. F. (2008) Proline modulates the intracellular redox environment and protects mammalian cells against oxidative stress. *Free Radic Biol Med* **44**, 671-681
15. Tallarita, E., Pollegioni, L., Servi, S., and Molla, G. (2012) Expression in Escherichia coli of the catalytic domain of human proline oxidase. *Protein expression and purification* **82**, 345-351
16. Price, F. W. e. (1950) *A Textbook of the Practice of Medicine*, 8th ed. ed., Geoffrey Cumberlege Oxford University Press, [S.l.]
17. Becker, D. F., and Thomas, E. A. (2001) Redox properties of the PutA protein from Escherichia coli and the influence of the flavin redox state on PutA-DNA interactions. *Biochemistry* **40**, 4714-4721
18. White, T. A., Krishnan, N., Becker, D. F., and Tanner, J. J. (2007) Structure and kinetics of monofunctional proline dehydrogenase from Thermus thermophilus. *The Journal of biological chemistry* **282**, 14316-14327
19. Wanduragala, S., Sanyal, N., Liang, X., and Becker, D. F. (2010) Purification and characterization of Put1p from Saccharomyces cerevisiae. *Arch Biochem Biophys* **498**, 136-142
20. Starkov, A. A. (2010) Measurement of mitochondrial ROS production. *Methods Mol Biol* **648**, 245-255
21. Hocker, B., Jurgens, C., Wilmanns, M., and Sterner, R. (2001) Stability, catalytic versatility and evolution of the (beta alpha)(8)-barrel fold. *Current opinion in biotechnology* **12**, 376-381
22. Zhang, M., White, T. A., Schuermann, J. P., Baban, B. A., Becker, D. F., and Tanner, J. J. (2004) Structures of the Escherichia coli PutA proline dehydrogenase domain in complex with competitive inhibitors. *Biochemistry* **43**, 12539-12548
23. Zhu, W., Gincherman, Y., Docherty, P., Spilling, C. D., and Becker, D. F. (2002) Effects of proline analog binding on the spectroscopic and redox properties of PutA. *Arch Biochem Biophys* **408**, 131-136
24. Goncalves, R. L., Rothschild, D. E., Quinlan, C. L., Scott, G. K., Benz, C. C., and Brand, M. D. (2014) Sources of superoxide/H2O2 during mitochondrial proline oxidation. *Redox biology* **2**, 901-909
25. Krishnan, N., and Becker, D. F. (2006) Oxygen reactivity of PutA from Helicobacter species and proline-linked oxidative stress. *J Bacteriol* **188**, 1227-1235

SUMMARY

SUMMARY AND FUTURE DIRECTIONS

The catabolism of proline has been shown to regulate many cellular processes, such as energy utilization, programmed cell death, cell reprogramming and development, oxidative stress resistance, and aging (1-4). ROS is implicated in all of these processes. For instance, oxidative stress limits the energy generation by the TCA cycle by inhibiting aconitase (7). In addition, according to the free radical theory of aging, ROS may induce the aging process or delay aging progression depending on the level of intracellular ROS (8). In many proline catabolic affected cellular processes, ROS induced by proline oxidation has been found to play a regulatory role (5). As discussed in chapter 1 and 2, a low amount of proline oxidation-induced ROS serves as a pro-survival signal, whereas a high concentration of proline oxidation-dependent ROS is deleterious to cells. This dissertation sought to gain further understanding of the relationship between proline-mediated ROS production and the effect of proline oxidation on cell survival during oxidative stress.

In Chapter 3, we explored the mechanism of proline oxidation-mediated protection against oxidative stress in *E. coli*. We first observed that proline pre-treatment of wild-type *E. coli* cells, but not *putA* mutant cells resulted in significantly higher survival rates in oxidative stress assays than in cells without proline

treatment. This indicates PutA is required for proline-mediated protection against oxidative stress. We than found that proline catabolism generates ROS as a signaling molecule which activates the OxyR regulon, including *katG*, thereby induces increased oxidative stress tolerance in *E. coli*. The source of proline oxidation-induced H_2O_2 was found to be potentially cytochrome *bo* terminal oxidase of the *E. coli* respiratory chain. In the future, the function of cytochrome *bo* in generating proline-induced ROS should be further studied using *E. coli* with impaired of cytochrome *bo* terminal oxidase. For example, if the proline oxidation-induced ROS formation is lower in cells with impaired cytochrome *bo* terminal oxidase, then the role cytochrome *bo* oxidase in generating proline-dependent ROS may be confirmed. In addition, inhibitors, such as aurachin C and D that have been shown to inhibit the activity of cytochrome *bo* oxidase may also be used (9). Another aspect that needs to be further studied is whether proline oxidation is capable of increasing oxidative stress resistance and/or promoting the infection process of bacterial pathogens. ROS was found to induce the infection process of many bacterial pathogens, such as *Porphyromonas gingivalis*, *Mycobacterium abscessus*, *Helicobacter pylori* and *Bacillus anthracis* (6). Proline-oxidation may increase the tolerance of these bacteria pathogens to oxidative stress, thereby pathogens may have a higher tendency to survive when attacked by the human immune system. Furthermore, studying the role of proline oxidation in regulating

oxidative stress resistance and pathogenesis in these bacteria may benefit the discovery of antibiotics specifically targeting bacteria with increased pathogenesis under oxidative stress.

In Chapter 4, the proline-induced ROS production was studied in human cell line, as well as isolated human and pig mitochondria. With proline supplementation, increased ROS production was observed in both human and pig mitochondria, suggesting proline-induced ROS production is a common occurrence in mammals. In CRL2429 and WM35 cells, we found cells with a higher ROS formation rate have an increased survival rate under H_2O_2 stress. We also found that the amount of ROS formed during proline oxidation is too low to cause oxidative stress, but is sufficient to activate pro-survival signaling pathways (e.g., Akt pathway). Therefore, it is highly plausible that proline oxidation-induced ROS may activate the Akt pathway and thereby enhance oxidative stress resistance. Using a human cell line with Tet-regulated MnSOD may be helpful to study the effect of proline-induced ROS on Akt activation. Phosphorylation of Akt could be analyzed with proline treatment in the absence and presence of MnSOD overexpression. Fluorescent western blotting may have to be used in order to capture proline oxidation-induced phosphorylation of Akt. In Chapter 4, we also noticed that mitochondria using proline as a substrate have lower respiration

efficiency, suggesting proline may have a unique effect on inducing ROS signalling. Because decreased mitochondrial potential or reduced expression of mitochondrial ETC enzymes may explain the low mitochondrial efficiency, two preliminary experiments can be done to understand the mechanism of proline in lowering mitochondrial efficiency. Last but not the least, it is an open question as to whether all the eukaryotes share the same sources of proline oxidation induced mitochondrial ROS. Future studies should explore the source of ROS production by proline catabolism in different organisms.

In Chapter 5, we expressed and purified human PRODH1, which specifically catalyzes the first and rate limiting step of proline oxidation. We made a human PRODH1 construct with a deleted mitochondria targeting signal (human PRODH1 ΔMTS). Purified human PRODH1 ΔMTS appeared to be a soluble apoprotein. However, with limited supplementation of flavin, the enzyme was active. The activity of human PRODH1 ΔMTS can be inhibited by L-THFA (*Ki*= 3.4 mM). We also found that molecular oxygen is not preferably used by human PRODH1 ΔMTS as electron acceptor, suggesting proline-induced ROS is not generated by a direct reaction between PRODH and oxygen. In the future, it will be critical to purify a form of human PRODH1 with fully incorporated flavin. It is also necessary to determine the structure of human PRODH1 ΔMTS. This may not only provide an answer to the incapability of the enzyme to bind flavin, but also provide the critical

piece of knowledge about the $(\beta\alpha)_8$ catalytic core of this enzyme. Secondary structure analysis of human PRODH1 ΔMTS indicated its catalytic domain has all the components of $(\beta\alpha)_8$ barrier, except sheet β2. Besides the catalytic domain, human PRODH1 ΔMTS also contains two additional domains with unknown function. It will be useful to understand the function of these domains since several missense mutagenesis in these domains are associated with the onset of schizophrenia.

References:

1. Xinwen Liang, Lu Zhang, Sathish Kumar Natarajan, and Donald F. Becker. *Antioxidants & Redox Signaling*. September 20, 2013, 19(9): 998-1011
2. Deuschle, K., Funck, D., Forlani, G., Stransky, H., Biehl, A., Leister, D., van der Graaff, E., Kunze, R., and Frommer, W. B. (2004) The role of [Delta]1-pyrroline-5-carboxylate dehydrogenase in proline degradation. *Plant Cell* **16**, 3413-3425
3. Pang, S., and Curran, S. P. (2014) Adaptive capacity to bacterial diet modulates aging in C. elegans. *Cell Metab* **19**, 221-231
4. Hare, P. D., and Cress, W. A. (1997) Metabolic implications of stress-induced proline accumulation in plants. *Plant Growth Regul* **21**, 79-102
5. Phang, J. M. (2012) Reprogramming of proline and glutamine metabolism contributes to the proliferative and metabolic responses regulated by oncogenic transcription factor c-MYC. *Proceedings of the National*
6. Paiva, C, N., and Bozza, M, T. (2014) Are Reactive Oxygen Species Always Detrimental to Pathogens? Antioxidant Redox Signal **20(6)**, 1000-1037
7. Tretter, L., Adam-Vizi, V. (2000) Inhibition of Krebs Cycle Enzymes by Hydrogen Peroxide: A Key Role of -Ketoglutarate Dehydrogenase in Limiting NADH Production under Oxidative Stress. *The Journal of Neuroscience* **20(24)**, 8972–8979
8. Si, Liochev. (2013) Reactive oxygen species and the free radical theory of aging. *Free radic Biol Med* **60**, 1-4
9. Meunier, B., Madgwick, S.A., Reil E., Oettmeier W., Rich P.R. (1995) New inhibitors of the quinol oxidation sites of bacterial cytochromes bo and bd. Biochmiestry **34(3)**,1076-83